

DOT/FAA/AR-04/5

Office of Aviation Research
Washington, D.C. 20591

The Investigation, Evaluation, and Application of Techniques for Correlating Rotorcraft Full-Scale Water Impact Tests Versus Analyses

June 2004

Final Report

This document is available to the U.S. public
through the National Technical Information
Service (NTIS), Springfield, Virginia 22161.



U.S. Department of Transportation
Federal Aviation Administration

NOTICE

This document is disseminated under the sponsorship of the U.S. Department of Transportation in the interest of information exchange. The United States Government assumes no liability for the contents or use thereof. The United States Government does not endorse products or manufacturers. Trade or manufacturer's names appear herein solely because they are considered essential to the objective of this report. This document does not constitute FAA certification policy. Consult your local FAA aircraft certification office as to its use.

This report is available at the Federal Aviation Administration William J. Hughes Technical Center's Full-Text Technical Reports page: actlibrary.tc.faa.gov in Adobe Acrobat portable document format (PDF).

1. Report No. DOT/FAA/AR-04/5	2. Government Accession No.	3. Recipient's Catalog No.	
4. Title and Subtitle THE INVESTIGATION, EVALUATION, AND APPLICATION OF TECHNIQUES FOR CORRELATING ROTORCRAFT FULL-SCALE WATER IMPACT TESTS VERSUS ANALYSES		5. Report Date June 2004	6. Performing Organization Code
7. Author(s) Gil Wittlin and Max Gamon		8. Performing Organization Report No.	
9. Performing Organization Name and Address Dynamic Response, Inc. 15207 Valley Vista Blvd. Sherman Oaks, CA 91403		10. Work Unit No. (TRAIS)	11. Contract or Grant No. N68335-02-D-3009 (DO-0002)
12. Sponsoring Agency Name and Address U.S. Department of Transportation Federal Aviation Administration Office of Aviation Research Washington, DC 20591		13. Type of Report and Period Covered Final Report	14. Sponsoring Agency Code ANM-102N
15. Supplementary Notes The FAA William J. Hughes Technical Center Program Manager was Gary Frings. The FAA William J. Hughes Technical Center Technical Monitor was Tim Smith.			
16. Abstract <p>This report presents the results of applying various correlation techniques between aircraft water impact tests and analysis. Various relationships, such as between floor accelerations and panel pressures amplitudes or between time and frequency domains, were also investigated.</p> <p>This report describes the investigation and evaluation of several procedures considered appropriate for correlation. The investigation included frequency filtering levels, the application of modal analysis and contribution, the application of power spectral density techniques, the Huang Hilbert Spectra analysis procedure, force reconstruction techniques, and automotive industry correlation procedures.</p> <p>The conclusions, drawn from the results, indicate that the use of different correlation techniques provides a better understanding of water impact testing versus analysis.</p>			
17. Key Words SAE class filter, Modal analysis, Power spectral analysis, PSD, Force reconstruction, Hilbert Spectra, Correlation, Full-scale crash test, Analytical model, Simulation, Water impact, Rotorcraft water impact, Rotorcraft ditching		18. Distribution Statement This document is available to the public through the National Technical Information Service (NTIS) Springfield, Virginia 22161.	
19. Security Classif. (of this report) Unclassified	20. Security Classif. (of this page) Unclassified	21. No. of Pages 106	22. Price

ACKNOWLEDGEMENTS

This research was performed under an interagency agreement between the U.S. Naval Air Warfare Aircraft Division and the Federal Aviation Administration William J. Hughes Technical Center in conjunction with Small Business Innovation Research Topic Number N95-147 and Contract N68335-02-D-3009 (DO-0002). The contributions and technical support provided by Gary Frings, Timothy Smith, and Steve Soltis are gratefully acknowledged.

TABLE OF CONTENTS

	Page
EXECUTIVE SUMMARY	xiii
1. INTRODUCTION	1-1
2. BACKGROUND	2-1
3. DISCUSSION	3-1
3.1 Correlation Tolerance	3-1
3.2 Filter Frequency Effects	3-2
3.3 Application of Power Spectral Density and Modal Analysis	3-12
3.3.1 Power Spectral Density Application to FEM Test-Analysis Correlation	3-12
3.3.2 Power Spectra Density Analysis of S1 and S2 Test and KRASH Model Results	3-14
3.3.3 Modal Analysis of KRASH Models	3-20
3.4 Huang Hilbert Transform	3-35
3.5 Force Reconstruction Techniques	3-35
3.6 Automotive Industry Crashworthiness Requirements and Practices	3-38
4. ANALYSIS	4-1
4.1 Correlation Criteria	4-1
4.2 Effect of Filter Frequency on Correlation Results	4-1
4.3 Evaluation of PSD and Modal Analyses Results for Water Impact	4-10
4.3.1 Evaluation of FEM and Test PSD Analysis Correlation	4-10
4.3.2 Power Spectral Density Analysis of Test and KRASH Model Acceleration Data	4-11
4.3.3 Analysis of UH-1H KRASH S1 and S2 Modal Contributions	4-19
4.3.4 Relationship Among Acceleration Time History, PSD Analysis, and Modal Analysis	4-22
4.4 Applicability of Hilbert Spectra and HHT	4-28
4.5 Applicability of Force Reconstruction Technique	4-31
4.6 Applicability of Automotive Industry Regulations and Practices	4-32

4.7	Comparison of S1 and S2 Test and Analysis Trends	4-33
4.8	Acceleration Pressure Transfer Function Relationships	4-38
5.	SUMMARY OF KEY POINTS	5-1
5.1	Previous S1 and S2 Correlation Results	5-1
5.2	Correlation Criteria	5-1
5.3	Floor Acceleration SAE Class 60 Filter Versus SAE Class 180 Filter Versus Unfiltered Results	5-2
5.4	Panel Pressure SAE Class 60 Filter Versus SAE Class 180 Filter Versus Unfiltered Results	5-2
5.5	Power Spectral Density Analysis of Test and KRASH Analysis Data	5-3
5.6	Modal Analysis of the KRASH Model	5-3
5.7	Relationship Between Time History, PSD, and Modal Acceleration Analysis Results	5-4
5.8	Relationship of Floor Acceleration and Panel Pressure Trends to Impact Severity	5-4
5.9	Relationship of Floor Acceleration Response to Underside Panel Pressure	5-5
5.10	Other Techniques	5-5
5.11	Application of FEM PSD TAC to Helicopter Water Impact Scenarios	5-5
5.12	Automotive Industry Correlation Procedures	5-5
5.13	Potential KRASH Improvements	5-6
5.14	Test Data Gathering and Reduction Improvements	5-6
6.	CONCLUSIONS	6-1
7.	REFERENCES	7-1

LIST OF FIGURES

Figure	Page
2-1 Test S1 and S2 Water Impact Scenarios	2-1
2-2 S1 Test Airframe Line Drawing	2-2
2-3 Locations for S1 Test Pressure Transducers, Accelerometers, and Occupant Weight Slabs	2-3
3-1 Filter Effect—S1 Floor Acceleration Test, FS 155 BL 35	3-6
3-2 Filter Effect—S1 Floor Acceleration Analysis, FS 146 BL 36	3-6
3-3 Filter Effect—S1 Slab Acceleration Test, FS 155 BL 14	3-7
3-4 Filter Effect—S1 Slab Acceleration Analysis, FS 146 BL 22	3-7
3-5 Filter Effect—S1 Panel Pressure Test, FS 139 BL 37	3-8
3-6 Filter Effect—S1 Panel Pressure Analysis, FS 129-155 BL 33	3-8
3-7 Effect of Interior Surface Water Impact—S2 Slab az Analysis, FS 146 BL 21.6	3-9
3-8 Effect of Interior Surface Water Impact—S2 Floor az Analysis, FS 129 BL 0.0	3-9
3-9 Effect of Different Sample Lengths on PSD Results	3-15
3-10 Time History Associated With PSD	3-15
3-11 S1 Floor az Correlation, FS 129 BL 14, SAE Class 180 Filter	3-16
3-12 S1 Floor az Test PSD, FS 129 BL 14, Three Filtering Levels—Logarithmic Scale	3-17
3-13 S1 Floor az Test PSD, FS 129 BL 14, Three Filtering Levels—Linear Scale	3-17
3-14 S1 Floor az Analysis PSD, FS 129 BL 14, Three Filtering Levels—Linear Scale	3-18
3-15 S1 Slab az Analysis PSD, FS 116.9 BL 21.6, Three Filtering Levels—Linear Scale	3-18
3-16 S1 Floor az PSD Correlation, FS 129 BL 14	3-19
3-17 DRI/KRASH Models S1	3-20
3-18 DRI/KRASH Models S2	3-21
3-19 S1 Modal Contribution Factors to az at Slab Grid Point 300	3-26

3-20	S1 Modal Contribution Factors to az at Floor Grid Point 3100	3-26
3-21	S1 Mode Shapes at BL 14 WL 22—First Six Modes Ordered by Contribution to az at Grid Point 3100	3-29
3-22	S2 Modal Contribution Factors to az at Slab Grid Point 300	3-31
3-23	S2 Modal Contribution Factors to az at Floor Grid Point 3100	3-31
3-24	S2 Modal Contribution Factors to az at Transmission Grid Point 700	3-34
3-25	S2 Modal Contribution Factors to az at Engine Grid Point 800	3-34
4-1	Filter Effect—S1 Floor Acceleration Test, FS 102 BL 37	4-2
4-2	Filter Effect—S1 Floor Acceleration Analysis, FS 102 BL 37.2	4-2
4-3	Filter Effect—S1 Slab Acceleration Test, FS 84.5 BL 14	4-3
4-4	Filter Effect—S1 Slab Acceleration Analysis, FS 84.9 BL 14	4-3
4-5	Filter Effect—S1 Panel Pressure Test, FS 105 BL 22.75	4-4
4-6	Filter Effect—S1 Panel Pressure Analysis, FS 102-109 BL 14	4-4
4-7	Filter Effect—S1 Panel Pressure Test, FS 81.15 BL 22.75	4-5
4-8	Filter Effect—S1 Panel Pressure Analysis, FS 74-102 BL 22	4-5
4-9	Comparison of Filtered S1 Test and Analysis Floor Acceleration, FS 102 BL 37.3	4-6
4-10	Comparison of Filtered S1 Test and Analysis Panel Pressure, FS 102-109 BL 12-22.75	4-7
4-11	Comparison of Filtered S1 Test and Analysis Slab Acceleration, FS 85 BL 14	4-7
4-12	Comparison of Filtered S1 Test and Analysis Panel Pressure, FS 74-102 BL 22	4-8
4-13	Comparison of Filtered S1 Test and Analysis Slab Acceleration, FS 42-47 BL 14-22	4-9
4-14	Comparison of Filtered S1 Test and Analysis Panel Pressure, FS 23-37 BL 21-22	4-9
4-15	S1 Slab az Time History Correlation, FS 84.5 BL 14, SAE Class 180 Filter	4-12
4-16	S1 Slab az PSD Correlation, FS 84.5 BL 14, Unfiltered Linear Scale	4-12
4-17	S1 Floor az Time History Correlation, FS 102 BL 37.3, SAE Class 180 Filter	4-13

4-18	S1 Floor az Time History Correlation, FS 102 BL 37.3, SAE Class 60 Filter	4-14
4-19	S1 Floor az PSD Correlation, FS 102 BL 37.3, Unfiltered Linear Scale	4-14
4-20	S1 Floor az Time History Correlation, FS 129 BL 36.3, SAE Class 180 Filter	4-15
4-21	S1 Floor az PSD Correlation, FS 129 BL 36.3, Unfiltered Linear Scale	4-15
4-22	S1 Floor az Time History Correlation, FS 155 BL 14 and BL 20, SAE Class 180 Filter	4-16
4-23	S1 Floor az PSD Correlation, FS 155 BL 14 and BL 20, Unfiltered Linear Scale	4-16
4-24	S1 Floor az Time History Correlation, FS 155 BL 35.21, SAE Class 180 Filter	4-17
4-25	S1 Floor az PSD Correlation, FS 155 BL 35.21, Unfiltered Linear Scale	4-17
4-26	S1 Floor and Slab az Time History Correlation, FS 42-47 BL 14-22, SAE Class 180 Filter	4-23
4-27	S1 Floor and Slab az PSD Correlation, FS 42-47 BL 14-22, Unfiltered Linear Scale	4-24
4-28	S2 Floor and Slab az Time History Correlation, FS 42-60 BL 14-22, SAE Class 180 Filter	4-26
4-29	S2 Floor and Slab az PSD Correlation, FS 42-60 BL 14-22, Unfiltered Linear Scale	4-27
4-30	Acceleration 2.0-Second Time History, FS 29 BL 22, Test S1 Channel 1	4-29
4-31	Hilbert Spectrum—Frequency vs Time—0.10 Second	4-29
4-32	Detailed Hilbert 3D Spectrum—Amplitude-Frequency-Time—0.10 Second	4-30
4-33	Marginal Hilbert and Fourier Spectra—Amplitude vs Frequency	4-30
4-34	Impact Scenario Trend Comparison—Analysis vs Test—Floor and Slab—Accelerations and Underside Panel Pressures	4-36

LIST OF TABLES

Table	Page
3-1 Comparison of Opposite Side Responses—S1 Test Data	3-1
3-2 FEM Mode Shapes and Frequencies	3-2
3-3 KRASH Model Floor and Slab Weights	3-3
3-4 Effect of Filter Frequency on Peak Accelerations—Test S1	3-3
3-5 Effect of Filter Frequency on Peak Pressures—Test S1	3-4
3-6 Comparison of Peak Pressures With and Without Filters—Test S1	3-5
3-7 Effect of Filter Frequency on Peak Vertical Accelerations—Test S2	3-10
3-8 Effect of Filter Frequency on Peak Longitudinal Accelerations—Test S2	3-10
3-9 Effect of Filter Frequency on Peak Pressures—Test S2	3-11
3-10 Comparison of Peak Pressures—Test S2	3-11
3-11 S1 and S2 KRASH Model Inertia Properties	3-21
3-12 S1 and S2 KRASH Model Sizes	3-22
3-13 UH-1H Normal Modes From Krash S1 Model	3-23
3-14 UH-1H Normal Modes From KRASH S2 Model	3-24
3-15 S1 Grid Points for Modal Contribution Analysis	3-25
3-16 S1 Top 20 Modal Contributions at Grid Points 300 and 500	3-27
3-17 S1 Top 20 Modal Contributions at Grid Points 3100 and 7100	3-28
3-18 S1 Top 20 Modes at Grid 3100 Sorted by Generalized Force	3-30
3-19 S2 Grid Points for Modal Contribution Analysis	3-30
3-20 S2 Top 20 Modal Contributions at Grid Points 300 and 500	3-32
3-21 S2 Top 20 Modal Contributions at Grids 3100 and 7100	3-33
4-1 S1 Normalized Peak Acceleration Amplitudes	4-18
4-2 Relationship of KRASH S1 Flexible Modes to FEM Modes	4-20

4-3	Relationship of KRASH S2 Flexible Modes to FEM Modes	4-20
4-4	S1 Acceleration Frequency Content Comparison—Time History vs PSD Results vs Modal Contribution	4-22
4-5	S2 Acceleration Frequency Content Comparison, PSD Results vs Modal Contribution	4-28
4-6	S1 and S2 Floor/Slab Accelerations and Underside Panel Trends—SAE Class 60 vs Unfiltered	4-34
4-7	S1 and S2 Floor/Slab Accelerations and Underside Panel Trends—SAE Class 180 vs Unfiltered	4-35
4-8	S1 and S2 Acceleration to Pressure Transfer Functions	4-38

LIST OF ACRONYMS

az	Vertical acceleration
BL	Buttock lines
c.g.	Center of gravity
CFR	Code of Federal Regulations
EMD	Empirical mode decomposition
FEM	Finite element model
FFT	Fast Fourier Transform
fps	Feet per second
FS	Fuselage station
g	Gravity
HHT	Huang Hilbert Transform
IMF	Intrinsic mode function
NFFT	Number of points in a Fast Fourier Transform
NPTS	Number of data points
PSD	Power Spectral Density
SAE	Society of Automotive Engineers
SNL	Sandia National Laboratories
TAC	Test Analysis Correlation
TF	Transfer function

EXECUTIVE SUMMARY

This report describes the investigation, evaluation, and application of several procedures considered appropriate for the correlation of full-scale rotorcraft water impact tests versus analysis. Included in the evaluation are different Society of Automotive Engineers class frequency filtering levels, the application of modal analysis, frequency analysis, and modal loading contributions, the application of Power Spectral Density techniques, the Huang Hilbert Transform Spectra analysis procedure, Force Reconstruction techniques, and automotive industry correlation procedures.

Previously, two full-scale, fully instrumented water impact tests of a helicopter were performed. Analytical models were also established and their results correlated with the test results. Correlation between test and analysis results was performed to validate the models and to develop an understanding of the significance of the test measurements, the analytical representation, and the differences between the two. To gain additional confidence in the analysis for eventual application to water impact and ditching requirements, a comprehensive evaluation of available correlation procedures was required.

As a result of this effort, there is a better understanding of the previously attained test and analysis results. There is also increased confidence in the ability of the analysis to represent water impact scenarios. These results can be incorporated into future procedures for full-scale water impact tests, improved analytical models, more comprehensive correlation procedures, and helicopter water impact and ditching regulatory requirements.

1. INTRODUCTION.

Several techniques used in the correlation between full-scale crash test data and analysis data were reviewed to determine their applicability to rotorcraft full-scale water impact testing. These techniques included (1) Society of Automotive Engineers (SAE) class 60 and class 180 filters, (2) modal analysis (frequency and mode shape), (3) Power Spectral Density (PSD) analysis (4) The Huang Hilbert Transform, (5) force reconstruction, and (6) automotive industry practices. The effort described in this report is for the purpose of (1) determining which techniques or combination of techniques best provide an understanding of test and analysis results, (2) improving the level of confidence one has in analytical simulations for water impacts, and (3) providing a future opportunity to address Title 14 Code of Federal Regulations (CFR) Parts 27 and 29 aircraft water impact and ditching requirements.

Documents that are related to this issue include:

- 14 CFR Part 27: Airworthiness Standards: Normal Category Rotorcraft
- 14 CFR Part 29: Airworthiness Standards: Transport Category Rotorcraft

2. BACKGROUND.

Two water impact tests have previously been performed [1]. The first test, designated S1, was an impact at 26 feet per second (fps) vertical, 0 fps longitudinal, and 0 degree pitch with a truncated UH-1H airframe. The second test, designated S2, had impact conditions of 28 fps vertical, 39 fps longitudinal, and 4 degrees nose-up pitch, using a full UH-1H aircraft with tail section and landing skids. These impacts are shown in figure 2-1.



S1 Vertical Impact



S2 Combined Vertical-Longitudinal Impact

FIGURE 2-1. TEST S1 AND S2 WATER IMPACT SCENARIOS

Floor and mass item accelerations and underside panel pressures were measured on each test. The tests were simulated using two computer codes. One code (DRI/KRASH) creates a lumped mass model. It is referred to as a hybrid approach. The hybrid approach models large regions of structure in a simplified and approximate manner and provides for the use of empirical and semiempirical data, heuristic reasoning, and supporting analytical data. The other code (MSC/DYTRAN) creates a model using a series of small beam and plate elements; hence it is referred to as a finite element model (FEM). The hybrid KRASH model is used in all analysis provided in this report.

A line drawing of the S1 truncated airframe is shown in figure 2-2.

Figure 2-3 shows a layout of the S1 test floor accelerometer locations and fuselage underside pressure locations. Weights representing seat and occupant masses were used. These weights are referred to as slabs. Fuselage stations (FS) and buttock lines (BL) are noted. The location of KRASH model mass points for S1 and S2 test measurement locations and KRASH model data points are in section 3.

The correlation between test data and analysis data for the S1 and S2 tests included:

- Airframe underside panel pressures, failures, and time of such occurrences
- Floor acceleration responses including peak gravity (g) and time of occurrence
- Airframe kinematics behavior, center of gravity (c.g.) acceleration, c.g. velocity change, water penetration, and pitch attitude

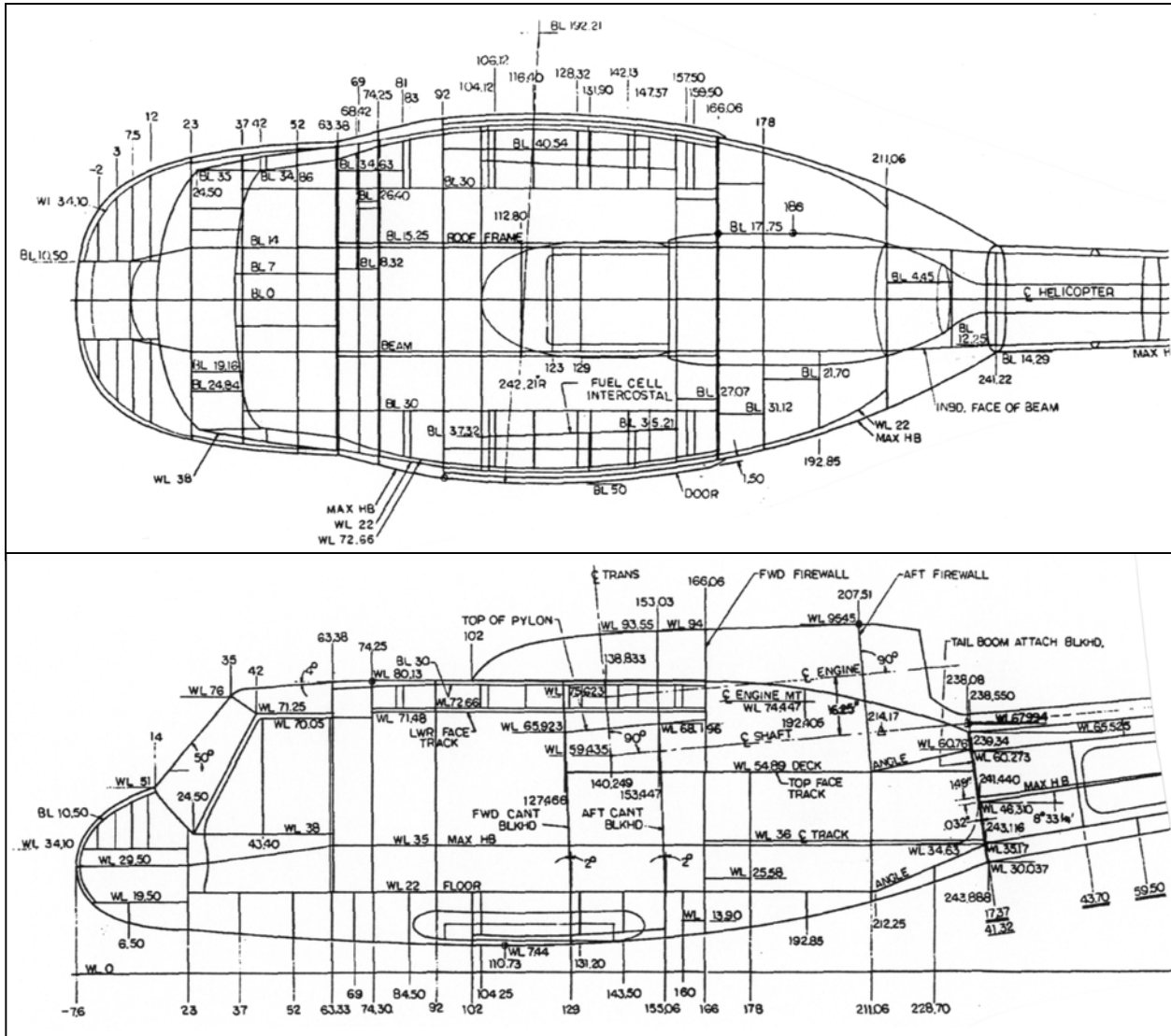


FIGURE 2-2. S1 TEST AIRFRAME LINE DRAWING

Correlation was performed in the following manner:

- Acceleration and panel pressure responses were filtered using an SAE class 180 (300 Hz) low-pass filter
- Peaks were compared on the basis of two criteria:
 1. Within $\pm 20\%$ peak value and 5 msec. of occurrence of peak
 2. Within $\pm 25\%$ peak value and 10 msec. of occurrence of peak

- Average floor and panel pressures were compared on the basis of percentage differences
- Panel damage was assessed based on observed failure (no quantitative data available to show when damage occurred) versus analytically predicted failure occurrence

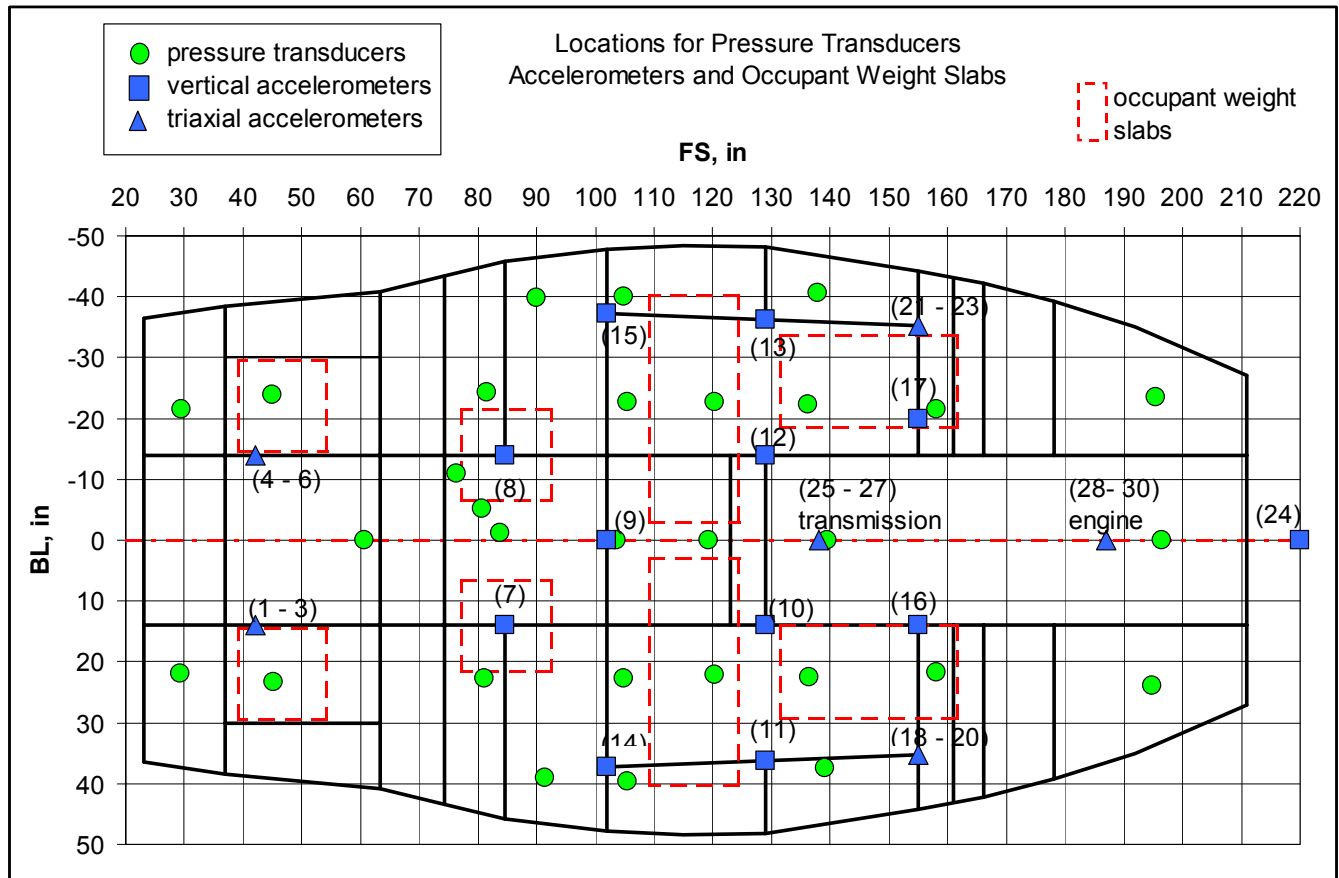


FIGURE 2-3. LOCATIONS FOR S1 TEST PRESSURE TRANSDUCERS, ACCELEROMETERS, AND OCCUPANT WEIGHT SLABS

Correlation results for S1 (26 fps sink speed), using a posttest analytical model, showed the analysis agreed with test data within the following percentages:

- c.g. vertical acceleration (az) 6.9%
- water penetration 8.3%
- c.g. velocity change 18.9%
- average floor acceleration 9.5%
- average panel pressure 8.2%

The analysis and test results were also compared with each other at various individual locations based on the looser criterion (25% and 10 milliseconds). These are referred to as discrete comparisons. The agreement for peak acceleration only and time of peak occurrence only was

41% and 78%, respectively. Simultaneous agreement of both acceleration peaks and time of peak occurrence was 33%. The corresponding discrete panel pressure agreement was 41%, 63%, and 25%, respectively. Panel failure and damage agreed both in location and failure or nonfailure and damage in about 80% of the comparisons. Based on previous accident data, the S1 test was considered moderately severe with substantial damage at about the limit of water impact survivability for civil helicopters.

The analytically determined floor acceleration pulse was 53-g peak, 0.0153-sec. rise time, and 5641 g/sec. onset rate versus a test-derived 45-g peak, 0.0135-sec. rise time, and 4245 g/sec. onset rate. The average test pressure was 30 psi versus 27 psi for the analysis.

The S2 test was a severe but survivable impact by U.S. Navy standards based on accident data. It showed substantially more severe underside panel damage. The analysis agreed with the damage assessment to a 80%-90% level. The comparisons between test and analysis were more limited in that there were only nine vertical and eight longitudinal floor accelerometers with which to compare data. The correlation was only performed with a pretest model.

The correlation results showed that the analysis agreed with the test data within the following percentages:

- c.g. longitudinal acceleration 8.3%
- c.g. az 17.6%
- average panel pressure 4.0%
- average floor az (slabs) 19.2%
- average floor az (all) 23.3%
- average floor longitudinal acceleration (slabs) 22.2%

For the S2 test discrete point comparisons, the acceleration agreement was 58%, 48%, and 25% for peak only, time only, and both peak and time of peak occurrence simultaneously, respectively. The corresponding S2 discrete point comparisons for panel pressure agreement were 47%, 63%, and 18%, respectively.

Based on average floor accelerations, the analytically determined floor az pulse was determined to be 37-g peak, 0.0143-sec. rise time, and an onset rate of 2874 g/sec. versus a test-calculated 30-g peak, 0.0180-sec. rise time, and 1667-g/sec. onset rate. For the longitudinal pulse, the oscillatory nature of both analysis and test data made for a difficult determination. Based on the c.g. acceleration, a representative analysis pulse is approximately 6-g peak with a rise time of around 0.075 sec., and a duration of 0.40 sec. Correspondingly, the test pulse can be characterized as a 7-g peak, 0.040-sec. rise time, and 0.35-second duration. The average test pressure is 34.4 psi versus 35.4 psi from the analysis.

The S2 test experienced some slab restraint failures that were not in the analytical model. The analysis also assumed some secondary internal water impact that may not have occurred during the test.

3. DISCUSSION.

3.1 CORRELATION TOLERANCE.

A summary of the S1 test opposite side-measured test peak accelerations and pressures is shown in table 3-1. From this data, it can be seen that the measured floor acceleration and pressure peak responses vary from left side to right side. The difference varies anywhere from less than 1% to as high as 63%. On average, the difference between opposite sides is from 20.3% to 22.5%. The time of peak occurrence for opposite side measurements (not shown) generally occurs within less than a 2-millisecond difference, and at most, less than 8 milliseconds. The closeness of the peak time of occurrence supports the notion that the impact is symmetrical. The test is by all accounts symmetrical. Among possible reasons for differences between opposite side measurements are (1) variation in structure, (2) location of pressure transducers relative to intended location because of obstructions, and (3) effective mass associated with mounting location of accelerometers.

TABLE 3-1. COMPARISON OF OPPOSITE SIDE RESPONSES—S1 TEST DATA

Acceleration							Pressure						
Ch No.	FS	BL	Left Side	Right Side	Peak g	% Variation	Ch No.	FS	BL	Left Side	Right Side	Peak psig	% Variation
							1	29.25	22			21.78	
							2	29.25	-21.6			33.63	
							Avg.	1&2		21.78	33.63	27.71	21.4%
1	42	14			54.09		3	45.25	23.25			26.49	
4	42	-14			62.96		4	45	-24			71.41	
Avg.	1&4		54.1	63	58.53	7.6%	Avg.	3&4		26.49	71.41	48.95	45.9%
7	84.5	14			27.19		6	81.15	22.75			25.49	
8	84.5	-14			27.21		10	81.5	-24.3			34.31	
Avg.	7&8		27.2	27.2	27.2	0.00	Avg.	6&10		25.49	34.31	29.9	14.7%
							11	91.5	39.13			21.24	
							12	90	-39.8			7.25	
							Avg.	11&12		21.24	7.25	14.25	49.1%
14	102	37.3			89		14	104.9	22.65			61.67	
15	102	-37			55.6		16	105.5	-22.8			52.12	
Avg.	14&15		89	55.6	72.3	23.1%	Avg.	14&16		61.67	52.12	56.90	8.4%
							13	105.5	39.6			22	
							17	104.8	-40.1		58	11.44	
							Avg.	13&17		22	11.44	16.72	31.6%
10	129	14			71.96		18	120.38	22.15			22.83	
12	129	-14			41.04		20	120.25	-22.8			20.88	
Avg.	10&12	14	72	41	56.5	27.4%	Avg.	18&20		22.83	20.88	21.86	4.5%
11	129	36.3			174.5		21	139.1	37.52			33.37	
13	129	-36			39.34		25	137.76	-40.7			21.26	
Avg.	11&13		174	39.3	106.9	63.2%	Avg.	21&25		33.37	21.26	27.32	22.2%
16	155.06	14			17.98		22	136.5	22.5			35.03	
17	155.06	-20			30.8		24	136.25	-22.3			33.84	
Avg.	16&17		18	30.8	24.39	26.3%	Avg.	22&24		35.03	33.84	34.44	1.7%
18	155.06	35.2			39.34		28	194.75	23.9			15.1	
21	155.06	-35			32		30	195.5	-23.6			16.35	
Avg.	18&21		39.3	32	35.67	10.3%	Avg.	28&30		15.1	16.35	15.73	4.0%

3.2 FILTER FREQUENCY EFFECTS.

Filtering of the response frequency has merit when one considers the fact that the normal modes of significance are generally much less than 100 Hz. For example, the first 11 flexible modes of the FEM models that are available to represent the S1 and S2 test articles are shown in table 3-2. The range of frequencies for different modes, shown in table 3-2, includes fuselage bending, fuselage torsion, engine, transmission pylon, and landing gear skid modes. All the modes shown are below 23 Hz.

TABLE 3-2. FINITE ELEMENT MODEL MODE SHAPES AND FREQUENCIES

Mode No.	Latest FEM (engine) Frequency (Hz)	Initial FEM (no engine) Frequency (Hz)	Description
7	3.37	3.28	Pylon roll ¹
8	3.61	3.31	Pylon pitch ¹
9	6.71	6.45	Fuselage 1 st lateral
10	8.51	7.72	Fuselage 1 st vertical
11	13.64	-----	Engine lateral
12	15.27	14.50	Landing gear lateral
13	16.14	14.74	Landing gear vertical
14	17.40	15.27	Fuselage 2 nd vertical
15	21.38	18.43	Fuselage torsion
16	21.95	16.55	Fuselage 2 nd lateral
17	22.93	22.36	Landing gear pitch
	-----	9.94, 20.7, 24.7	Other landing gear modes

¹ Pylon supports the main rotor around the transmission weight = 8577 lb.

Most major mass items on their supports, i.e., engine, transmission, occupant/seat, and fuel/fuel cell installation fall into a low-frequency (<25 Hz) regime. Thus, the use of an SAE class 60 filter (cutoff frequency of 100 Hz) is appropriate for these particular items.

The use of unfiltered data and SAE class 180 data is also valuable in the clarification of pulse definition and velocity change as well as for failure assessment.

The use of class 60 or 180 filters in lieu of SAE class 60 or 180 filters may also be used throughout the report.

When comparing test and analysis data, consideration has to be given to the weights associated with the test and analytical model. The analytical model represents occupant/seat systems as lumped masses ranging in weight from 260 to 650 lb., depending on how many occupants are being represented. These masses are referred to as slabs. Other than discrete masses to represent known mass items (engine and transmission), the remaining aircraft structure is represented by a series of lighter weights. The weights associated with the KRASH model mass locations mentioned throughout this report are noted in table 3-3.

TABLE 3-3. KRASH MODEL FLOOR AND SLAB WEIGHTS

Slab Model Mass No.	Slab Weight (lbs.)	Floor Model Mass No.	Floor Weight (lbs.)
3	260.0	31	11.0
4	260.0	41	9.0
5	520.0	51	11.0
6	650.0	61	9.0
		62	11.6
		71	5.3
		72	7.8
		81	6.3
		82	9.0

The slab weights were intended to match the weights that were added to the test to represent the seats and occupants at various locations. The weights at the other floor locations were intended to be representative of the weight distribution provided in mass data for the aircraft.

The S1 and S2 test data and the corresponding KRASH model pressure and acceleration data were organized so that unfiltered, class 180 filter, and class 60 filter results were obtained. The results for the S1 test are shown in tables 3-4 and 3-5 for the accelerations and panel pressures, respectively. From the data in table 3-4 it can be seen that when measurements are taken on relatively heavy mass items, such as slabs, the filtering of the response has very little effect on the results. This is also true of the analysis results. From accelerometer channel locations on slabs, the effect of class 60 versus 180 filtering is about 10% and even less on model masses 3, 4, 5, and 6. However, the floor measurements show extremely high effects. When comparing class 60 to class 180 filtered results, the changes are easily 50% or more.

TABLE 3-4. EFFECT OF FILTER FREQUENCY ON PEAK ACCELERATIONS—TEST S1

Channel Number	TEST DATA							KRASH ANALYSIS DATA						
	FS	BL	Peak g's			% Diff. 60 vs 180	Comment	Mass Number	FS	BL	Peak g's			% Diff. 60 vs 180
			Unfilt	SAE 180	SAE 60						Unfilt	SAE 180	SAE 60	
1	42	14	207.8	54	42.1	22	floor	3	46.7	22	55.3	56.2	55.0	2
4	42	-14	254.3	63	45.0	29	floor	31	42	14	293	142.1	68	52
7	84.5	14	28.5	27.2	25.2	7	slab	4	84.9	14	59.8	59.8	59.8	0.0
8	84.5	-14	29.6	27.2	24.6	10	slab	51	84.9	14	288	126.5	62	51
14	102	37.3	234.1	89	35.5	60	floor	62	102	37.2	147.3	60.9	33.2	45
15	102	-37.3	302.6	55.6	28.2	49	floor	62	102	-37.2	147.3	60.9	33.2	45
10	129	14	155.9	72	16.6	77	floor	71	129	14	394	62	56	-10
11	129	36.3	521.1	175	64.8	63	floor	72	129	36	163.6	77.6	56	28
12	129	-14	219.8	41	17.8	57	floor	5	117	21.6	37.2	37.2	36	3
13	129	-36.3	152.6	39.3	19.1	51	floor							
16	155.06	14	20.6	18	16.4	9	slab	6	146	21.6	36.3	36.3	36.3	0
17	155.06	-20	36.9	30.8	20.8	32	slab	81	146	14	508	70.3	37	47
18	155.06	35.21	309.1	39.3	16.1	59	floor	82	146	36	193.8	80.8	42	48
21	155.06	-35.21	177.3	31.9	14.0	56	floor							
24	241	0	14.1	11.8	11.8	0	slab	120	241	0	16.0	15.9	15.9	0

TABLE 3-5. EFFECT OF FILTER FREQUENCY ON PEAK PRESSURES—TEST S1

TEST DATA						KRASH ANALYSIS DATA							Estimated Allowable psi
Channel Number	Lower Surface FS	Skin Contour BL	Peak Pressure - psig			Lift Surface No.	Mass No.	FS range	BL center	Peak Pressure - psig			
			Unfilt	SAE 180	SAE 60					Unfilt	SAE 180	SAE 60	
1	FS23-30 29.25	BL±22 22	24.0	21.8	3.0	2	21	23-37	21	27.8	27.8	25.0	25-42
2	29.4	-21.6	46.0	33.6	18.8	2	21	23-37	21	27.8	27.8	25.0	
AVG			35.0	27.7	10.9	AVG				27.8	27.8	25.0	
3	FS 45-60 45.25	BL±24 23.25	149.0	26.0	23.6	4	31	37-63	21	11.5	11.5	10.0	24-40
4	45	-24	169.0	71.0	33.3	4	31	37-63	21	11.5	11.5	10.0	
AVG			159.0	48.5	28.5	AVG				11.5	11.5	10.0	
5	FS45-60 60.63	BL0.0 0	29.0	25.0	19.0	3	30	37-63	0	11.6	11.6	10.0	24-30
AVG.			29.0	25.0	19.0	19	41	68.3	0	34.0	32.0	28.0	
						AVG				22.8	21.8	19	
6	FS76-84 81.15	BL±24 22.75	34.0	25.6	24.0	6	51	74-102	22	26.0	26.3	24.0	35-40
10	81.5	-24.25	40.0	34.0	28.5								
AVG	81.25		37.0	29.8	26.3	AVG		88		26.0	26.3	24.0	
7	FS76-84 83.75	BL0.0 -1.18	34.0	14.4	12.0	5	50	74-102	0	21.8	21.8	15.0	34-40
9	76.25	-11	18.0	22.6	17.0	17	40	63-74	0	17.0	17.0	16.4	
AVG	80		26.0	18.5	14.5	AVG		82		19.4	19.4	15.7	
11	FS90-95 91.5	BL±40 39.13	25.0	22.0	9.2	7	52	74-102	36	9.9	9.8	10.0	21-28
12	90	-39.75	13.0	7.0	6.2	7	52	74-102	-36	9.9	9.8	10.0	
AVG			19.0	14.5	7.7	AVG				9.9	9.8	10.0	
13	FS105 105.5	BL±40 39.6	77.0	22.0	22.0	10	62	102-129	33	15.6	15.5	15.5	21-28
14	104.8	-40.7	14.0	11.0	8.0								
15	104.9	22.65	69.0	61.0	36.7								
16	105.5	-22.75	53.0	50.0	32.3	9	61	102-109	14	27.0	27.0	26.0	21-35
AVG	FS105		53.3	36.0	24.8	AVG		115		21.3	21.3	20.8	
18	FS120 120.38	BL±22 22.15	26.0	22.5	18.7	9	61	102-129	14	27.0	27.0	27.0	21-35
20	120.25	-22.75	26.0	21.0	14.2	10	62	102-129	33	15.6	15.6	14.2	
AVG	FS120.3		26.0	21.8	16.5	AVG		FS115		21.3	21.3	20.6	
21	FS136-140 139.1	BL±40 37.52	42.0	33.0	20.0	13	82	129-155	33	18.3	18.2	17.0	30-66
25	137.76	-40.67	33.0	21.0	15.2								
AVG	FS138.5		37.5	27.0	17.6	AVG				18.3	18.2	17.0	
22	FS136-140 136.5	BL±24 22.5	162.0	35.0	21.0	12	81	129-155	14	45.9	45.9	45.0	25-40
24	136.25	-22.25	42.0	34.0	15.0								
AVG	FS136.25		102.0	34.5	18.0	AVG				45.9	45.9	45.0	
26	FS158-166 158	BL±22 21.75	140.0	89.0	46.5	20	91	155-166	23	91.5	91.5	85.0	60-80
27	158	-21.5	149.0	80.0	34.6	20	91	155-166	-23	91.5	91.5	85.0	
AVG	FS158		144.5	84.5	40.6	AVG		FS160.5		91.5	91.5	85.0	
28	FS166-211 194.75	BL±24 23.9	68.0	15.0	3.4	15	103	166-211	21	11.3	11.3	11.0	14-17
29	196.5	-23.6	58.0	16.3	3.7	15	103	166-211	-21	11.3	11.3	11.0	
30	195.5	0	25.0	6.0	5.0	14	100	166-211	0	9.4	9.4	9.0	
AVG	196		50.3	12.4	4.0	AVG				10.7	10.7	10.3	

Table 3-5 provides a comparison of the test and analysis data between unfiltered, class 60, and class 180 filtered pressure responses. The test data for the most part indicates sharp responses whose peak value is significantly affected by filtering. The test measurements are obtained using a pressure transducer with a small area imbedded in the lower fuselage skin surface. Thus, the pressures obtained are more localized. By way of contrast, the analysis pressures developed in KRASH tend to be of longer duration than the test pressures and are unaffected by filtering.

The use of a class 60 filter may not be appropriate for pressures. As is the case for airframe forces causing structural failure, panels under water impact force fail due to the force they experience. Filtering is a postprocessing technique that does not influence failure pressures. Table 3-5 shows that if the test data were subjected to a class 60 filter, the pressures associated with panel failures would be unduly reduced and the wrong interpretation could be given to the overall pressure. Whether unfiltered or class 180 filters for test data are appropriate is difficult to say. From the KRASH analysis results there is no difference. With test data filtered to 300 Hz, the overall test pressure is lower (29 psi) than the unfiltered pressure (47 psi), as noted in table 3-6. Intuitively, one would think from a failure perspective that unfiltered pressures are appropriate. How one compares test-measured pressure and analytically determined pressure is a point to be considered. This is discussed further in section 4.

TABLE 3-6. COMPARISON OF PEAK PRESSURES WITH AND WITHOUT FILTERS—TEST S1

Lower Surface FS	Skin Contour BL	Unfiltered			SAE Class 180 Filtered			SAE Class 60 Filtered			Estimated Allowable psi
		Test	KRASH Analysis	Analysis -Test	Test	KRASH Analysis	Analysis -Test	Test	KRASH Analysis	Analysis -Test	
23-30	±22	35.0	28.0	-20.0%	28.0	28.0	0.0%	11.0	25.0	127.3%	40
45-60	0.0	29.0	22.8	-27.2%	25.0	21.8	-12.8%	19.0	19.0	0.0%	
76-84	±24	37.0	30.0	-18.9%	30.0	29.0	-3.3%	26.0	24.0	-7.7%	40
76-84	0.0	26.0	19.0	-26.9%	19.0	19.0	0.0%	15.0	16.0	6.7%	40
90-95	±40	19.0	10.0	-47.4%	15.0	10.0	-33.3%	8.0	10.0	25.0%	35
105	±40	53.0	16.0	-69.8%	36.0	16.0	-55.6%	25.0	16.0	-36.0%	35
120	±22	26.0	21.0	-19.2%	22.0	21.0	-4.5%	16.0	21.0	31.3%	35
120.38	22.15	26.0	27.0	3.8%	22.5	27.0	20.0%	18.7	27.0	44.4%	35
120.25	-22.75	26.0	15.6	-40.0%	21.0	15.6	-25.7%	14.2	14.2	0.0%	35
136-140	±40	38.0	18.0	-52.6%	27.0	18.0	-33.3%	18.0	17.0	-5.6%	40
136-140	±24	102.0	46.0	-54.9%	35.0	46.0	31.4%	36.0	45.0	25.0%	40
158-166	±22	145.0	92.0	-36.6%	85.0	92.0	8.2%	41.0	85.0	51.8%	80
166-211	±24	50.3	10.7	-78.7%	12.4	11.0	-11.3%	4.0	10.3	157.5%	17
Average		47.1	27.4	-41.8%	29.1	27.3	-6.2%	21.0	27.5	30.8%	39

Figures 3-1 through 3-6 illustrate the time histories associated with floor accelerations, slab accelerations, and panel pressures. Figures 3-1 and 3-2 illustrate the sensitivity of the peak response to filtering for a floor analysis and a corresponding test response, respectively.

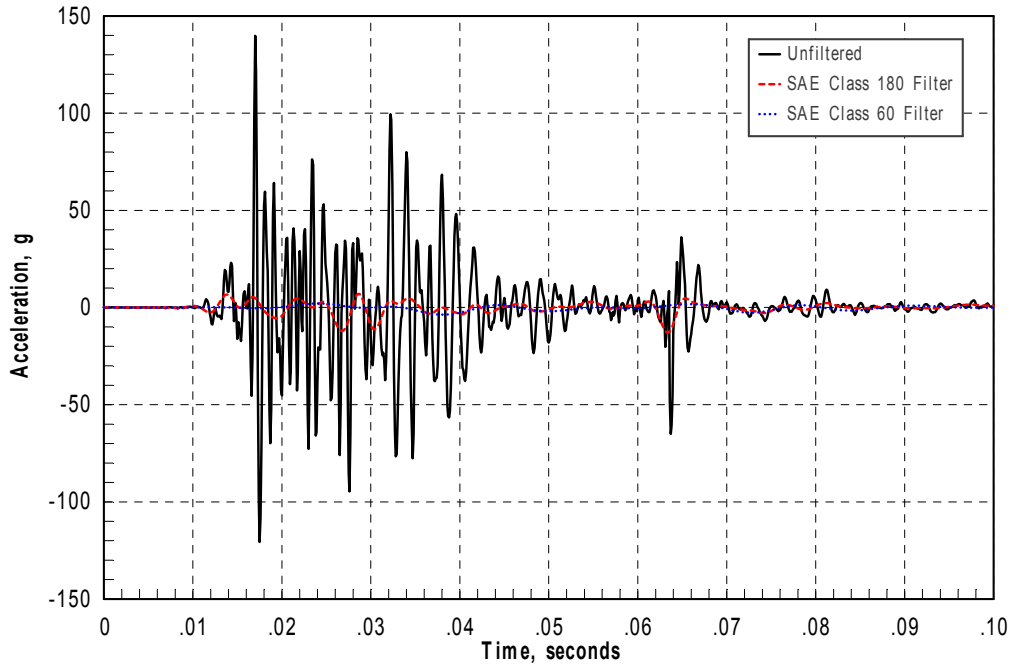


FIGURE 3-1. FILTER EFFECT—S1 FLOOR ACCELERATION TEST, FS 155 BL 35

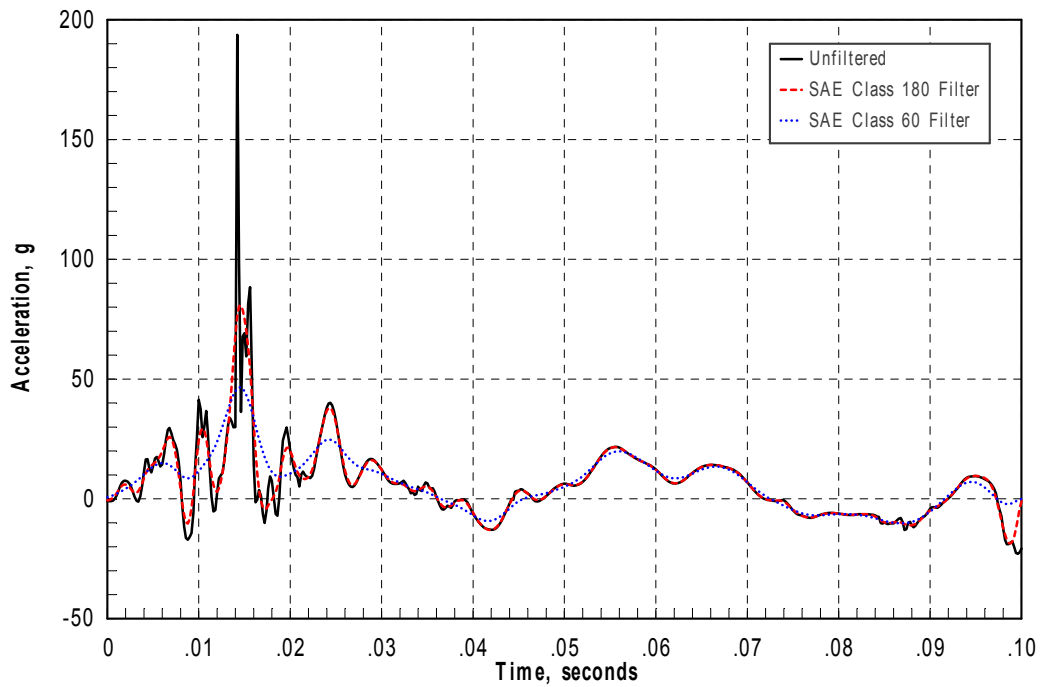


FIGURE 3-2. FILTER EFFECT—S1 FLOOR ACCELERATION ANALYSIS, FS 146 BL 36

Figures 3-3 and 3-4 illustrate that the filtering has little effect on peak response for a slab analysis and a corresponding test response, respectively.

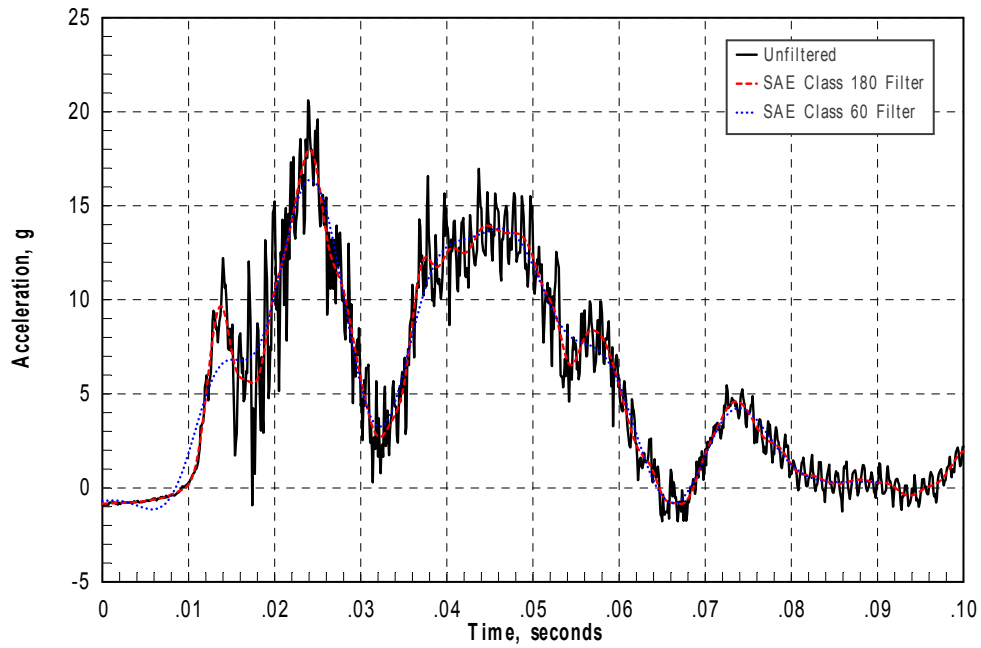


FIGURE 3-3. FILTER EFFECT—S1 SLAB ACCELERATION TEST, FS 155 BL 14

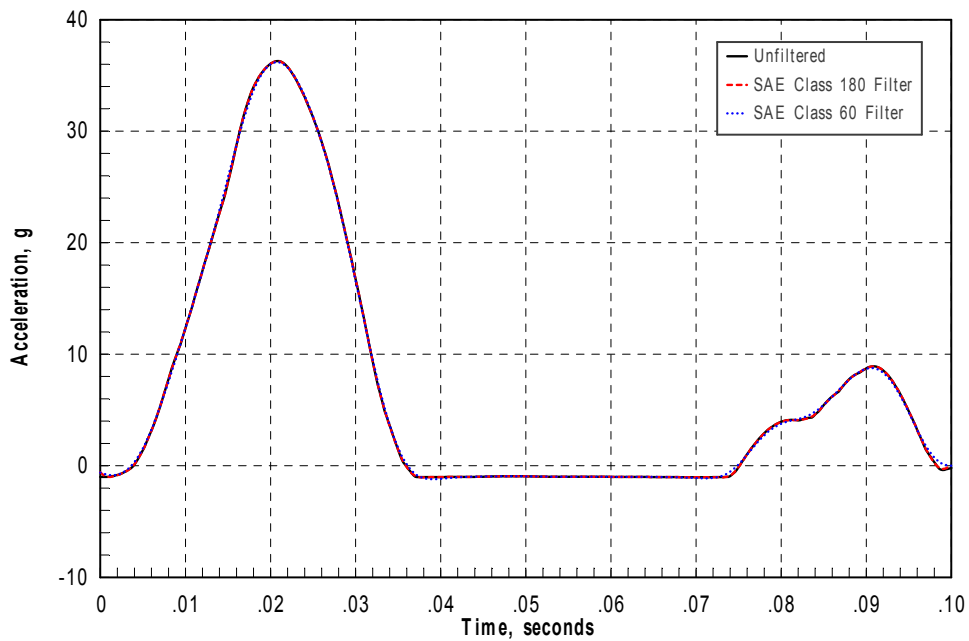


FIGURE 3-4. FILTER EFFECT—S1 SLAB ACCELERATION ANALYSIS, FS 146 BL 22

Figures 3-5 and 3-6 illustrate the effect of class filtering for a panel pressure analysis and a test response, respectively. The analysis response is not sensitive to filtering, whereas the test response exhibits sensitivity to the filter level.

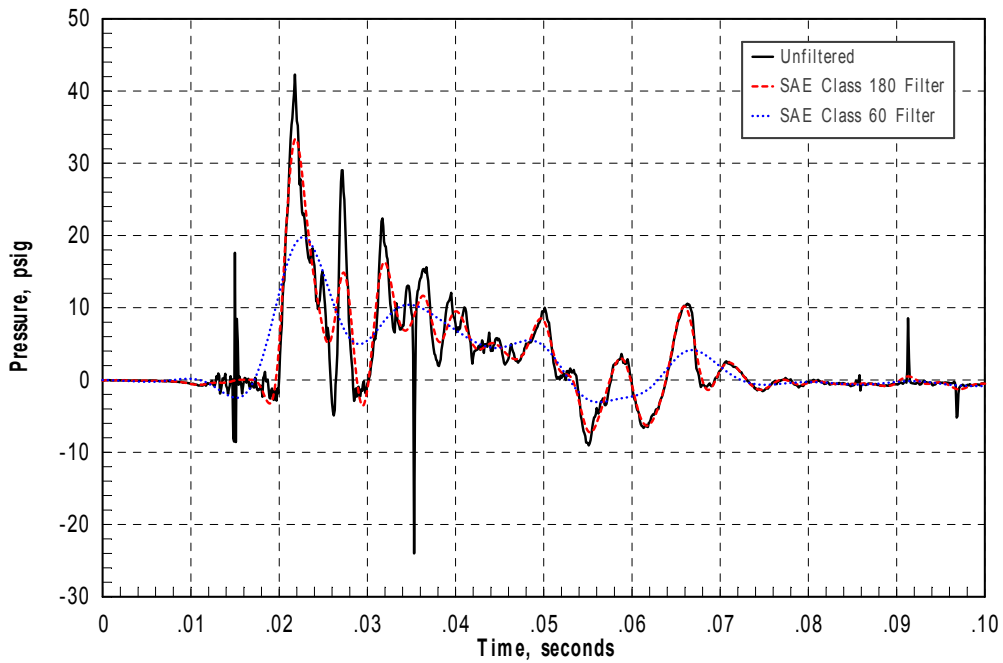


FIGURE 3-5. FILTER EFFECT—S1 PANEL PRESSURE TEST, FS 139 BL 37

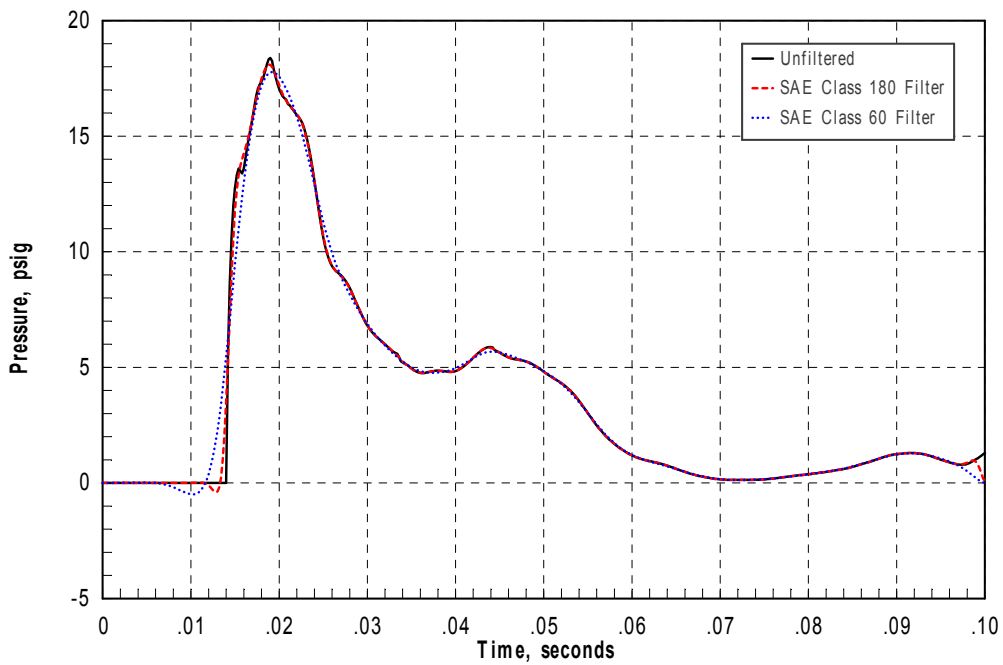


FIGURE 3-6. FILTER EFFECT—S1 PANEL PRESSURE ANALYSIS, FS 129-155 BL 33

The effect of filtering for the combined velocity impact condition, test S2, was also reviewed. Since the analysis showed some postimpact underside panel interior impacts to the floor (secondary impacts), which are not observed in the test data, the S2 model was modified to minimize or reduce this occurrence. The effect of this change on the az response is illustrated in figures 3-7 and 3-8. Some responses can be altered due to secondary impacts. Figure 3-7 clearly shows that the secondary impact is significant for the slab location shown. However, the response at the floor location shown in figure 3-8 is not as affected due to the secondary impact. For the purpose of evaluating filter frequency as a factor in the interpretation of the responses, the revised S2 model was used since secondary impacts during the test are considered not to have occurred to any significant degree.

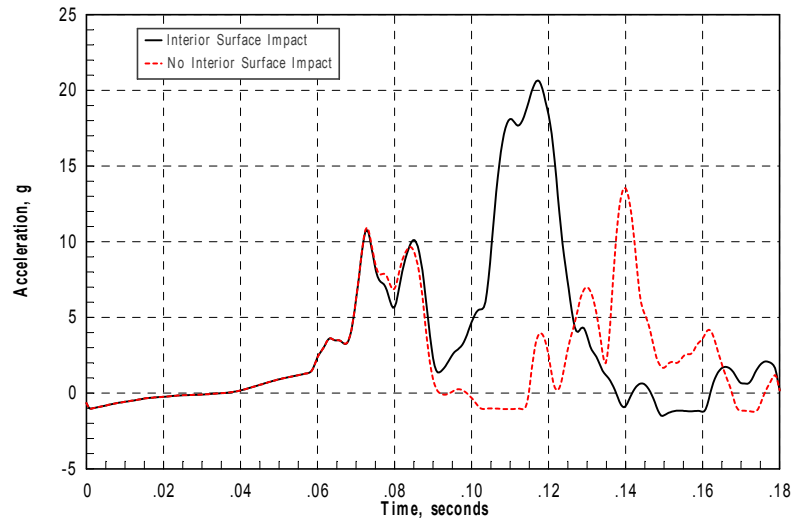


FIGURE 3-7. EFFECT OF INTERIOR SURFACE WATER IMPACT—S2 SLAB AZ ANALYSIS, FS 146 BL 21.6

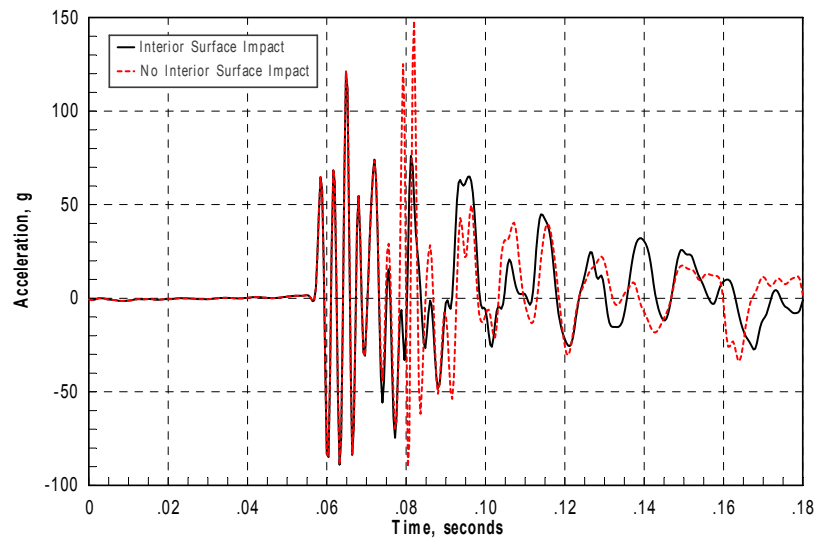


FIGURE 3-8. EFFECT OF INTERIOR SURFACE WATER IMPACT—S2 FLOOR AZ ANALYSIS, FS 129 BL 0.0

Summary results for the S2 floor az and longitudinal acceleration are shown in tables 3-7 and 3-8, respectively. The pressure results are shown in tables 3-9 and 3-10. Table 3-10 shows, like in the S1 summary, the average unfiltered test pressure is as high as 63 psi. The unfiltered analysis overall pressure is 39 psi.

TABLE 3-7. EFFECT OF FILTER FREQUENCY ON PEAK VERTICAL ACCELERATIONS—TEST S2

Channel Number	TEST DATA							KRASH ANALYSIS DATA							
	FS	BL	Peak g's			% Diff. 60 vs 180	Comment	Mass Number	FS	BL	Peak g's			% Diff. 60 vs 180	Comment
			Unfilt	SAE 180	SAE 60						Unfilt	SAE 180	SAE 60		
1 4	FS 42 pilot/co		32.6	27.5	24.9	9.5%	slab	3	60	22	43.9	43.9	43.2	1.6%	slab
	55	22													
	55	-22													
7 9	FS 93.62 fwd troop		32.2	28.6	26.2	8.4%	slab	4	85	14	53.1	53.1	51.8	-2.4%	slab
	93.62	14.81													
	93.62	-14.81													
11 15 18 13	FS 121 mid troop		201	71.6	25.0	65.1%	floor	70	129	0	297	148.2	36.3	75.5%	floor
	121.25	0													
	132.5	19.75													
	132.5	-19.75													
	121.5	-35													
19 22	FS 149 aft troop		24.2	18.1	17.2	5.0%	slab	6	146	22	36.3	36.2	36.2	-6%	slab
	149.5	19.75													
	149.5	-19.75													
Average				22.7									37.5		

TABLE 3-8. EFFECT OF FILTER FREQUENCY ON PEAK LONGITUDINAL ACCELERATIONS—TEST S2

Channel Number	TEST DATA							KRASH ANALYSIS DATA							
	FS	BL	Peak g's			% Diff. 60 vs 180	Comment	Mass Number	FS	BL	Peak g's			% Diff. 60 vs 180	Comment
			Unfilt	SAE 180	SAE 60						Unfilt	SAE 180	SAE 60		
3 6 Avg.	FS 42 pilot/co		21	11.5	9.9	14%	slab	3	60	22	22.0	20.5	19.0	7%	slab
	55	22													
	55	-22													
8 10 Avg.	FS 93.62 fwd troop		13.3	10	7	30%	slab	4	85	14	15.1	12.9	10.7	-17.1%	slab
	93.62	14.81													
	93.62	-14.81													
12 17 Avg.	FS 121 mid troop		181	25.5	5.9	77%	floor	70	129	0	16	15.2	14.5	5%	floor
	121.25	0													
	132.5	19.75													
21 24 Avg. Floor	FS 149 aft troop		24.2	6.5	4.7	28%	slab	6	146	22	11.7	10.4	9.8	-6%	slab
	149.5	19.75													
	149.5	19.75													
			22.1	5.6	4.5	9%	slab	6	146	22	11.7	10.4	9.8	-6%	slab

TABLE 3-9. EFFECT OF FILTER FREQUENCY ON PEAK PRESSURES—TEST S2

TEST DATA						KRASH ANALYSIS DATA							Estimated Allowable psi				
Channel Number	Lower Surface FS	Skin Contour BL	Peak Pressure - psig			Lift Surface No.	Mass No.	FS range	BL center	Peak Pressure - psig							
			Unfilt	SAE 180	SAE 60					Unfilt	SAE 180	SAE 60					
1	FS40-50 46	BL±22 23.2	58.2	40.2	17.6	3	30	42	0	23.4	23.2	22.8	30-40				
			154	83.5	42.7					30.4	30.2	30.0					
4	FS60-90 83.5	BL±24 22.5	29.6	23.3	19.4	6	51	84.5	14	39.6	37.4	33.4	30-40				
			27.9	24.0	17.2					39.9	39.2	38.5					
7	FS 89.5 89.5	BL±40 40	11.6	9.3	4.5	7	52	84.5	30	44.4	37.6	25.6	35-45				
			249	109	54.6					44.4	37.6	25.6					
9	FS105 105	BL±40 40	53.1	50.0	43.1	10	62	102	37.3	62.5	63.7	52.5	35-65				
			45.9	29.1	18.4					9	61	102		14	35	35	35
			37.3	27.0	12.5					10	62	102		37.3	62.5	63.7	53
14	FS120 120.3	BL±22 22	81.5	42.8	30.1	13	82	138	35	65.5	60.0	47.0	35-66				
			29	23.5	15.2					11	80	138		0	35	35.0	35.0
			20.4	17.5	9.3					13	82	138		35	65.5	60.0	47.0
17	FS143-158 143	BL±40 37	33.5	28.5	18.0	13	82	138	35	65.5	60.0	47.0	40-66				
			47.5	35.1	21.2					12	81	138		14	40	40	40
			18.1	17.6	15.3					12	81	138		-14	40	40	40
			120.	47.8	23.4					13	82	138		-35	65.5	60.0	47.0
			52.5	43.9	31.1												
			66.5	50.1	34.5												
			115.	68.7	39.9												
28	FS166-211 194	BL±24 26	17.6	11.1	9.7	15	103	192	14	17.0	17.0	17.0	14-35				
			21.9	16.2	8.5					15	103	192		-14	17.0	17.0	17.0
										16	110	211		0	24.4	20.7	20.2
										14	100	192		0	33.8	29.2	12.8
AVG			58.7	36.3	22.1					42.6	40.3	34.3					

TABLE 3-10. COMPARISON OF PEAK PRESSURES—TEST S2

Lower Surface FS	Skin Contour BL	Unfiltered Peak Pressure			SAE 180 Filtered Peak Pressure			SAE 60 Filtered Peak Pressure			Estimated Allowable Pressure	
		Test	KRASH Analysis	Analysis Test	Test	KRASH Analysis	Analysis Test	Test	KRASH Analysis	Analysis Test	min	max
40-60	±22	106.3	26.9	-74.7%	61.9	26.7	-56.9%	30.2	26.4	-12.6%	30	40
60-90	±24	79.5	42.1	-47.0%	41.6	38.0	-8.7%	23.9	30.8	28.9%	30	40
105-120	±40	44.5	54.3	22.0%	31.6	52.5	66.1%	21.4	44.4	107.5%	35	64
143-158	±37	64.9	46.3	-28.7%	41.7	43.3	3.8%	26.2	38.7	47.7%	40	65
166-211	±26	19.8	23.1	16.7%	13.7	21.0	53.3%	9.1	16.8	84.6%	14	35
Average		63	39	-38.8%	38.1	36.3	-4.7%	22.2	31.4	41.8%	30	48.8

The analysis shows about 86% of the panels failed, which is consistent with the severity of the test. When one compares the average pressures from test S1 (table 3-6) and test S2 (table 3-10), the latter values are about 30% higher for both test and analysis, particularly for the class 180 filtered and more so for the unfiltered results.

The S2 results are similar to the S1 results in the following respects:

- Filter frequency has less of an effect on slab-measured or analyzed acceleration responses than on lighter weight floor responses.
- The use of class 60 filtering improves the correlation at floor locations where lightweight masses exist, but does not materially change the correlation for slab locations.
- The KRASH panel pressures are less sensitive to filter frequency than the test panel pressures.

3.3 APPLICATION OF POWER SPECTRAL DENSITY AND MODAL ANALYSIS.

3.3.1 Power Spectral Density Application to FEM Test-Analysis Correlation.

The Test-Analysis Correlation (TAC) procedure using PSD analysis [2] is described for the purpose of achieving the ability to better quantify the accuracy of crash simulation results generated by nonlinear, transient dynamic, and finite element codes. The following is a discussion of the TAC results from reference 2.

TAC is considered for comparison of peak loads, pressures, accelerations, time histories of acceleration, velocity and displacement, gross motion of the vehicle, components and human surrogates, and other parameters. To accurately diagnose and address TAC issues, greater understanding of the structure is needed, and TAC in the frequency domain can provide much of the missing knowledge. TAC in both the time and frequency domains will together form a robust assessment of model fidelity and provide cleaner indications of model and test deficiencies that will facilitate understanding and correction of issues.

The approach to evaluate the TAC technique is as follows:

- Conduct evaluation on the as-is test versus analysis correlation.
- Streamline and automate the data reduction of test data and analysis to create a situation that is tenable for large heavily instrumented tests and for simulations that produce channels of interest. To accomplish this current data acquisition, equipment and new signal-processing techniques will be applied to test data and to finite element results for structural test specimens. TAC will be conducted on two categories of structural specimens: (1) elemental metallic beam and plate structures that are being evaluated under carefully controlled impact conditions and (2) composite energy-absorbing fuselage section.

- Following the understanding of the correlation of test and finite element results, current standards will be evaluated for suitability and recommendations will be developed as required.
- Proven signal-processing techniques will be applied to quantify correlation of large-scale crash simulation results with test results.
- Perform FEM analysis to simulate the tests.

Applications have been performed with elemental beam specimens, where the test matrix consisted of steel versus aluminum, flat versus T-section, pinned-roller versus pinned-pinned, and flat versus stiffened plate specimens.

Tests were conducted so that (1) no permanent deformation occurred and (2) moderate deformation occurred. Tests were based on symmetry, repeatability, and modal and frequency domains. PSD or Fourier Transforms (on unfiltered strain data) was performed.

For drop tests in either the elastic and inelastic behavioral range, the lower frequencies (36, 120, and 220 Hz) were exhibited in the PSD with appropriate phasing. Preliminary conclusions from reference 2 are:

- Free vibration modes for the test are matched with the FEM.
- For modal comparison, the impact or forced portion of the test data must be cropped away.
- Even with rigorous control over instrumentation and test parameters, some experimental deviation will occur. Quantification and understanding of experimental deviation is important in understanding correlation.
- Free vibration results were repeatable. Some higher frequencies of interest are eliminated with an SAE-J211 class 60 filter.

In addition, substructure testing in both the elastic (3 fps) and inelastic (25.3 fps) range was performed using a composite energy-absorbing fuselage section (six frames) with geometrically simple structure. For the test in the elastic range, the Fourier Transform of the raw unfiltered acceleration data provided frequency domain data said to compare well, but not perfectly, with MSC-DYTRAN analysis modal frequencies.

In the inelastic test, the frequency of the lower mode was reduced from approximately 25 to 20 Hz compared to the first test, as expected. However, more effort is required to develop means and criteria to identify similar modes between elastic and inelastic modeling. The test showed that (1) inadvertent roll and pitch changes could be induced and (2) some channels may exhibit additional peaks and valleys not observed in other channels, which was attributed to structural responses relative to small pitch and roll at impact. In addition, these tests raised many questions about which data should be used in correlation and what criteria should be used. In addition,

questions arose with regard to whether the evaluation should include (1) effect of mass that the accelerometer is mounted on, (2) lateral symmetry, (3) filtering rates, and (4) data acquisition strategies.

Other considerations that are being followed in this continuing research are:

- Time history comparison and assessment of qualification for each channel
- Frequency domain comparison for each channel
- Assessment of phasing with mode shape
- Assessment of suitability of correlating forced response MSC-DYTRAN results with forced response test results
- Quantify test variation
- Evaluate elastic mode as an aid in modeling

Analyses of these and other results are discussed in section 4.3.1.

3.3.2 Power Spectral Density Analysis of S1 and S2 Test and KRASH Model Results.

PSD analysis was applied to the hybrid model and S1 and S2 test data. The following are the results of that application.

Figures 3-1 through 3-4 show that filtering can affect the amplitude of the acceleration response, depending on the location at which a test or analysis response is obtained. If one were trying to define a pulse, at some locations that is difficult without filtering. At other locations, namely at heavy mass items, the pulse shape and amplitude are relatively unaffected by filtering. Thus, the application of PSD analysis included investigating the effects of filtering in the comparison between time and frequency domain. In addition, the effects of sample rate and sample size on PSD results were evaluated. For the PSD analysis, a representative set of test and analysis acceleration responses at or near FS 129 BL 14 are used.

The effect of different sample lengths is shown in figure 3-9. This is for test channel 10, with PSDs calculated with unfiltered data for time spans of 0.1, 0.2, and 1.0 second. The basic pulse is contained in 0.1 second (see the time history in figure 3-10, showing the first 0.3 second). The longer sample lengths cause the PSD to decrease in amplitude across the frequency range, since the overall average acceleration is lower.

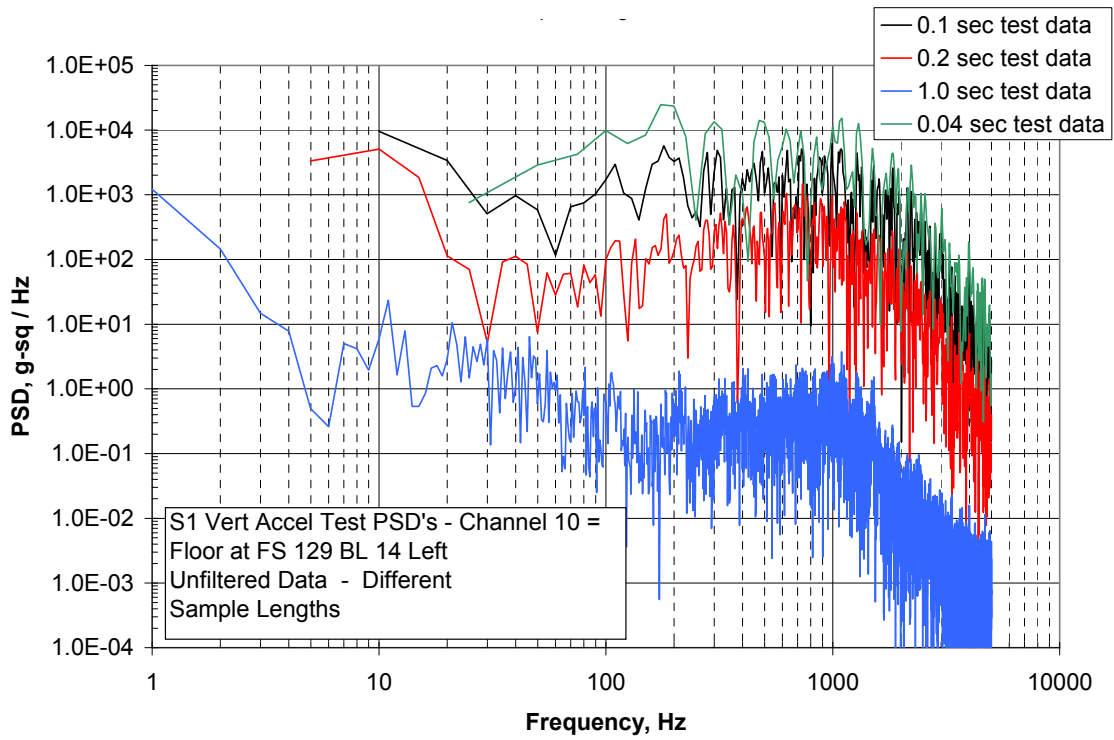


FIGURE 3-9. EFFECT OF DIFFERENT SAMPLE LENGTHS ON PSD RESULTS

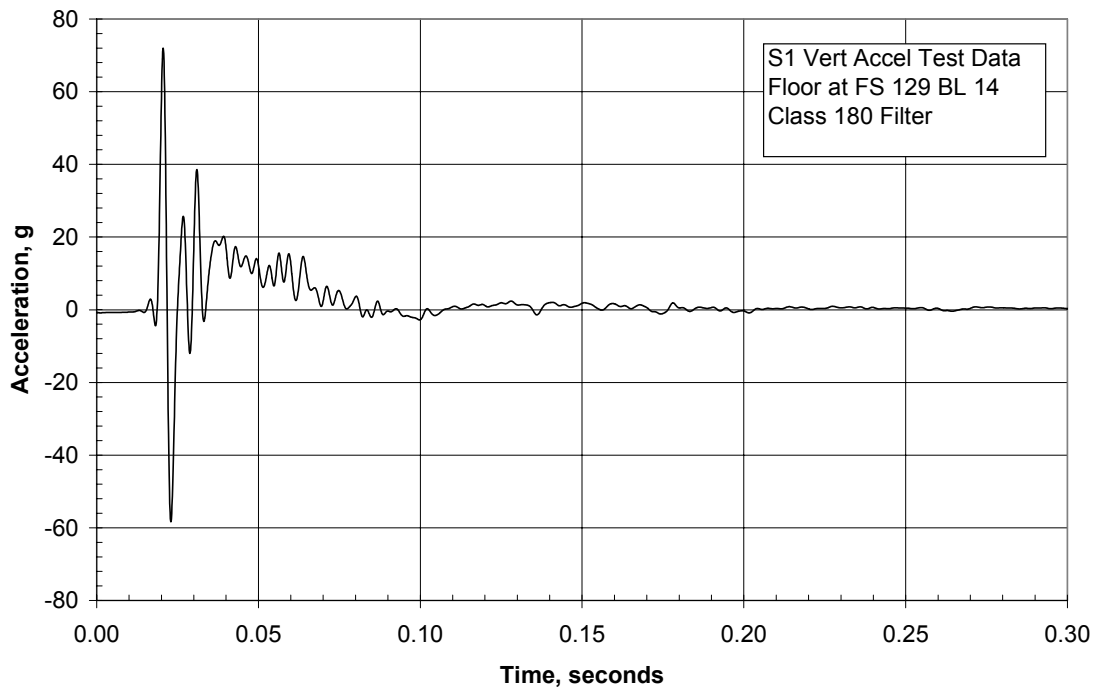


FIGURE 3-10. TIME HISTORY ASSOCIATED WITH PSD

The longer time span, or sample length, allows calculating the PSD to a lower frequency, down to 1 Hz for a 1.0-second sample length. The 0.2-second sample length appears to give good resolution of the PSD in the 10-400-Hz frequency range compared to the 0.1-second sample length, while the 1-second sample provides hashy results above 30 Hz or so. So, the 1-Hz resolution seems to be too fine, while the 5-Hz resolution that goes with the 0.20-second sample length gives the best results in terms of readability.

The maximum frequency for the PSD is one-half the sample rate. In this case, the test data sample rate is 10,000 Hz (time interval = 0.0001 second), so the maximum PSD frequency is 5000 Hz. The analysis data with a time interval of 0.0002 has a sampling rate of 5000 Hz or samples/sec. The minimum PSD frequency, which is also equal to the resolution or step size or spacing, is the inverse of the sample length. So, for the sample lengths of 0.1, 0.2, and 1.0 second, the PSD minimum frequencies are 10, 5, and 1 Hz. These relationships are only true if the total number of data points (NPTS) is used for the number of points in a Fast Fourier Transform (NFFT) parameter in the PSD calculation. It is possible to use a lower value for NFFT, which causes a higher minimum frequency for the PSD. In fact, the minimum frequency is actually $1/NFFT$ rather than $1/NPTS$. In the published test results, $NFFT = 512$ was used, causing the minimum frequency to be around 20 Hz. One might want to change this to get more resolution.

The test and analysis responses using the class 180 filter are shown in figure 3-11. For the responses at this particular floor location, PSD results as a function of filter frequency are noted in figures 3-12 (logarithmic amplitude scale) and 3-13 (linear amplitude scale) for the test data.

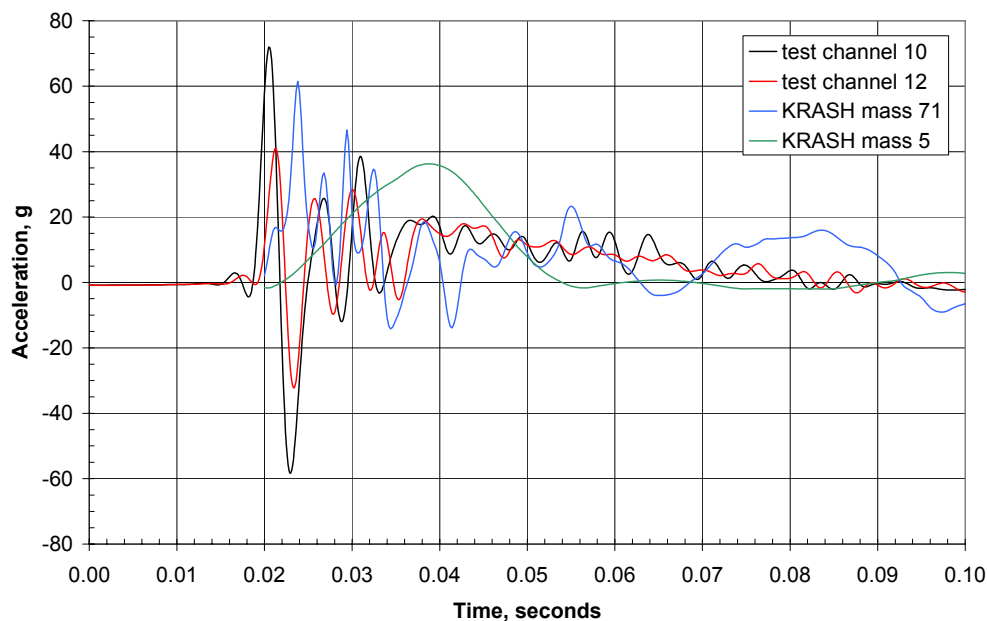


FIGURE 3-11. S1 FLOOR AZ CORRELATION, FS 129 BL 14, SAE CLASS 180 FILTER

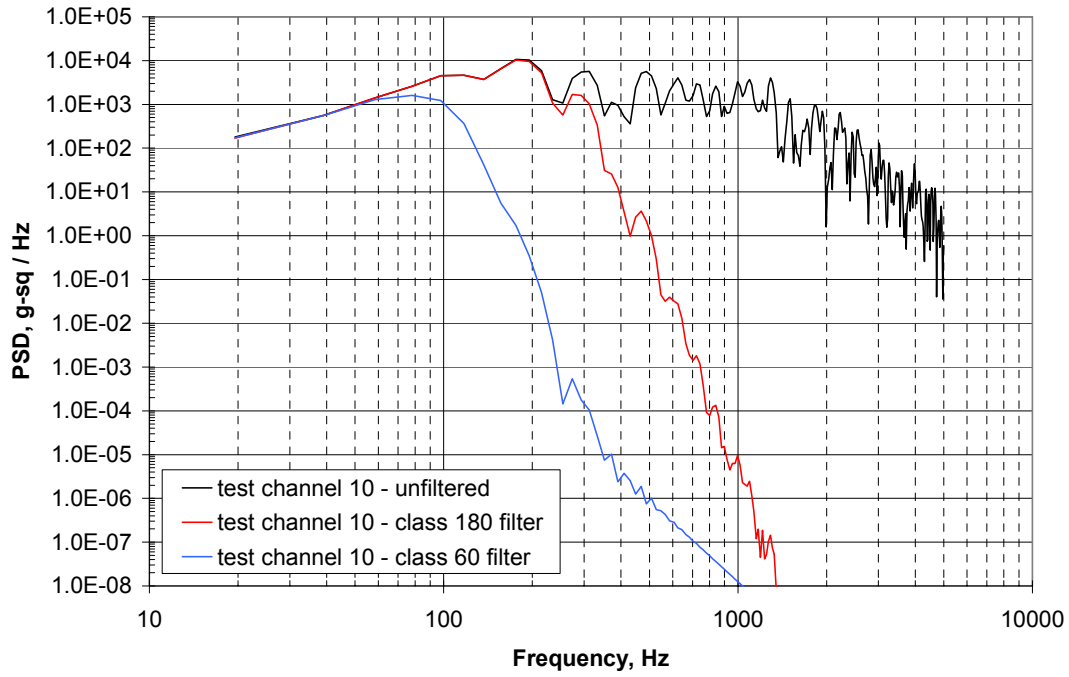


FIGURE 3-12. S1 FLOOR AZ TEST PSD, FS 129 BL 14, THREE FILTERING LEVELS—LOGARITHMIC SCALE

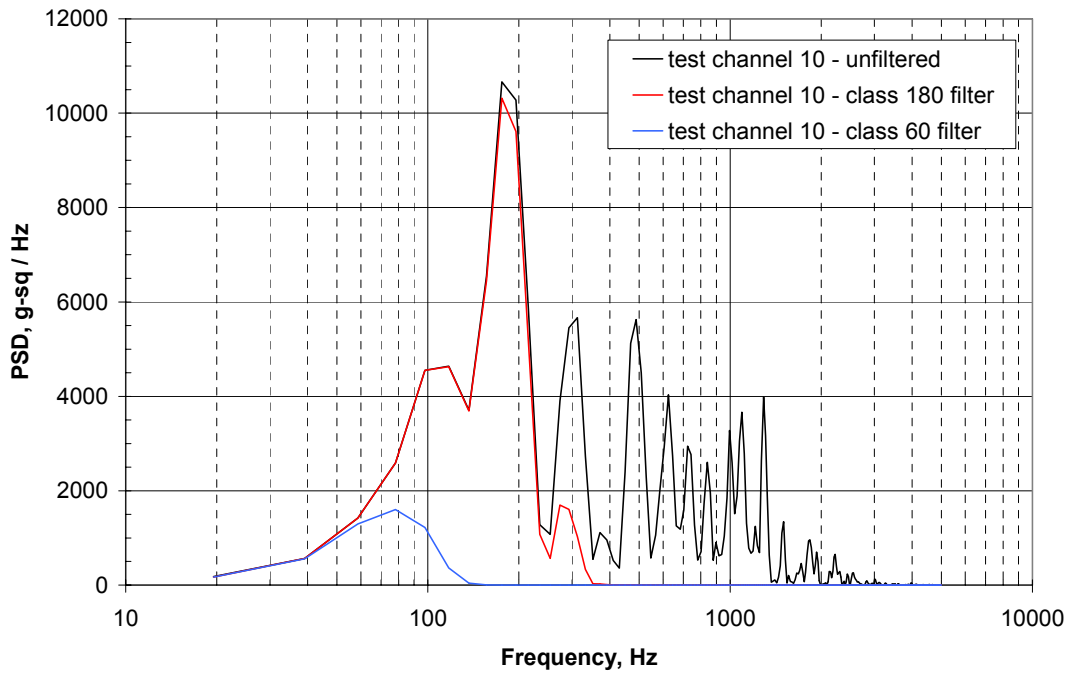


FIGURE 3-13. S1 FLOOR AZ TEST PSD, FS 129 BL 14, THREE FILTERING LEVELS—LINEAR SCALE

Figure 3-14 presents linear PSD data for the KRASH analysis results at a floor location of a light floor weight (8 lb.), whereas figure 3-15 presents linear PSD analysis of KRASH data at a nearby heavy mass (650 lb.) slab location.

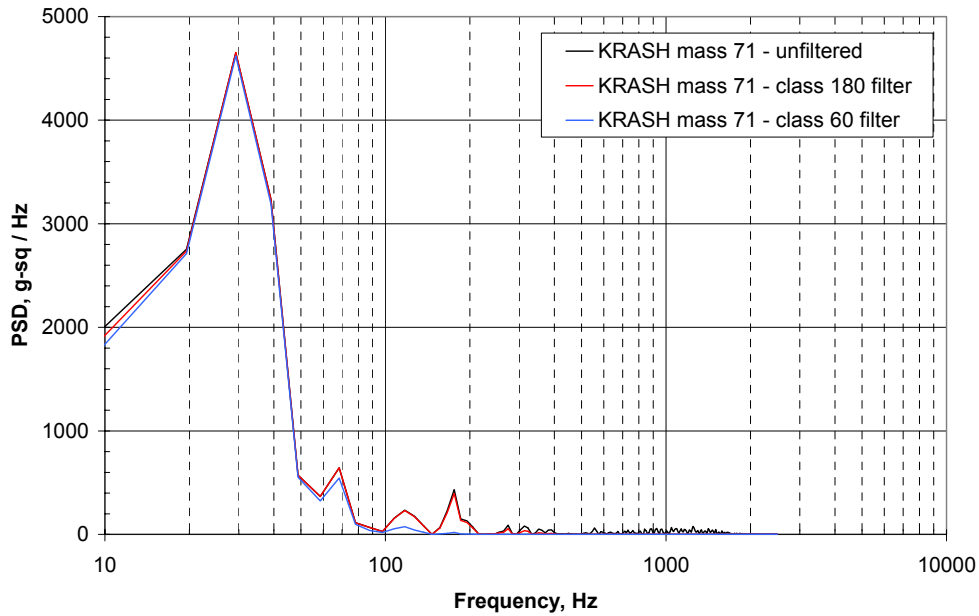


FIGURE 3-14. S1 FLOOR AZ ANALYSIS PSD, FS 129 BL 14, THREE FILTERING LEVELS—LINEAR SCALE

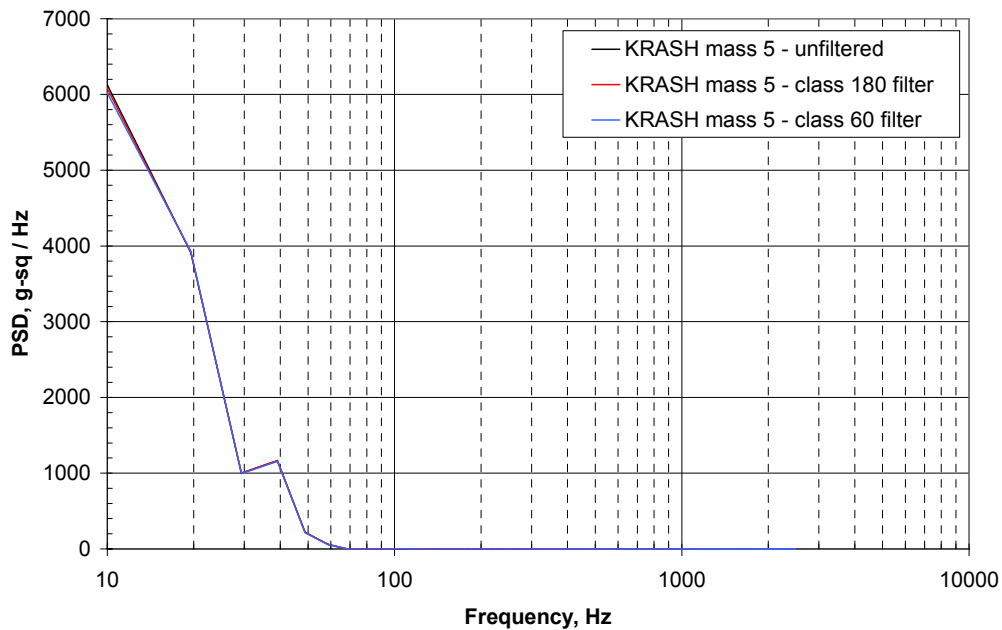


FIGURE 3-15. S1 SLAB AZ ANALYSIS PSD, FS 116.9 BL 21.6, THREE FILTERING LEVELS—LINEAR SCALE

It can be observed that

- filtering, as expected, eliminates or minimizes the amplitude contribution from frequencies above the cutoff frequencies of 300 and 100 Hz for class 180 and class 60 filters, respectively.
- the linear amplitude scale provides a better opportunity than the logarithmic amplitude scale to see the contributing frequencies.
- the analysis results tend to show more of a lower-frequency (< 100 Hz) contribution. This is more apparent at the heavier weight slab location than at the lighter weight floor location.
- PSD results of the S1 test data fails to show amplitudes associated with frequencies less than 20 Hz, due to lack of sampling duration, so any comparisons with analysis data should be for data above 20 Hz.

A comparison of the test and analysis PSD data for the FS 129 location using linear scaling and unfiltered data is shown in figure 3-16. The figure shows that the KRASH slab mass 5 provides much of its energy below 30 Hz, the KRASH floor mass 71 contributes in the range of 30 Hz, and the test floor response contributes more at 100 Hz and above. For the PSD results in figure 3-16, the test data was analyzed with NFFT = 512, rather than NFFT = NPTS = 1000. So, the minimum frequency and resolution are both around 20 Hz. If an NFFT of 1000 were used, a minimum frequency and resolution of 10 Hz would have resulted.

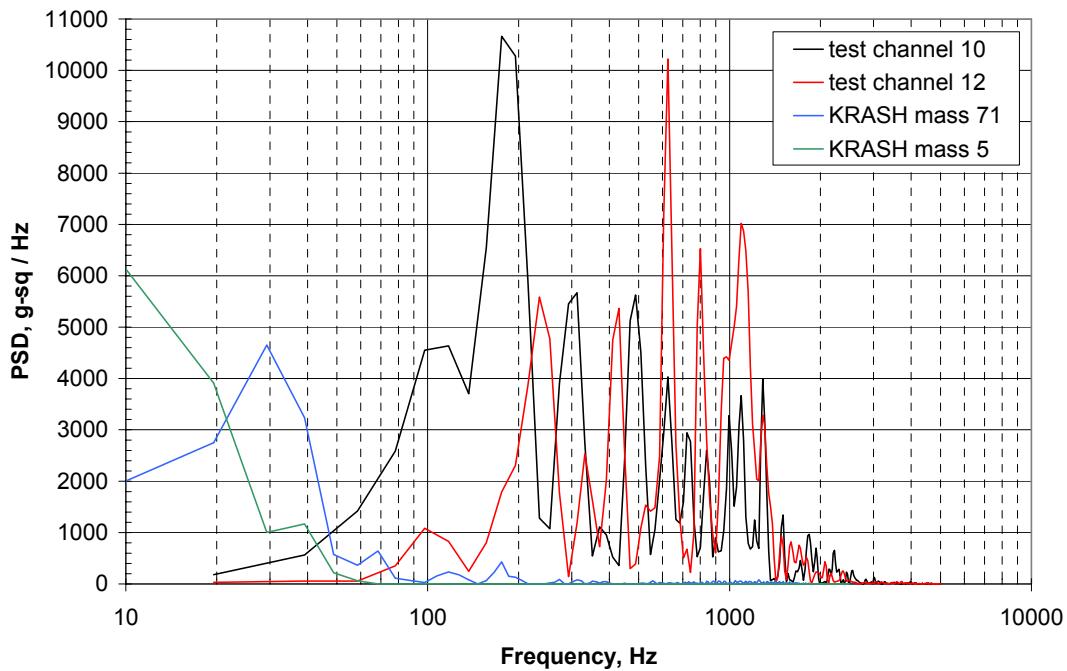


FIGURE 3-16. S1 FLOOR AZ PSD CORRELATION, FS 129 BL 14

The analysis data also used NFFT = 512, which is almost equal to the NPTS (501), resulting in a minimum frequency and resolution of around 10 Hz. Also of interest is the difference in contribution from the opposite test sides. While they exhibit many similar frequencies, the peak amplitudes are at different frequencies. The right side amplitude is about half the left side amplitude, which does coincide with the amplitude difference in the time history plot (figure 3-11).

In performing a PSD analysis, one must bear in mind that this technique is generally applicable to free vibration analysis. What is shown in crash impact testing is a primary pulse or series of pulses. One should be able to deduce what primary and secondary frequencies exist from the time histories of the acceleration. To this extent, modal analysis (along with time histories and PSD analyses) may help to understand the test and analysis results.

A comprehensive evaluation of PSD results is provided in section 4.3.2.

3.3.3 Modal Analysis of KRASH Models.

The two analytical models, denoted S1 and S2, are shown in figures 3-17 and 3-18. The S1 model represents a test configuration without a tail and with steel masses representing the engine and transmission. A steel plate at the aft end of the cabin structure represents the tail weight. The S2 test configuration includes the tail, engine, transmission, and rotor hub, as well as landing skids. Both configurations use steel plates to represent the weight of the seats and occupants. Neither configuration accounted for fuel. The inertia properties for the two configurations are shown in table 3-11.

V2

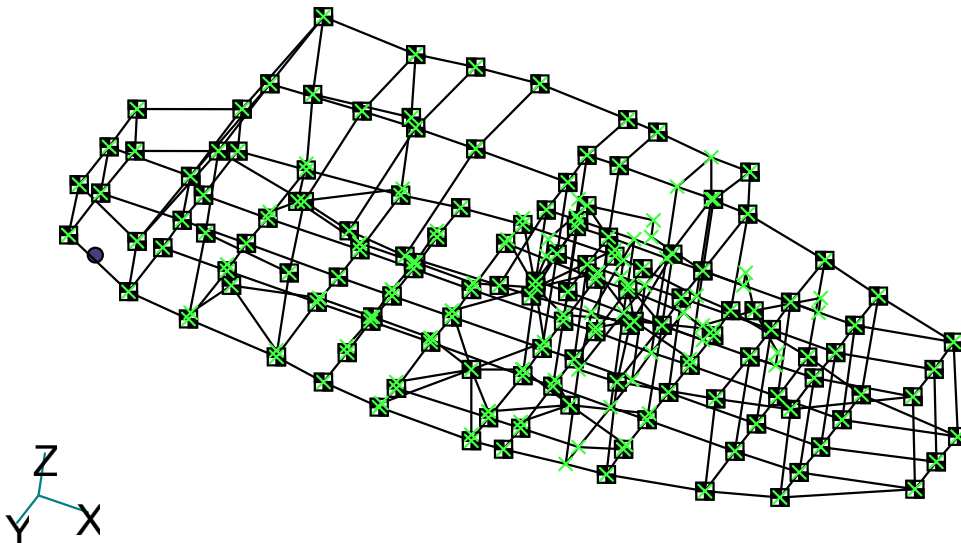


FIGURE 3-17. DRI/KRASH MODELS S1

V2

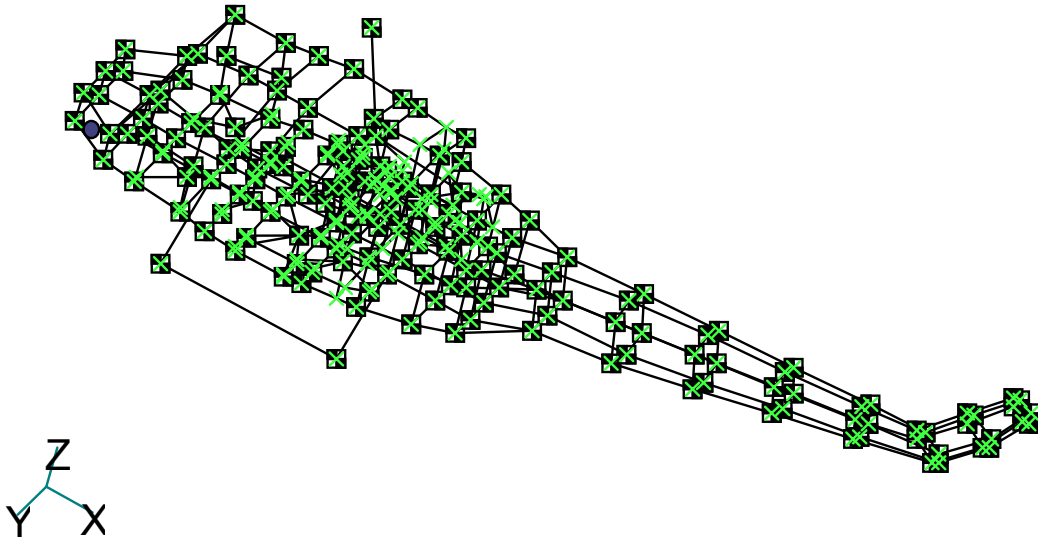


FIGURE 3-18. DRI/KRASH MODELS S2

TABLE 3-11. S1 AND S2 KRASH MODEL INERTIA PROPERTIES

	S1	S2
Wt	7571	7955
FScg	134.76	143.64
BLcg	0.00	0.00
WLcg	41.68	46.34
Ix	18643	36692
Iy	75749	171082
Iz	75647	154884
Izx	6535	18005

In order to perform a modal analysis, the KRASH model was converted to a linear NASTRAN model. The NASTRAN model includes CBAR elements to represent the linear characteristics of the KRASH beams, CONM2 elements to represent the concentrated inertia properties of the KRASH lumped masses, and grid points to represent the mass and node point location geometry. For example, NASTRAN grid points 300 and 3100 represent KRASH masses 3 and 31, respectively.

The KRASH model sizes for these two configurations are shown in table 3-12, along with the corresponding NASTRAN sizes.

TABLE 3-12. S1 AND S2 KRASH MODEL SIZES

	S1	S2
DRI/KRASH		
masses	135	182
node points	78	84
beams	319	415
NASTRAN		
grid	213	266
conm2	135	182
cbar	319	415

Both models are symmetrical full-vehicle models. The NASTRAN models are then used to calculate normal modes for both configurations. For each configuration, 500 modes are calculated, all normalized to unit generalized mass. For the S1 model, the modal frequencies range from 6.0 to 275 Hz, while for the S2 model, they range from 3.0 to 165 Hz. The presence of the tail section in the S2 model lowers the frequency range relative to the S1 model.

Table 3-13 shows a summary of the first 20 flexible modes for the S1 model, while table 3-14 shows the same results for the S2 model. For the S2 model, the addition of the skids generates a number of modes with significant skid motion. The S2 results in table 3-14 are considered more representative of a normal UH-1H, since the S1 model lacks a tail, skids, and an actual engine and transmission.

The purpose of this study is to identify which normal modes contribute significantly to the responses of interest, which are the az's at selected floor locations and large mass items such as the engine and transmission. The methodology for modal selection is based on an approximation of the generalized force and its effect on the responses of interest. For each normal mode, the governing dynamic equation is

$$F_i \cong M_i \ddot{q}_i \quad (3-1)$$

where

- F_i = Generalized force for i^{th} normal mode
- M_i = Generalized mass for i^{th} normal mode
- \ddot{q} = Generalized acceleration for i^{th} normal mode

TABLE 3-13. UH-1H NORMAL MODES FROM KRASH S1 MODEL

Mode	Frequency (Hz)	Symmetrical	Description
1	6.05	yes	Fuselage vertical bending
2	8.49	no	Fuselage torsion
3	9.93	no	Fuselage lateral bending and torsion
4	10.58	yes	Fuselage vertical bending—transmission vertical
5	10.79	yes	Fuselage vertical bending—transmission vertical
6	11.39	no	Fuselage lateral bending and torsion
7	11.91	yes	Forward fuselage vertical bending
8	12.06	no	Fuselage lateral bending—tail torsion
9	12.58	yes	Fuselage vertical bending—floor slab vertical
10	13.00	no	Forward fuselage vertical bending—transmission
11	13.03	no	Forward fuselage vertical—aft fuselage torsion
12	13.72	no	Fuselage vertical and lateral bending—floor slab vertical
13	13.90	no	Roof vertical—floor slab and transmission vertical
14	14.60	no	Roof lateral
15	14.70	no	Roof vertical and lateral
16	15.22	no	Roof and forward fuselage torsion
17	15.49	no	Fuselage torsion, lateral and vertical bending
18	16.18	no	Windshield lateral—floor slab vertical
19	16.68	no	Tail vertical bending—engine/transmission vertical
20	16.87	yes	Fuselage vertical bending—transmission vertical

Equation 3-1 ignores the contribution of the generalized stiffness and damping terms, which is a valid simplification for the purpose of modal selection. The actual az at any grid point (k) is given by

$$az_k = \sum_{i=1}^N v_{ik} q_i \quad (3-2)$$

where

v_{ik} = Eigenvector for vertical direction at grid point k for the i^{th} mode

The summation in equation 3-2 is over the total number of modes N . The generalized force in equation 3-1 is given by

$$F_i = \sum_{j=1}^M v_{ij} F a_j \quad (3-3)$$

TABLE 3-14. UH-1H NORMAL MODES FROM KRASH S2 MODEL

Mode	Frequency (Hz)	Symmetrical	Description
1	3.01	yes	Tail vertical bending
2	3.56	no	Tail lateral bending
3	3.92	yes	Fuselage and tail 1 st vertical bending—rotor mast fore-aft
4	5.39	no	Fuselage torsion and lateral bending
5	7.45	no	Fuselage torsion and tail rotor lateral
6	7.79	yes	Fuselage and tail 2 nd vertical bending
7	9.56	no	Fuselage torsion and tail lateral bending
8	10.36	no	Fuselage torsion and tail lateral bending and torsion
9	10.93	yes	Fuselage and tail 3 rd vertical bending
10	11.53	yes	Fuselage and tail 4 th vertical bending
11	14.06	no	Fuselage vertical/lateral bending—engine, trans, skids
12	15.07	no	Forward fuselage torsion—skids
13	15.46	no	Forward fuselage torsion—skids fore-aft and lateral
14	15.60	no	Engine/trans vertical—skids fore-aft and lateral
15	15.89	no	Skids lateral and vertical
16	16.05	no	Fuselage lateral bending—skids fore-aft
17	16.20	no	Fuselage lateral bending—skids fore-aft—trans vertical
18	16.39	yes	Skids fore-aft
19	16.53	yes	Fuselage vertical bending—skids and engine fore-aft
20	17.00	no	Fuselage lateral and vertical bending—skids and engine fore-aft

The summation in equation 3-3 is over all the applied force locations j , with M applied forces Fa_j , and v_{ij} is the eigenvector for mode i , location j . Combining equations 3-1 and 3-2, one develops the following expression for az_k

$$az_k = \sum_{i=1}^N v_{ik} \frac{F_i}{M_i} \quad (3-4)$$

The combination of equations 3-3 and 3-4 allows one to estimate the contribution of each normal mode to the total az_k at k . Since the modes are normalized to unit generalized mass, the M_i term in equation 3-4 can be ignored (set to 1.0). The resulting equation for the i^{th} modal contribution to az_k is

$$az_{ik} = v_{ik} \sum_{j=1}^M v_{ij} Fa_j \quad (3-5)$$

Once again, the subscripts are i for mode, j for applied force location (ranging from 1 to M), and k for acceleration location.

The applied forces Fa_j are approximated as follows:

- S1—Assume uniform vertical forces over the entire lower floor structure, since the S1 impact condition is a level landing. Set Fa_j to 1.0 for all M lower floor locations in equation 3-5.
- S2—Assume a variation in Fa_j from 1.0 at the initial contact point to zero at forward and aft extremes along the lower floor. The S2 initial attitude at impact is 4 degrees nose-up. The initial contact point is around FS 138.

Note that the forces and accelerations in equation 3-5 are actually time-varying responses, but for the purpose of modal selection, one is characterizing the responses as a single value. The calculations are performed using a total of 400 modes. For purposes of this effort, this is more than enough modes, since frequencies below 200 Hz are of primary interest.

3.3.3.1 S1 Modal Contribution Results.

To illustrate the modal contribution differences at a large floor mass slab and at a light floor structure, modal data at grids 300, 500, 3100, and 7100 are generated. The particulars regarding these two locations are noted in table 3-15.

TABLE 3-15. S1 GRID POINTS FOR MODAL CONTRIBUTION ANALYSIS

Grid	FS	BL	WL	Weight	Description
300	46.7	-22.0	24.0	260.0	Floor slab at pilot station
500	116.9	-21.6	24.0	650.0	Floor slab at troop station
3100	42.0	-14.0	22.0	10.9	Location on floor near pilot station
7100	129.0	-14.0	22.0	5.3	Location on floor near troop station

WL = water line

Figure 3-19 shows the modal contributions to the floor slab az at grid 300, plotted versus frequency. The numbers indicate the mode. Both positive and negative modal contributions are shown, indicating the possibility of modal cancellations. Figure 3-18 shows that the modal contributions are concentrated at frequencies below 30 Hz with some limited higher-frequency inputs up to 100 to 120 Hz. The fundamental mode (number 1) at 6 Hz is a significant contributor. A plot of the modal contributions to the floor slab az at grid 500 would show similar results to the grid 300 plot.

For grid point 3100, figure 3-20 shows the modal contributions. At this location, there are significant modal contributions at all frequencies up to the 180 Hz limit examined. Clearly, the light mass for this grid point results in numerous high-frequency modal contributions. A plot of

the modal contributions to the floor az at grid 7100 would show similar results to the grid 3100 plot.

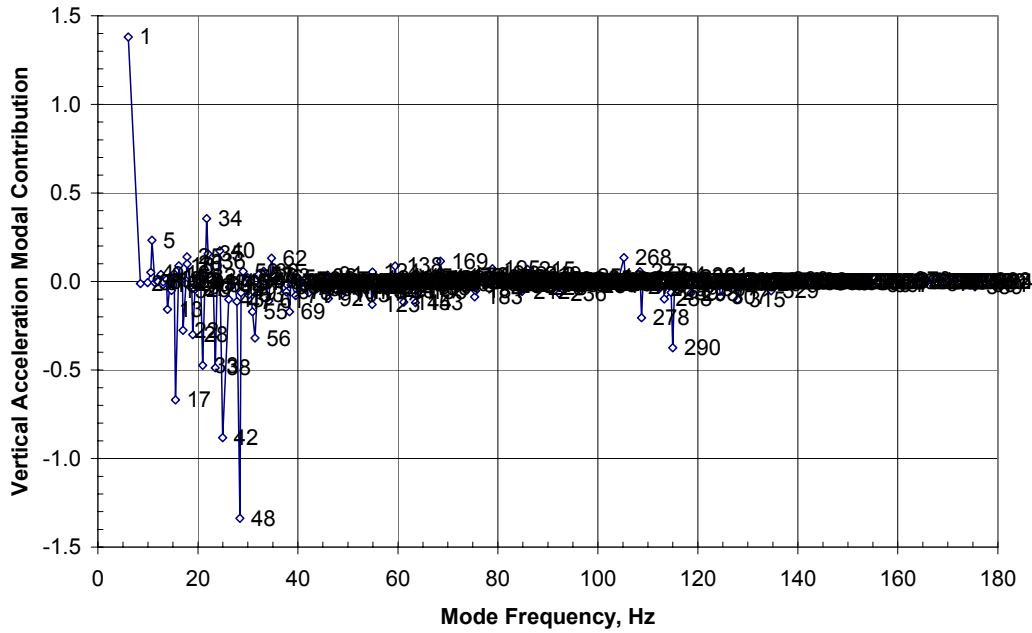


FIGURE 3-19. S1 MODAL CONTRIBUTION FACTORS TO AZ AT SLAB GRID POINT 300

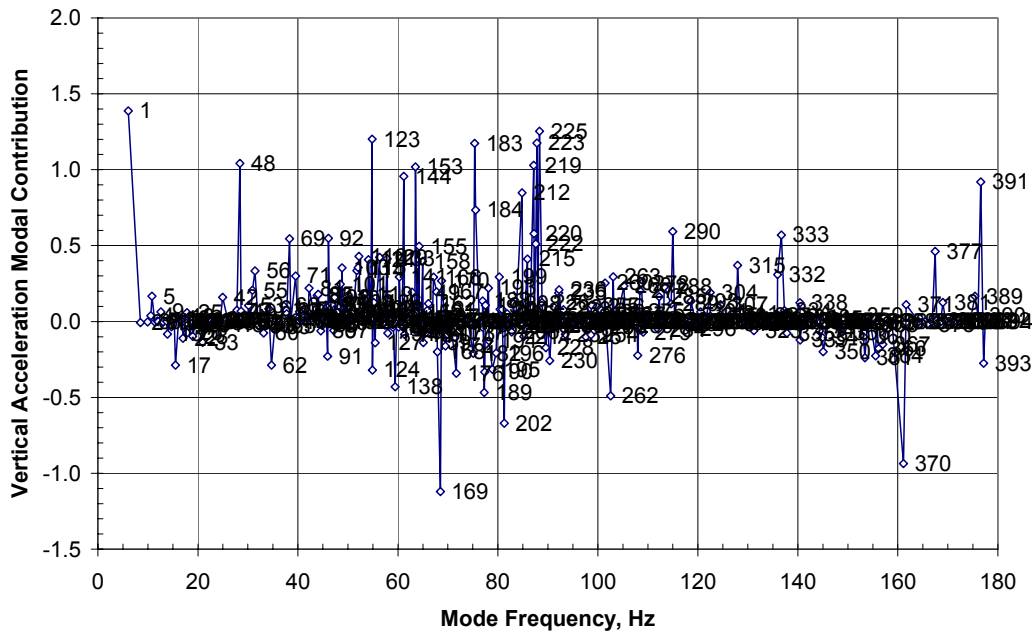


FIGURE 3-20. S1 MODAL CONTRIBUTION FACTORS TO AZ AT FLOOR GRID POINT 3100

Tables 3-16 and 3-17 show the modal contribution data for the first 20 significant modes, sorted by modal contribution to the az at grid points 300 and 3100 and 500, and 7100, respectively. In the tabular data, the absolute value of each modal contribution is taken before the sorting. The color coding for the modal frequencies noted in tables 3-16 and 3-17 sorts the frequencies in ranges from 0-60 Hz, 60-120 Hz, and > 120 Hz. These results again show the relative lack of higher-frequency modal contributions to the az's at the heavier floor slab locations and a greater propensity for higher frequencies at the floor lightweight location.

TABLE 3-16. S1 TOP 20 MODAL CONTRIBUTIONS AT GRID POINTS 300 AND 500

Grid Point 300			Grid Point 500		
20 Mode Sum		8.396	20 Mode Sum		4.406
Mode No.	Frequency (Hz)	az-fact	Mode No.	Frequency (Hz)	az-fact
1	6.05	1.380	17	15.49	0.575
48	28.38	1.338	22	17.01	0.527
42	24.96	0.882	1	6.05	0.467
17	15.49	0.669	9	12.58	0.304
38	23.48	0.488	13	13.90	0.271
33	20.96	0.474	116	52.21	0.239
290	114.97	0.374	18	16.18	0.219
34	21.76	0.355	33	20.96	0.213
56	31.42	0.320	133	57.84	0.197
28	18.96	0.300	42	24.96	0.164
22	17.01	0.275	49	28.63	0.162
5	10.79	0.233	215	85.89	0.157
278	108.71	0.205	25	17.81	0.147
40	24.39	0.173	10	13.00	0.132
69	38.33	0.171	143	60.85	0.124
55	30.91	0.171	40	24.39	0.109
13	13.90	0.158	28	18.96	0.107
35	22.02	0.156	34	21.76	0.102
25	17.81	0.138	12	13.72	0.096
268	105.18	0.134	144	61.20	0.093
	< 60 Hz				
	60-120 Hz				

TABLE 3-17. S1 TOP 20 MODAL CONTRIBUTIONS AT GRID POINTS 3100 AND 7100

Grid Point 3100			Grid Point 7100		
20 Mode Sum		18.301	20 Mode Sum		17.060
Mode No.	Frequency (Hz)	az-fact	Mode No.	Frequency (Hz)	az-fact
1	6.05	1.388	215	85.89	3.053
225	88.33	1.254	219	87.16	1.918
123	54.86	1.201	205	81.85	1.337
223	87.79	1.175	214	85.19	1.103
183	75.35	1.174	236	92.24	0.896
169	68.50	1.120	208	83.05	0.813
48	28.38	1.042	220	87.24	0.782
219	87.16	1.029	391	176.59	0.751
153	63.50	1.019	329	134.66	0.748
144	61.20	0.957	389	175.42	0.633
370	161.11	0.936	1	6.05	0.613
391	176.59	0.919	304	122.45	0.597
212	84.86	0.848	226	88.83	0.570
184	75.55	0.735	71	39.53	0.543
202	81.29	0.670	290	114.97	0.499
290	114.97	0.593	277	108.43	0.496
220	87.24	0.580	116	52.21	0.483
333	136.71	0.569	121	54.10	0.455
92	46.11	0.548	278	108.71	0.392
69	38.33	0.546	101	48.48	0.378
	< 60 Hz				
	60-120 Hz				
	> 120 Hz				

Figure 3-21 shows the mode shapes along BL 14 for the first six modes contributing to the az at grid point 3100. Also shown is the overall maximum and minimum vertical modal deflection. Except for a couple points, the modes having maximum vertical floor deflections are not among the top six modes contributing to az at grid 3100. This is presumably because the generalized force for those modes is too low to make the top six group.

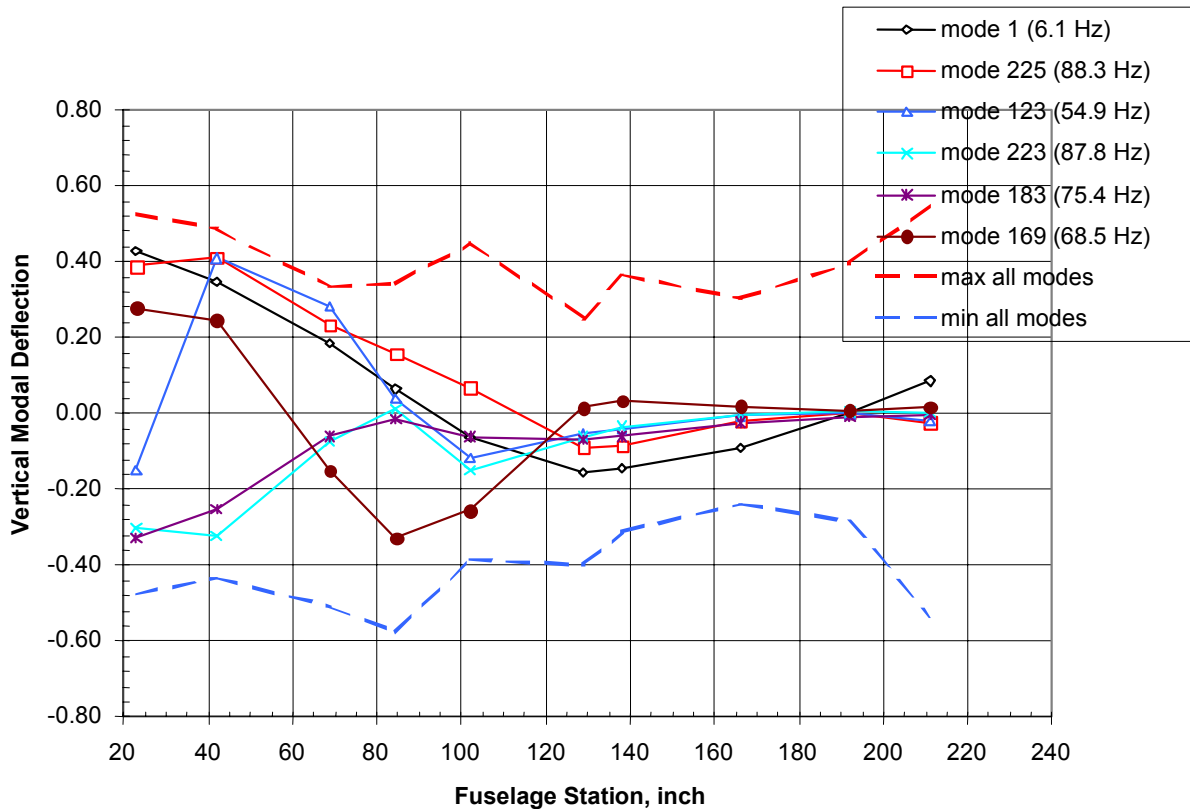


FIGURE 3-21. S1 MODE SHAPES AT BL 14 WL 22—FIRST SIX MODES ORDERED BY CONTRIBUTION TO AZ AT GRID POINT 3100

Table 3-18 shows a sorted list of the top 20 modes for grid 3100 ranked by absolute value of generalized force. In general, this ranking does not correlate well with the rankings based on modal contribution to az (equation 3-5, shown in tables 3-14 and 3-15. Common modes occur for 7 of the top 20 modes for grid point 3100 (shown shaded in gray in table 3-18). From these results, it is clear that both the forcing function (generalized force) and the mode shape at the location of interest must be considered in determining the modal contributions. Those are the considerations in the derivation of equation 3-5.

3.3.3.2 S2 Modal Contribution Results.

The modal contributions to the same grid points as the S1 data are also presented, along with transmission and engine mass items. The associated weights and locations are shown in table 3-19.

TABLE 3-18. S1 TOP 20 MODES AT GRID 3100 SORTED BY GENERALIZED FORCE

Rank	Mode	Frequency (Hz)	Generalized Force
1	329	134.66	8.407
2	215	85.89	7.641
3	219	87.16	7.640
4	48	28.38	7.327
5	315	127.94	6.339
6	220	87.24	6.283
7	391	176.59	6.267
8	116	52.21	6.052
9	389	175.42	5.725
10	307	124.48	5.636
11	304	122.45	5.580
12	166	67.15	5.571
13	195	78.91	5.547
14	205	81.85	5.501
15	290	114.97	5.459
16	236	92.24	5.298
17	226	88.83	5.225
18	183	75.35	4.666
19	169	68.50	4.537
20	301	120.54	4.447

TABLE 3-19. S2 GRID POINTS FOR MODAL CONTRIBUTION ANALYSIS

Grid	FS	BL	WL	Weight	Description
300	60.000	-22.060	24.090	266.3	Floor slab at pilot station
500	121.20	-21.38	24.11	680.1	Floor slab at troop station
700	138.20	0.00	85.33	634.4	Transmission
800	186.80	0.00	79.17	629.0	Engine
3100	42.0	-14.00	22.00	12.0	Location on floor near pilot station
7100	129.0	-14.00	22.00	23.8	Location on floor near troop station

Figures 3-22 and 3-23 show the modal contributions to the floor slab (grid point 300) and light floor mass (3100) az, plotted versus frequency. The numbers indicate the mode. The data in these figures are consistent with the S1 results for modal contributions at slabs versus light floor

masses. The results for grid points 500 and 7100, not shown, are similar to that at grid points 300 and 3100, respectively.

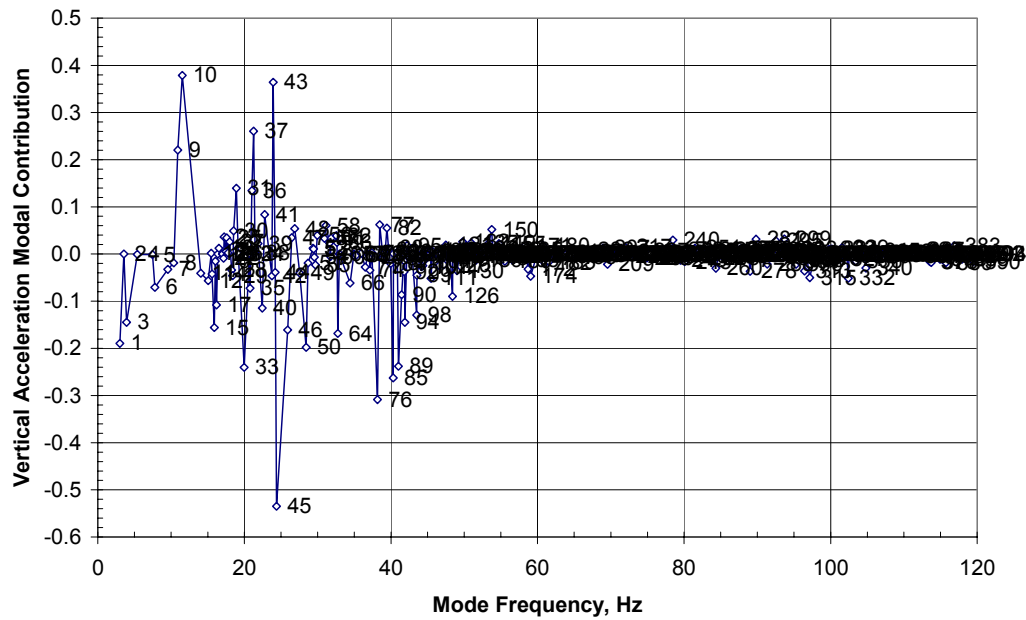


FIGURE 3-22. S2 MODAL CONTRIBUTION FACTORS TO AZ AT SLAB GRID POINT 300

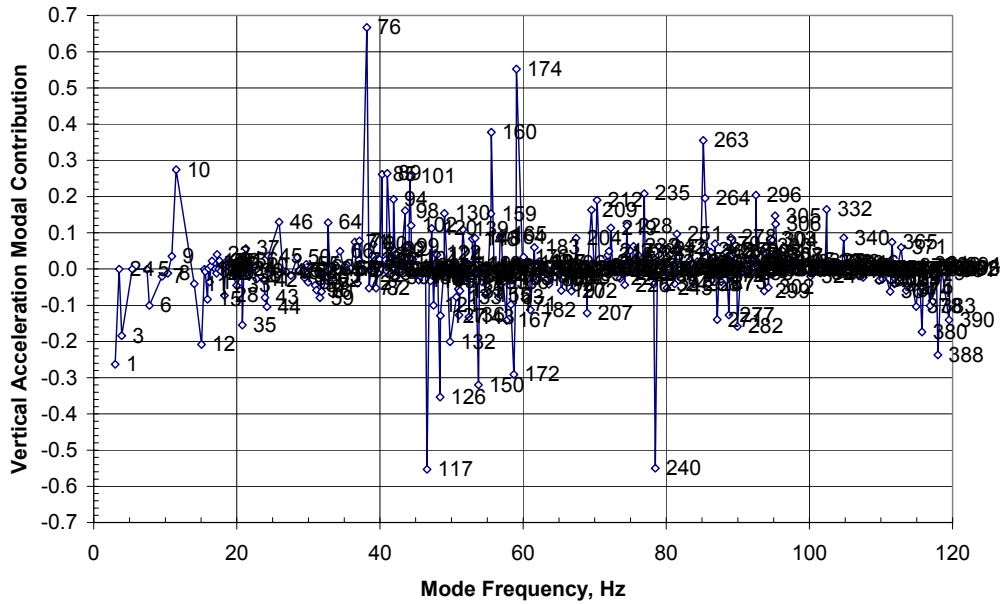


FIGURE 3-23. S2 MODAL CONTRIBUTION FACTORS TO AZ AT FLOOR GRID POINT 3100

Tables 3-20 and 3-21 show the modal contribution data for the first 20 significant modes, sorted by modal contribution to the az at grid points 300, 500, 3100, and 7100. In the tabular data, the absolute value of each modal contribution is taken before the sorting. The color coding for the modal frequencies noted in tables 3-20 and 3-21 covers frequency ranges of < 50 Hz, 50-100 Hz, and >100 Hz. These results again show the relative lack of higher-frequency modal contributions to the az at the high mass floor slab locations and the expected high incidence of high-frequency contributions.

TABLE 3-20. S2 TOP 20 MODAL CONTRIBUTIONS AT GRID POINTS 300 AND 500

Grid Point 300			Grid Point 500		
20 Mode Sum		4.488	20 Mode Sum		3.900
Mode No.	Frequency (Hz)	az-fact	Mode No.	Frequency (Hz)	az-fact
45	24.38	0.5350	59	31.62	0.4176
10	11.53	0.3787	17	16320	0.3313
43	23.95	0.3639	12	15.07	0.3243
76	38.15	0.3086	35	20.79	0.2825
85	40.31	0.2625	40	22.45	0.2822
37	21.25	0.2603	41	22.78	0.2530
33	19.97	0.2404	117	46.59	0.2139
89	41.03	0.2379	14	15.60	0.1786
9	10.93	0.2205	149	53.37	0.1779
50	28.44	0.1979	66	34.43	0.1734
1	3.01	0.1895	46	25.91	0.1697
64	32.76	0.1686	10	11.53	0.1413
46	25.91	0.1608	31	18.91	0.1362
15	15.89	0.1557	44	24.22	0.1269
3	3.92	0.1450	61	31.85	0.1261
94	41.92	0.1447	50	28.44	0.1256
31	18.91	0.1397	15	15.89	0.1247
36	21.04	0.1343	33	19.97	0.1094
98	43.52	0.1294	42		0.1064
40	22.45	0.1145	263	85.17	0.0994
	< 50 Hz				
	50-100 Hz				

TABLE 3-21. S2 TOP 20 MODAL CONTRIBUTIONS AT GRIDS 3100 AND 7100

Grid Point 3100			Grid Point 7100		
20 Mode Sum		6.593	20 Mode Sum		7.434
Mode No.	Frequency (Hz)	az-fact	Mode No.	Frequency (Hz)	az-fact
76	38.15	0.6672	242	79.07	0.6920
117	46.59	0.5530	117	46.59	0.6863
174	59.07	0.5519	332	102.40	0.6436
240	78.47	0.5502	182	61.02	0.5253
160	55.55	0.3777	172	58.72	0.4743
263	85.17	0.3554	263	85.17	0.4474
126	48.39	0.3537	240	78.47	0.4241
150	53.75	0.3201	59	31.62	0.3970
172	58.72	0.2910	183	61.57	0.3792
10	11.53	0.2740	66	34.43	0.3584
89	41.03	0.2641	160	55.55	0.2970
1	3.01	0.2634	383	116.86	0.2876
85	40.31	0.2617	85	40.31	0.2810
101	44.19	0.2551	155	54.74	0.2580
388	117.95	0.2372	167	57.69	0.2319
12	15.07	0.2083	327	101.27	0.2224
235	76.92	0.2082	149	53.37	0.2205
296	92.54	0.2042	375	113.72	0.2164
132	49.80	0.2008	371	112.81	0.1985
264	85.43	0.1956	219	72.25	0.1926
	< 50 Hz				
	50-100 Hz				
	> 100 Hz				

Modal contributions for large discrete mass items such as the transmission and engine (grids 700 and 800) are shown in figures 3-24 and 3-25. For the most part, these also show few contributions from high-frequency modes. The exception is the engine, grid point 800, which has a number of significant modal contributions from modes above 40 Hz and as high as 120 Hz.

As is the case of the S1 modal analysis results (figure 3-21 and table 3-18), the S2 modes, having maximum floor deflections, are usually not among the top six modes contributing to the az at a particular grid point, and both forcing function and mode shape are important.

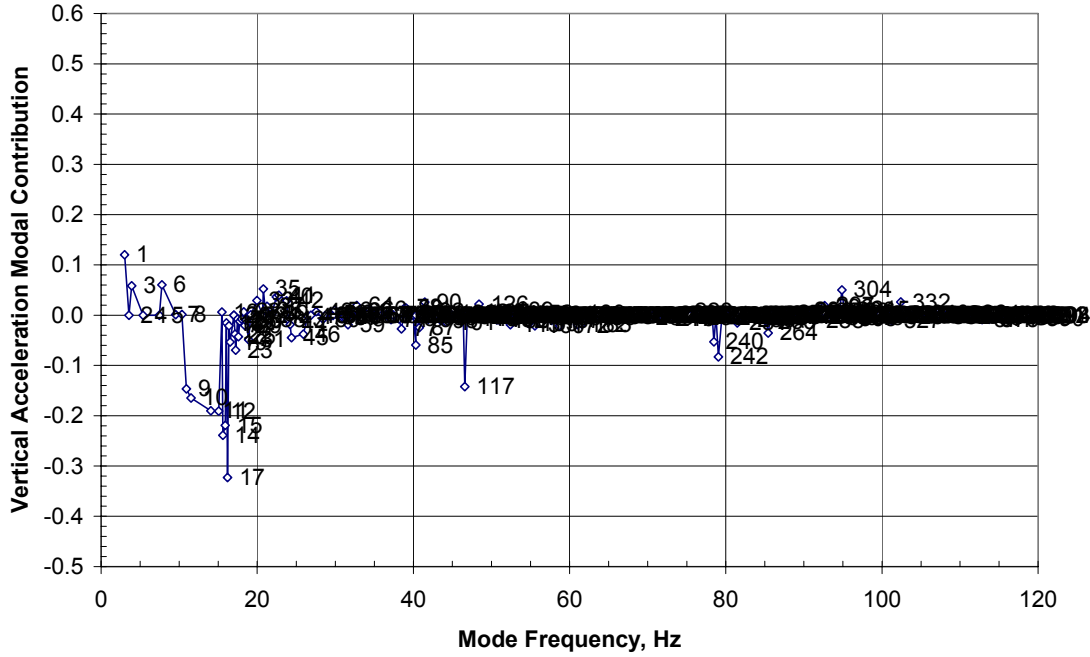


FIGURE 3-24. S2 MODAL CONTRIBUTION FACTORS TO AZ AT TRANSMISSION GRID POINT 700

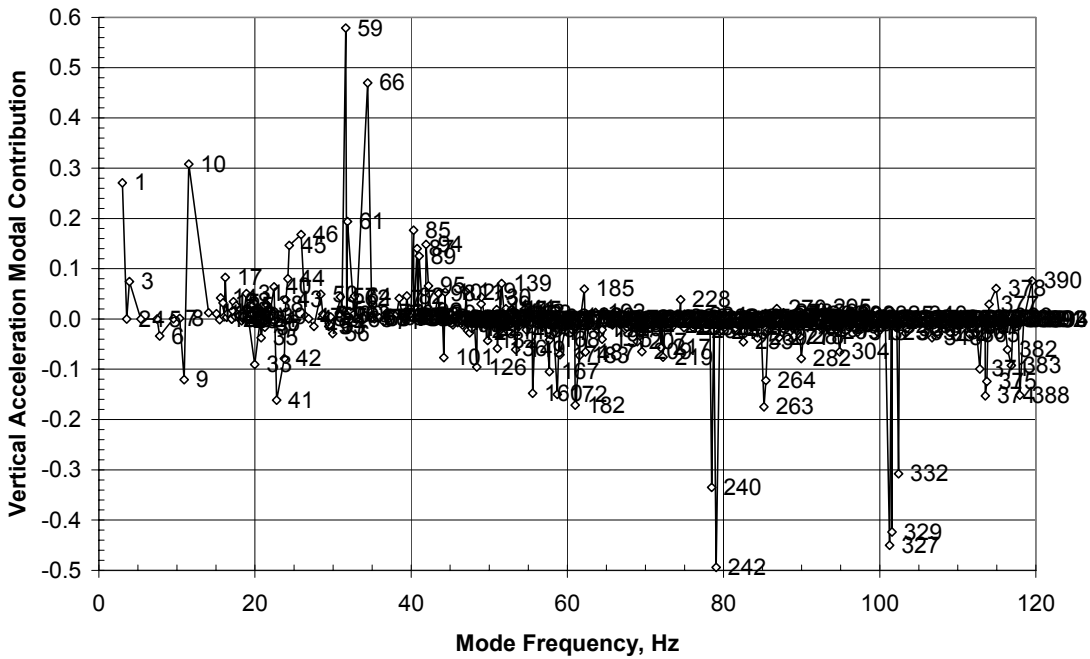


FIGURE 3-25. S2 MODAL CONTRIBUTION FACTORS TO AZ AT ENGINE GRID POINT 800

3.4 HUANG HILBERT TRANSFORM.

Reports [3 and 4] provided by NASA Goddard Space Flight Center regarding the application of time series analysis using empirical mode decomposition (EMD) and Hilbert Spectra or the Huang Hilbert Transform (HHT) were reviewed. The following is a synopsis of the procedure based on information in those reports.

The purpose of the procedure is (1) to decompose complicated sets of data into finite collections of intrinsic mode functions (IMF) that exhibit well-behaved Hilbert transforms and (2) to analyze time series data that represents nonstationary and nonlinear processes.

The method is a contrast to classical methods, i.e., Fourier analysis, that are generally applicable to periodic or stationary data that represent a linear process. The method is based on the concept of EMD.

An IMF, loosely defined, is an oscillation mode that is embedded in the data to be analyzed and that is associated with a local time scale of data. IMFs are based on (1) local properties of the signal to be analyzed and which give meaning to the concept of instantaneous frequency and (2) the introduction of instantaneous frequencies for complicated sets of data, which frequencies eliminate the need for spurious harmonics to represent nonlinear and nonstationary processes.

The final presentation of the results is an energy-frequency-time distribution designated the Hilbert spectra.

Several limitations are noted that would affect results. Among these are:

- Overshoot and undershoot problems
- Criteria in the sifting process has to be chosen judiciously
- Further studies and quantitative criteria are worthwhile
- Corruption of data under some conditions
- Weak signals embedded in stronger ones
- Need for oversampled data to define the instantaneous frequency precisely
- Cannot separate signals when frequencies are too close
- Does not provide a well-defined physical meaning

Further analysis of this procedure is provided in section 4.4.

3.5 FORCE RECONSTRUCTION TECHNIQUES.

Reports [5 and 6] were provided by the Sandia National Laboratories (SNL) on the subject of force reconstruction. The following is a discussion of the information provided in those reports.

Using an example of the slap-down impact test for a nuclear transportation cask, the procedure is used to provide a better estimate of forces acting on a rigid structure (cask) during a test than conventional methods. The conventional method is to digitally filter an acceleration measurement after the test to a value, which is considered to be the rigid-body acceleration of the

cask. The rigid acceleration is then multiplied by the mass to obtain an estimate of the applied force. The frequency content of this force is restricted to the cutoff frequency (3-dB point) of the digital filter, which is typically about 1/2 of the lowest elastic mode of the cask. Additionally, the rise time of the force is restricted to the rise time of the digital filter.

The application that is presented is a slap-down of a scale model steel spent fuel cask onto an unyielding surface. The purpose of the test was to evaluate the response of two impact limiters and their attachments to a 10 degree slap-down orientation. Slap-down at small angles occurs when one end of the cask impacts the target before the other end with higher deceleration forces resulting from the secondary impact.

The requirements are an accelerometer with resonant frequency that can be used in an environment where the usable frequency range is about 1/5 of its resonant frequency. Elastic modes for the structure must be eliminated for the force reconstruction.

The approach is to:

- Analytically predict the elastic modes, i.e., bending, ovaling.
- Experimentally measure the modes using seven rings, eight circumferential triaxial locations per ring, plus end cap accelerometers; at least 170 accelerometers.
- For this specimen, the cutoff frequency for filtering the acceleration data to eliminate elastic response is 500 Hz or about 1/2 the first modal frequency.
- A frequency bandwidth of 1500 Hz was chosen for the new force reconstruction technique; so the reconstructed force provides three times the frequency content available from the conventional technique of filtering acceleration.

The techniques used:

- SWAT uses the modal characteristics to calculate weighting functions that allow summing of acceleration measurements from different points on the specimen to reconstruct the force.
- DECON makes use of measured frequency response functions that are combined with the measured responses to reconstruct the force.

The SWAT procedure:

- Consists of two sets of weighting factors that are determined from modal analysis results:
 - One set of weighting factors, having units of mass, reconstructs the resulting force vector.

- The second set of weighting factors, having units of mass, is used to reconstruct the moment vector.
- These factors eliminate the elastic response so that one sum of acceleration yields the rigid-body translation acceleration (acceleration of center of mass) from which the resultant applied force may be determined. The other sum yields the rotational acceleration from which the resultant applied moment may be determined.
- The number of accelerometers, required for force reconstruction in a particular frequency bandwidth is related to the number of elastic and rigid-body modes of the structure in that bandwidth.

The DECON procedure:

- Infers the applied force by combining the measured acceleration with impulse response functions.
- Requires that the point of application of the forces on the structure be known. Forces applied at other points can contaminate the deconvolution force reconstruction and cannot be separated from the desired forces without reformulation of the problem.
- Theoretically the number of accelerometers required is equal to the number of forces to be reconstructed, but the technique is more successful if there are more accelerometers than forces.

Implementation and calibration of the reconstruction techniques (lateral force):

- For the SWAT technique, each of the eight accelerometer responses are multiplied by the appropriate weight for force and moment; a summation of weighted accelerations is formed for the force and moment.
- For the DECON technique, a matrix of frequency response from all the force input points to the measured accelerometers is required. In the case presented, there were two force inputs and two accelerometer responses (each response was the average of two accelerometer signals).

Potential limitations appear to be:

- The number of force points that can be analyzed
- The type of impact surface
- Simple nonfailing structure
- Impact force reconstruction only from test data

- The exact knowledge and application area of force is needed to produce acceptable results

The applicability of this technique to water impact crash test and analysis is discussed in section 4.5.

3.6 AUTOMOTIVE INDUSTRY CRASHWORTHINESS REQUIREMENTS AND PRACTICES.

The automotive industry has extensive crash design and test regulations. If, and how, analysis is integrated into the crash design, the compliance cycle is considered a valuable source of potential influence on the aircraft industry. Thus, several contacts were made with companies that had some knowledge of automotive industry practices. The Cranfield Impact Center in England and the German Research Laboratory in Stuttgart were main contributors. These organizations provided sources of information, including websites, contacts with automobile industry colleagues, and knowledge about automotive industry practices.

Several website locations were provided and were visited. These include:

- Federal Motor Vehicle Safety Standards (FMVSS)
<http://www.crash-network.com/Regulations/regulations.html>
- U.S. FMVSS mandatory rules 571 (for cars) and 572 (for dummies)
http://www.access.gpo.gov/nara/cfr/waisidx_98/49cfrv5_98.html
- Description of crash analysis criteria
<http://www.crash-network.com/Download/crashfunc.pdf>
- European car safety information
<http://www.euroncap.com>

A series of questions were posed. These included questions related to:

- How the test conditions are defined.
- Where and how structure-related measurements are taken during tests.
- Data reduction techniques that are used.
- The role that analysis plays in the design process.
- The types of analysis and criteria used in comparing test and analysis.
- What data is obtained during a crash test.
- How test analysis correlation is judged.
- How injury levels are determined.

The automotive industry follows a series of Motor Vehicle Safety Standards, dictated in the U.S. or by the European Union or community. For example, in the U.S. the FMVSS define how a vehicle has to comply with certain safety standards. It is still necessary to show in a real test that the vehicle fulfills the requirements. The tests have to be performed in a certain way and with

equipment that fulfills certain requirements. These requirements are defined by SAE J211-Part 1 (Electronic Instrumentation for Impact Test) and SAE J211-Part 2 (Photographic Instrumentation for Impact Test). Injury Calculation Guidelines are defined in SAE J1727.

The various safety standards are:

- FMVSS No. 201—Occupant Protection in Interior Impact
- FMVSS No. 203—Impact Protection for the Driver From the Steering Control System
- FMVSS No. 206—Door Locks and Door Retention Components
- FMVSS No. 207—Steering Systems
- FMVSS No. 208—Occupant Crash Protection
- FMVSS No. 209—Seat Belt Assemblies
- FMVSS No. 210—Seat Belt Assembly Anchorage
- FMVSS No. 213—Child Restraint Systems
- FMVSS No. 214—Side Impact Protection
- FMVSS No. 216—Roof Crush Resistance
- FMVSS No. 224—Rear Impact Protection

A European document entitled “Description of Crash Analysis Criteria” clearly presents the injury criteria that are used for the evaluation of automotive crash tests. There is a description of the criteria, followed by the mathematical calculation. There is also an explanation of how the individual input quantities are determined (filtered), followed by information about the laws and specifications connected with the algorithm. Criteria is prescribed for, but not limited to, the (1) head, (2) femur, (3) tibia, (4) abdomen, and (5) vehicle and sled.

With regard to the responses to the questions related to automobile industry modeling practices that were posed, the following was ascertained:

1. There are well-defined impact scenarios, such as frontal, side, and rollover, that the occupants must be protected against. Extensive analysis of test data is performed because there are well-defined criteria for different body parts and the regulations require that occupant protection be demonstrated.
2. There are two sets of parameters being used to correlate simulation results with test results:
 - a. Structure-related—time history of test pulse, collapse mechanism, sequence of failure, etc.
 - b. Driver-related—injury-related indices for any body segment contact with the vehicle interior, i.e., head, knee, chest, etc.
3. There is no standard simulation code. Each company decides on their own simulation code. FEM codes such as PAM-CRASH and LS-DYNA-3D are two such codes used in the analysis of structures. One company indicated that they use the FE dummy, which is included in the LS-DYNA-3D software, or alternately, they use MADYMO. Current

practice at some companies is to use a rigid-body occupant/seat model, i.e., MADYMO for a first assessment. This is then followed up with detailed DYNA dummy analysis. Within a company, various departments have different interests and use different codes.

4. Simulation is not enough to show a car is of good crash design. However, simulation might be used to evaluate some crash behavior aspects of the design. There is no quantitative measure applied to the simulation. Simulations are carried out unofficially and that is an internal decision made by each company to reduce the required time (and costs) for development of new cars.
5. When modeling various impacts, there are several parameters of importance that are defined. For the frontal impact, these would include (1) the failure mechanisms around the foot-well area (at the driver's feet), (2) the acceleration time history for point at or near the B pillar base (on the driver's side), (3) the acceleration at the vertical frame behind the front door (with three sensors at each side), and (4) the steering wheel excursion into the driver's space.
6. The automobile industry does not use spectral or modal analysis in interpreting test or analysis data.
7. There is no stated, published, or agreed to criteria that quantifies test-analysis correlation agreement. It is unlikely that even a very well-developed model can reproduce the test results, and a certain amount of argument concerning the effectiveness of the model is very likely. Everyone agrees that there should be good agreement between test and analysis. The comparison between test and analysis is often done in an optical way, which means that if it looks good, it is OK. If the impression is that there are larger discrepancies between test and simulation pulses then they would try to find out the reason. A difference of 10%-20% appears to be reasonable.
8. Various SAE filters call for SAE J211-1.
9. High-speed videos (at selected points) are used to compare deformations/displacements of the test and simulation.
10. An important response for car crashes is the time when the velocity reaches zero.
11. Simulation and test results are normally not published; if they are published, it is done in a qualitative way, i.e., without a scale on the axes

A discussion of the evaluation of the automobile industry crash regulation and compliance practices and how they relate to the aircraft industry is provided in section 4.6.

4. ANALYSIS.

4.1 CORRELATION CRITERIA.

When comparing opposite side measurements, the variation in test data peak accelerations and pressures was shown to be, on average, in the range of 20.5% to 22.5% for class 180 filter data. The comparative time of occurrence for the test opposite side peaks was shown to be less than 7 msec., which supports the contention that the impact is indeed symmetrical. For a symmetrical impact and structure, there can be a deviation in measured data from one side to another. Possible contributing factors are that there is no certainty that the structure is truly symmetrical, nor that the placement of the instrumentation is on exactly the same location or structural component with regard to left versus right side. Past history has shown that from one test to another, with supposedly identical airframes and measurement locations, repetitive results may not occur.

The problem for an analysis is that unless mass and stiffness are identical to the test data being compared at every location, in all likelihood, it will not match. This is particularly true of hybrid modeling where approximations are the strength of the process. In the hybrid modeling effort, a correlation criterion of a peak acceleration and pressure amplitude match within 25% and a time of peak occurrence agreement within 10 msec. was used with a class 180 filter. This criterion appears compatible with the test variation that was obtained. The use of different filter levels could alter the variation in opposite side test data. With a class 60 filter, the average opposite side test acceleration and pressure variations are 12.2% and 31%, respectively.

While the choice of tolerance criteria applied to analysis versus test results is arbitrary, it would seem rational to impose similar limits on the analytical process as is acceptable for test data.

4.2 EFFECT OF FILTER FREQUENCY ON CORRELATION RESULTS.

Figures 4-1 through 4-4 show the comparison of filtering on test and analysis results for the floor acceleration peaks (figures 4-1 and 4-2) and the slab acceleration peaks (figures 4-3 and 4-4). Figures 4-5 through 4-8 show the comparison of filtering on test and analysis results for underside panel peak pressures at locations in proximity to the floor acceleration locations (figure 4-5 and 4-6) and to the slab locations (figures 4-7 and 4-8).

Figure 4-1, which represents floor acceleration at around FS 102 BL 37, shows that the S1 unfiltered test data exhibits a frequency in the range of 750-800 Hz. As class 180 (300 Hz) and class 60 (100 Hz) filters are applied, the shift in frequency and amplitude is observed. The class 180 filter at 300 Hz shows less oscillatory response, but still has several short-duration peaks. At the lower 100 Hz filter, associated with the class 60 filter, there is a more defined pulse.

If the unfiltered test data from figure 4-1 were chosen as a measure of the floor pulse, it would be characterized as a series of oscillating positive and negative 200 g or less peaks, each with a 1-millisecond duration. This is unrealistic for three reasons. First, the energy from the positive pulses is offset by the energy from the negative pulses. Second, no test facility would be able to reproduce such a pulse shape. Third, the occupant/seat system, being a low-frequency system, is

not expected to respond to such a high frequency. That leaves the use of filtered data as a more probable representation of the floor pulse.

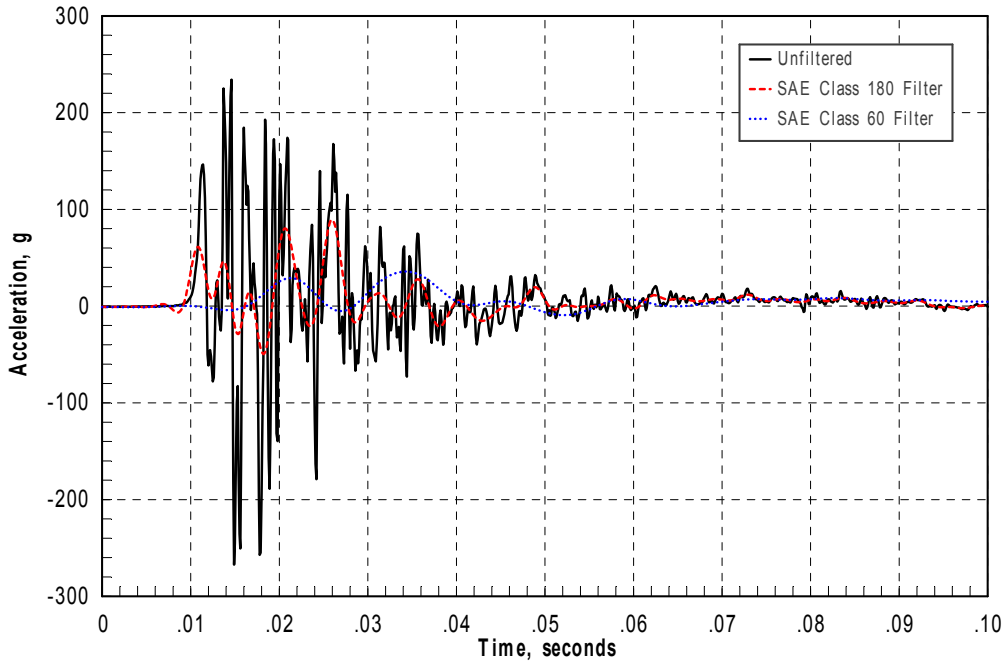


FIGURE 4-1. FILTER EFFECT—S1 FLOOR ACCELERATION TEST, FS 102 BL 37

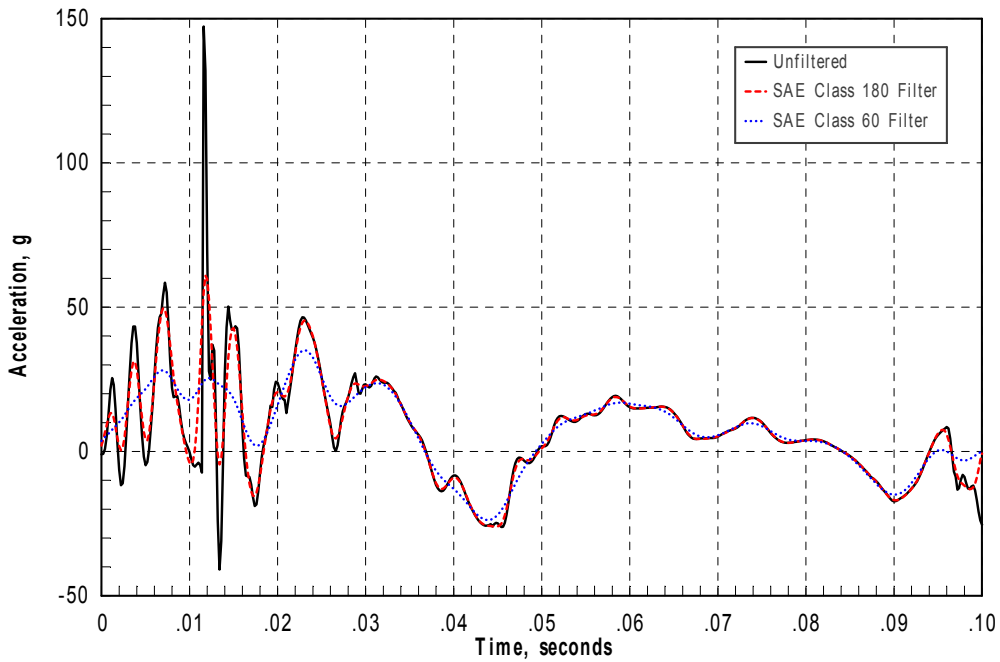


FIGURE 4-2. FILTER EFFECT—S1 FLOOR ACCELERATION ANALYSIS, FS 102 BL 37.2

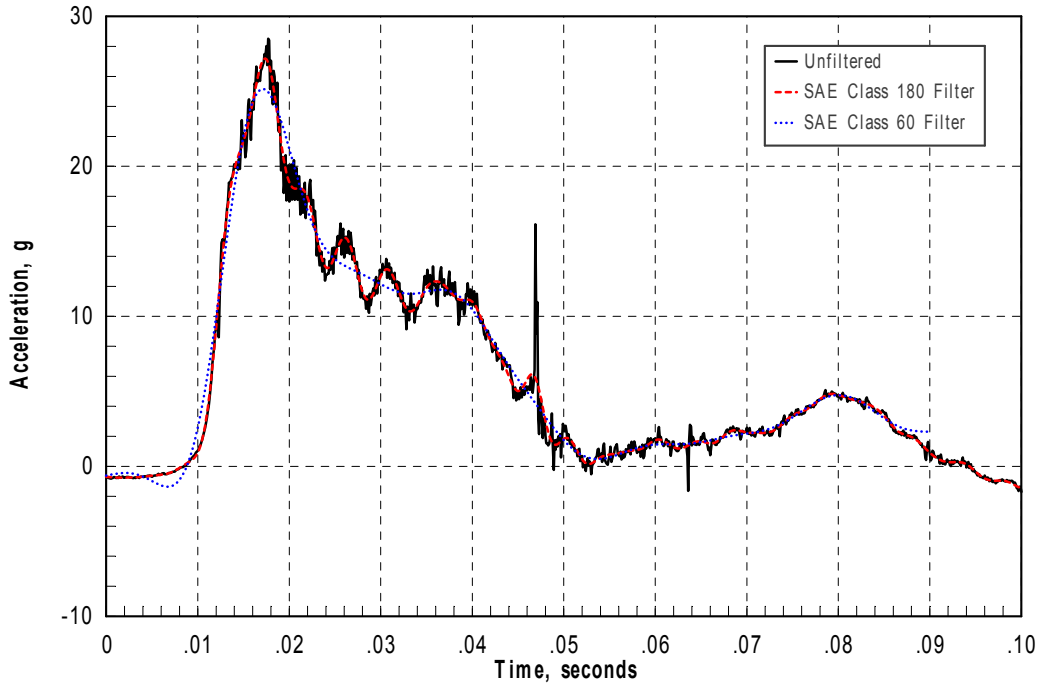


FIGURE 4-3. FILTER EFFECT—S1 SLAB ACCELERATION TEST, FS 84.5 BL 14

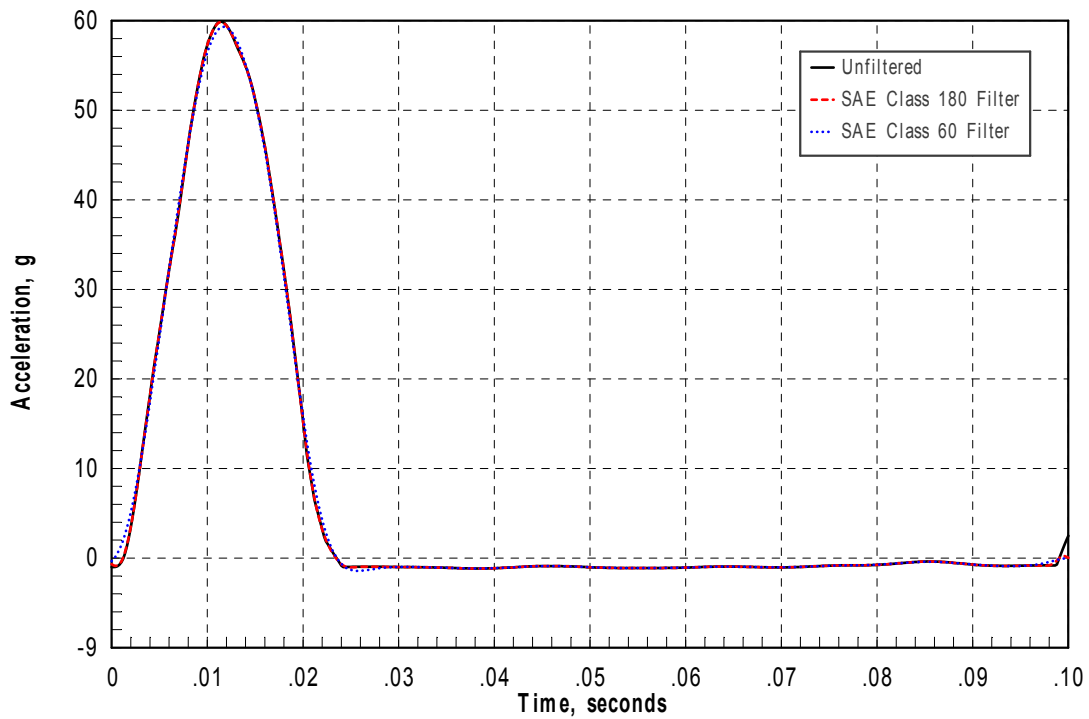


FIGURE 4-4. FILTER EFFECT—S1 SLAB ACCELERATION ANALYSIS, FS 84.9 BL 14

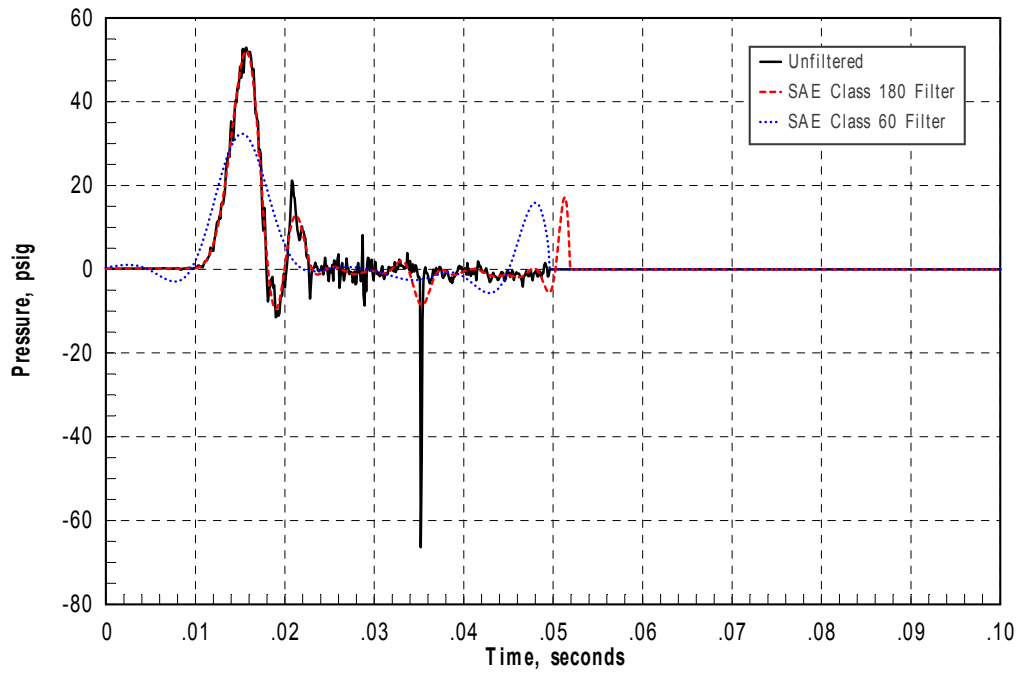


FIGURE 4-5. FILTER EFFECT—S1 PANEL PRESSURE TEST, FS 105 BL 22.75

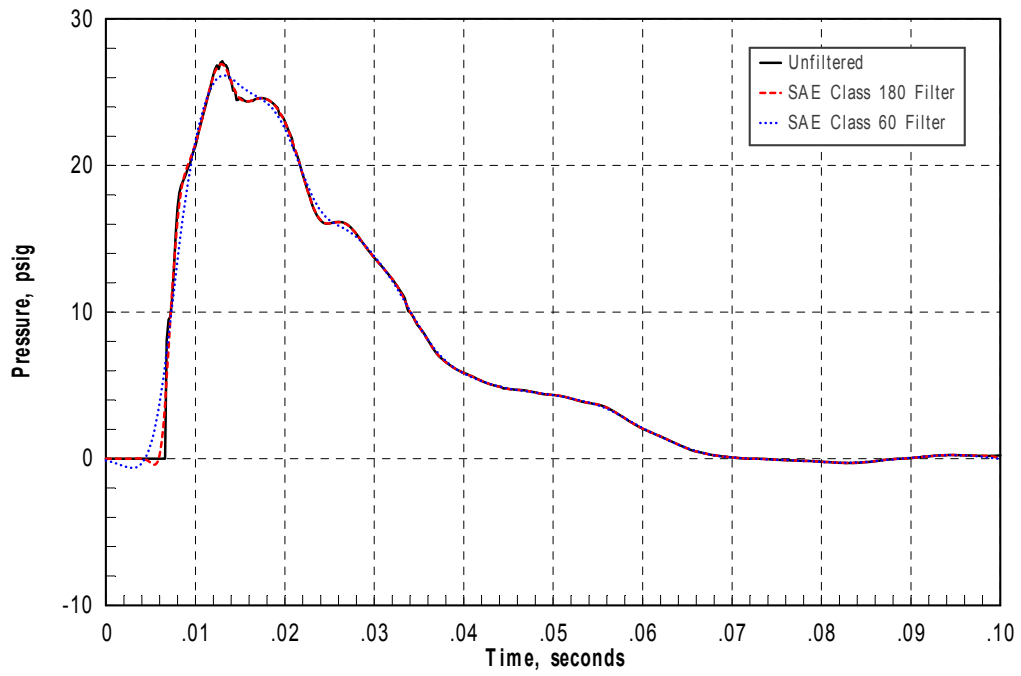


FIGURE 4-6. FILTER EFFECT—S1 PANEL PRESSURE ANALYSIS, FS 102-109 BL 14

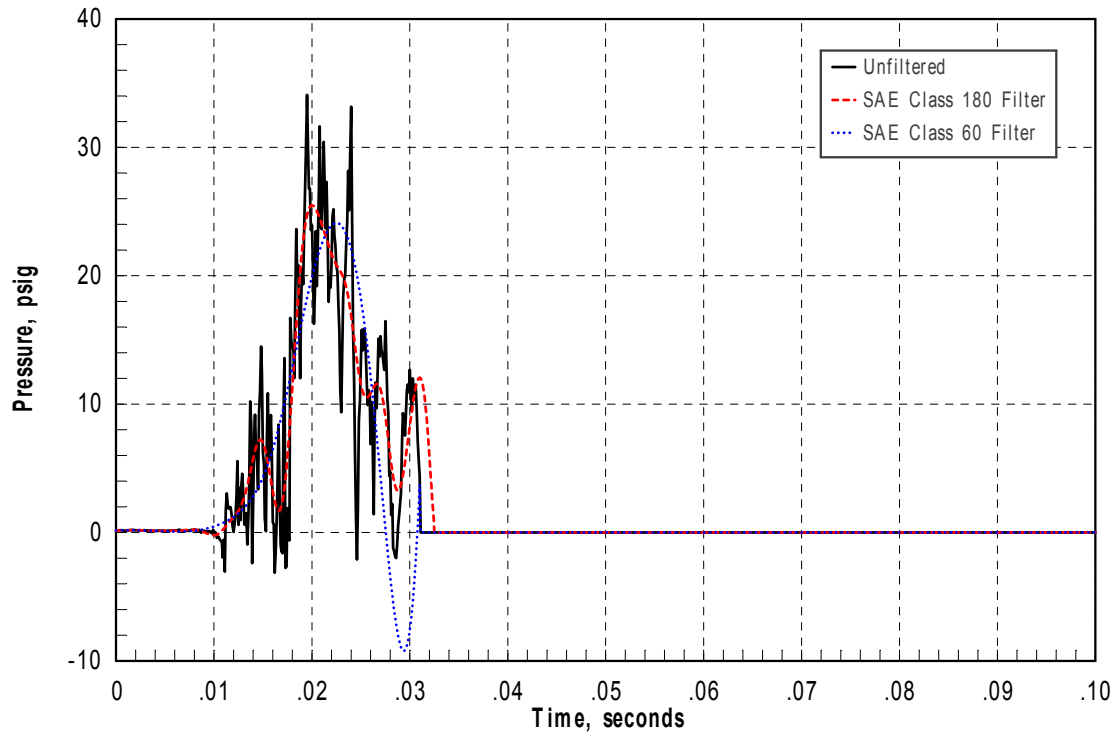


FIGURE 4-7. FILTER EFFECT—S1 PANEL PRESSURE TEST, FS 81.15 BL 22.75

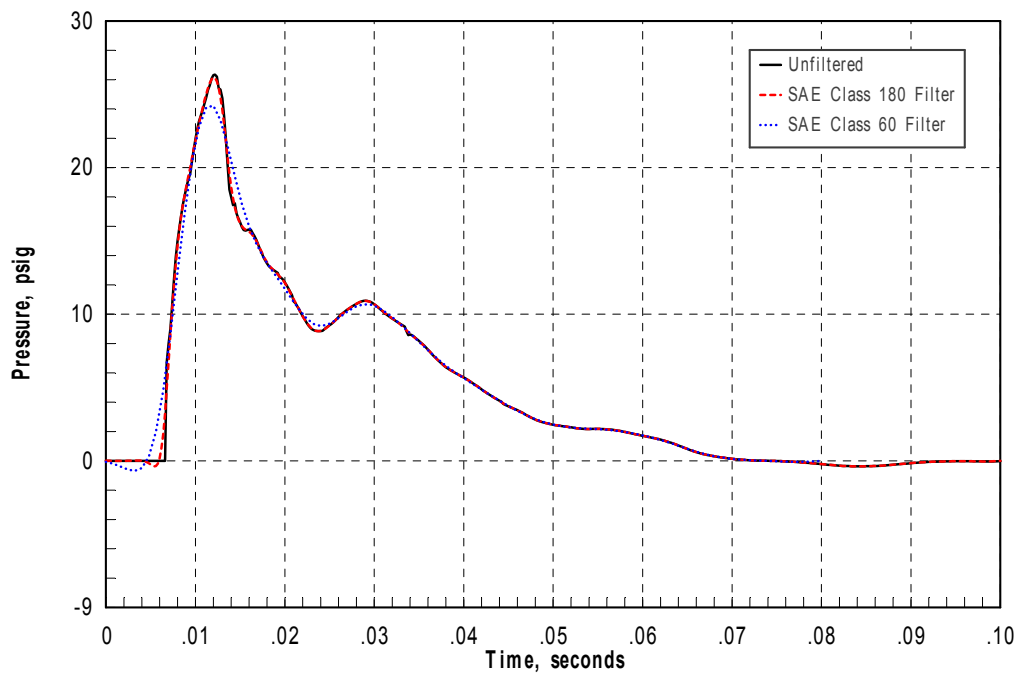


FIGURE 4-8. FILTER EFFECT—S1 PANEL PRESSURE ANALYSIS, FS 74-102 BL 22

The corresponding analysis response to filtering is shown in figure 4-2. In the latter situation, the unfiltered analysis exhibits a 300 Hz response, as does the class 60 filter data. With a class 60 filter, the pulse is more muted.

Figures 4-3 and 4-4 represent floor pulses measured and analyzed at locations representative of a heavier mass item, such as a slab. The location is at approximately FS 84.5 BL 14. As shown at this location, there is really no significant effect on the pulse due to filtering, either for the test or analysis. There is a clear definition of the pulse.

The data shown in figures 4-5 through 4-8 for FS 102 and FS 84.5 indicate that the pressure pulses at this location are not significantly affected by the filter frequency. Throughout the structure this is true for most of the analytically determined pressures, but less so for the test-measured pressures. Table 3-6 showed that the average analytical pressure (approximately 27.5 psi) is not affected by filtering, but that the average test pressure is 21 psi, 29 psi, and 47 psi for the class 60 filter, class 180 filter, and unfiltered data, respectively.

Figures 4-9 and 4-10 show comparisons between test and analysis floor acceleration and underside panel pressure in the region of FS 102-109 BL 14-22 for both the class 60 and class 180 filters. At the lower frequency, both the test and analysis acceleration pulses are reasonably close, as are the pressure pulses. At the higher filter frequency, the peak acceleration and peak pressure for the test are higher than the corresponding peaks obtained from the analysis, which is a consistent trend.

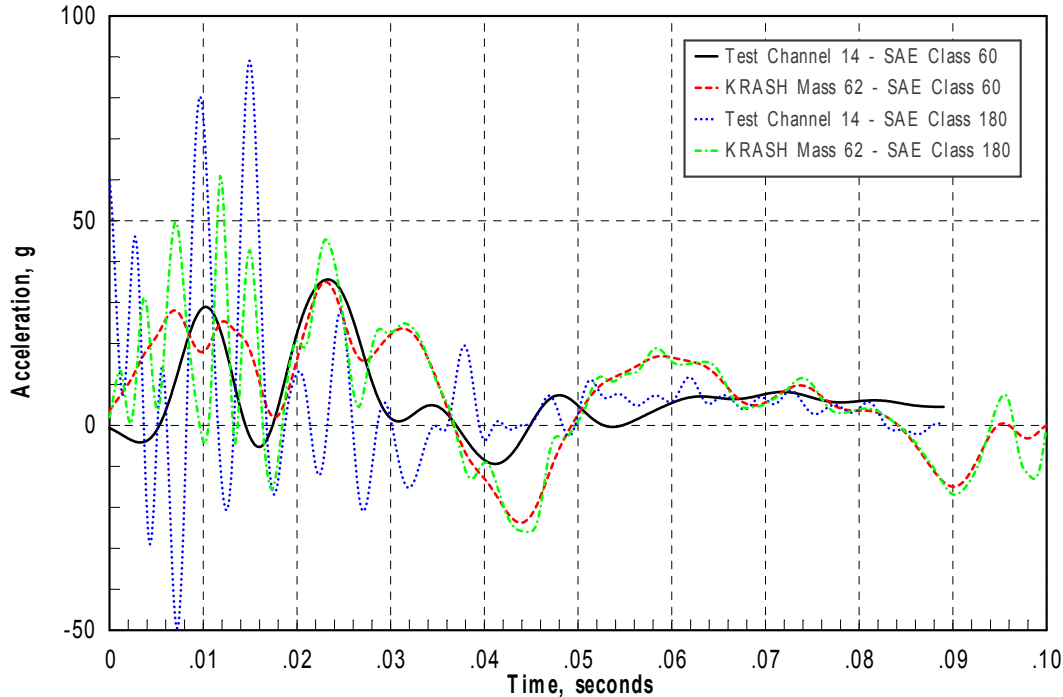


FIGURE 4-9. COMPARISON OF FILTERED S1 TEST AND ANALYSIS FLOOR ACCELERATION, FS 102 BL 37.3

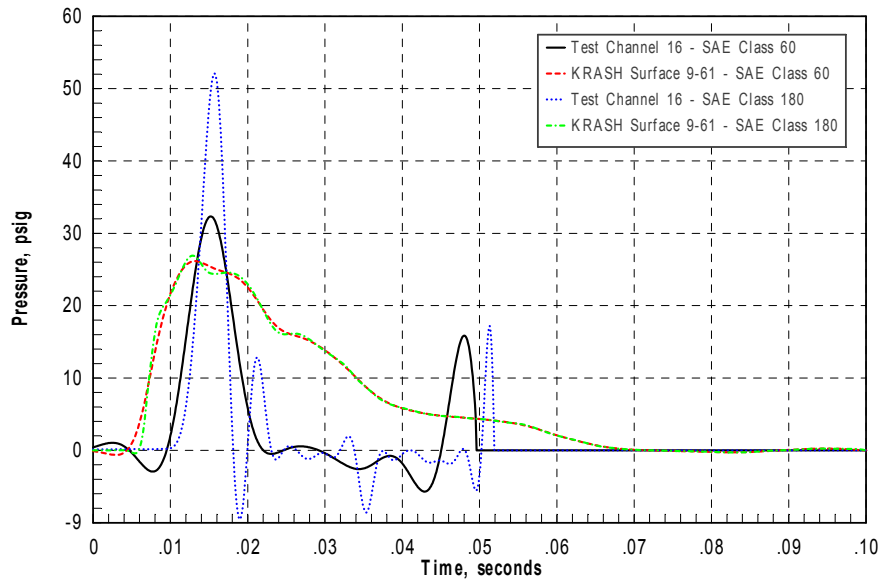


FIGURE 4-10. COMPARISON OF FILTERED S1 TEST AND ANALYSIS PANEL PRESSURE, FS 102-109 BL 12-22.75

Figure 4-11 shows a comparison between test and analysis floor acceleration at FS 84.5 BL 14. Figure 4-12 shows a comparison between test and analysis pressure at FS 74-102 BL 22. Both the acceleration and pressure data are presented for class 60 and class 180 filters. The panel pressure correlation between test and analysis (figure 4-12) appear to compare favorably. The floor acceleration correlation between test and analysis (figure 4-11) compares less favorably. In the comparison, the analysis peak floor acceleration is more than twice as high as the test value.

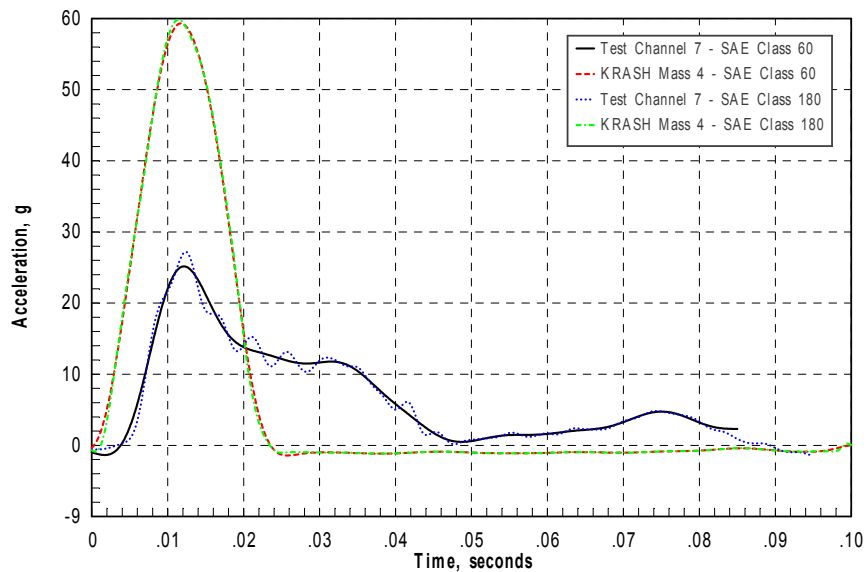


FIGURE 4-11. COMPARISON OF FILTERED S1 TEST AND ANALYSIS SLAB ACCELERATION, FS 85 BL 14

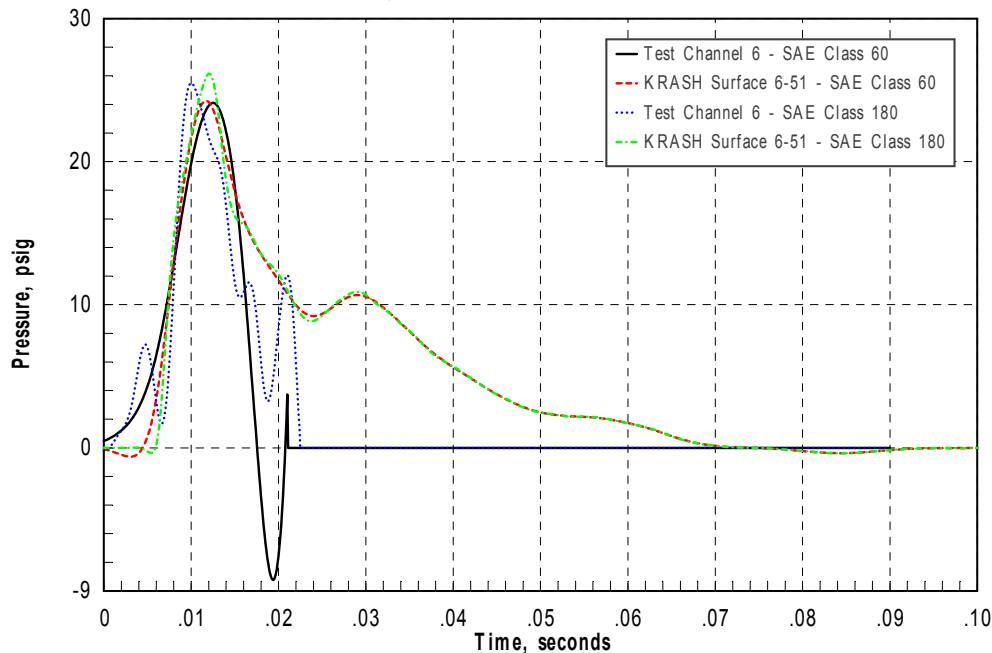


FIGURE 4-12. COMPARISON OF FILTERED S1 TEST AND ANALYSIS PANEL PRESSURE, FS 74-102 BL 22

If the force experienced by the floor is directly related to a panel pressure that is in close proximity, one would expect that both the pressure and acceleration correlations would match. One possible explanation is that while the panel pressure is equal, the panel force for the test, which is more likely a measure of peak local pressure, should be higher, or conversely, the analysis panel pressure, which is representative of an average pressure, should be lower. Unfortunately, there is no measure of force obtained in the test to compare with the hydrodynamic force predicted in the analysis. Another possibility is that the analytical model representation of the mass at the floor location does not match the test effective mass at that location. Possible solutions to achieve equal floor acceleration peaks would be to reduce the pressure match by altering the panel representation or to alter the mass at the floor. This might be more feasible in a single degree of freedom system with only one location in question, but there are multiple pressure and acceleration locations involved in the full-scale test. The KRASH hybrid model represents larger structure with simulation properties and locations, which is why overall values are more likely a better measure of the ability to simulate test data.

Figures 4-13 and 4-14 provide similar comparisons of acceleration and pressure test-analysis correlation as do figures 4-11 and 4-12, except at FS 23-47 BL 14-22, which is closer to the pilot/copilot location. The KRASH slab mass 3 is representative of an occupant/seat weight. The opposite side test pressure measurements near that location varied and were also affected by the filter level. Test channel 2 was the least affected by the filter and thus was used. The data in figures 4-13 and 4-14 (and tables 3-4 and 3-5) show that the correlation is not affected by filter level and that the relationship between acceleration and pressure is relatively constant. For example, if the analysis acceleration to pressure ratio is taken, based on mass 3 and lift

surface 2-21 values, it is 2.03 and 2.2 with class 180 and class 60 filters, respectively. The corresponding test ratios, based on acceleration channel 1 and pressure channel 2, are 1.94 and 2.23 for the class 180 and the class 60 filter, respectively.

The comparisons from figures 4-11 through 4-14 show that the use of a class 60 filter in lieu of a class 180 filter does not affect the results nor significantly alter any relationship between panel pressure and floor acceleration. In all, there are an equal number of times that a class 60 filter improves the correlation, worsens the correlation, and has no significant effect on the correlation.

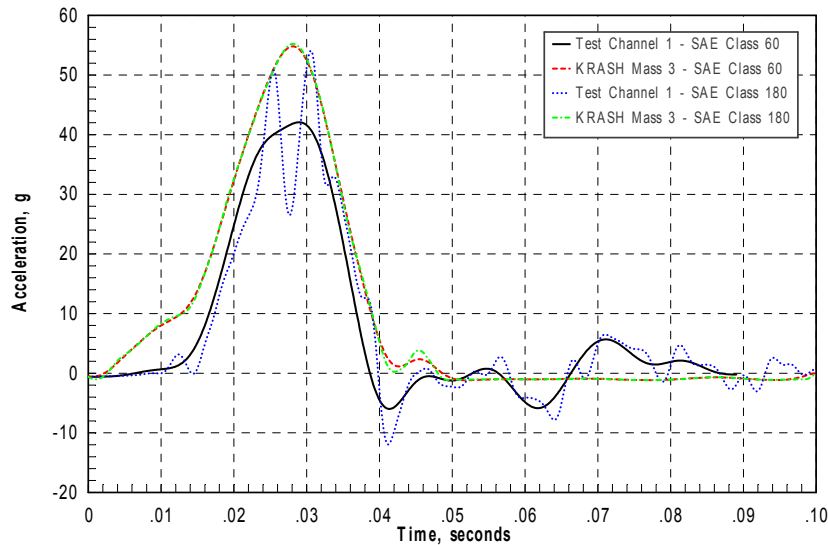


FIGURE 4-13. COMPARISON OF FILTERED S1 TEST AND ANALYSIS SLAB ACCELERATION, FS 42-47 BL 14-22

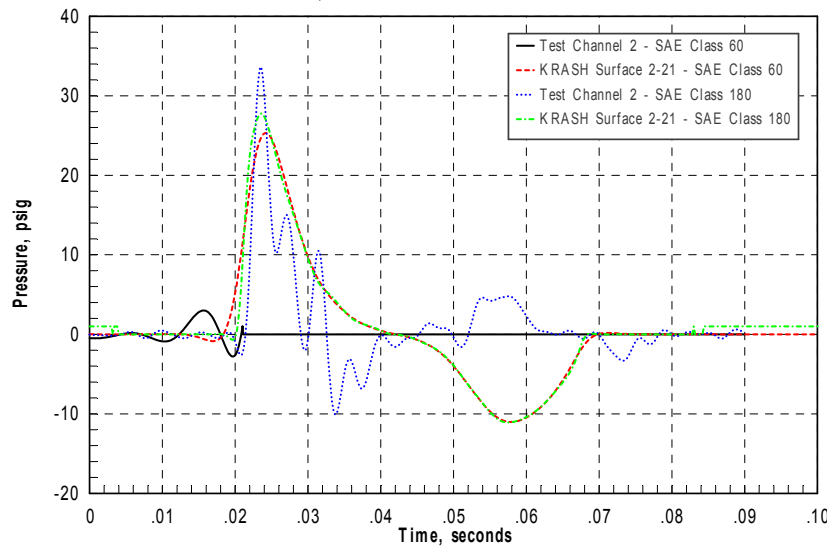


FIGURE 4-14. COMPARISON OF FILTERED S1 TEST AND ANALYSIS PANEL PRESSURE, FS 23-37 BL 21-22

4.3 EVALUATION OF PSD AND MODAL ANALYSES RESULTS FOR WATER IMPACT.

4.3.1 Evaluation of FEM and Test PSD Analysis Correlation.

The effort described in section 3.3.1 is only partially complete and only a portion of the initial testing and FEM correlation of simple elements is available. It is important to recognize that as more TAC testing and analysis is performed, the results could change. The following preliminary results are findings taken directly from reference 2.

- Even with simple tests, it was difficult to hold rigorous variables completely static so that the isolation of the required information is achieved. In symmetric configurations and impact conditions, there was considerable asymmetry in results as well as test-test variability. Both the asymmetrical response and the test-test variability were resolved sufficiently to continue the desired test matrix. However, while many fixes and procedures were introduced, the cause of the problems were never quantified nor completely understood.
- It is possible to identify correlation in both time and frequency domain. However, a process will need to be developed to identify and quantify frequency-time domain correlation.
- Correlation between test and FEM results are better achieved with strains and displacements than with accelerations. The use of FEM to design structures for crash impacts will invariably be a process that is somewhat different than with lumped mass models. The latter provides forces and accelerations from which design loads can be developed. The FEM provides a direct calculation of structural behavior from strains and deflections in addition to accelerations and forces. Preliminarily, it was shown that the analytical methodology imposes some limitations that have to be addressed, i.e., higher than traditional sampling rates. A need to extract simulation data at high frequencies is computationally challenging for current Windows NT.

Many of the preliminary TAC results can be related to the PSD analysis of hybrid models, full-scale water impact tests, and correlation techniques being evaluated in this effort. Several in particular are noteworthy:

1. The application of PSD analysis in the TAC application, as described in section 3.3.3.1, is oriented toward FEM modeling and to date has been achieved for relatively simple structure subject to a well-defined ground impact. By contrast, the PSD analysis described in this effort is oriented toward hybrid analysis results and uses existing full-scale water crash impact test data. In some respects, the applications to date are consistent with the intended application of the methodologies. That is, FEM is more detail-oriented, while hybrid modeling is designed for overall and average results and less toward discrete comparisons.
2. The preliminary TAC results are provided for well-defined fundamental mode shapes that are in the range of 140 to 500 Hz, with the exception of one modal frequency at 37 Hz. By contrast, the PSD full-scale water impact test application deals with modal

frequencies predominantly in the range of 3 to 20 Hz and perhaps as high as 70 Hz. Many of the modes in the latter situation are coupled.

3. In both applications, it is recognized that test data variation with regard to symmetry and repeatability has to be a consideration. In fact, the results from both applications suggest that there is a tendency to accept test data as the true measure of accuracy and to distrust the analysis. The truth actually lies somewhere in between, and one has to establish the accuracy of the test data as well as the accuracy of the analysis.
4. Both applications show some consistent trends that help explain the correlation between analysis and test but also indicate some inconsistencies that lead to currently unanswered questions.
5. The TAC results show promise for understanding the test and FEM analysis results provided appropriate parameters, such as strain, are monitored. However, to date, on simple structures, neither strain nor acceleration correlation has been close in magnitude. Meaningful strains are difficult to accurately measure in full-scale aircraft crash tests.
6. The PSD analysis application to the full-scale water impact tests shows that relationships between modal analysis, time history responses, and PSD analysis provide a degree of consistency but may also be improved with further investigation.
7. All procedures have limitations and present challenges before they can be fully understood and implemented.
8. Correlation criteria needs to be established, whether it be quantitative or in combination with qualitative assessments.

4.3.2 Power Spectral Density Analysis of Test and KRASH Model Acceleration Data.

The application of PSD analysis to hybrid modeling correlation provides a mixed bag of results. For purposes of clarity, time histories are presented for class 180 filter results. However, the PSD analysis is unfiltered so that a full range of frequencies can be observed. In reality, frequencies below 300 Hz in the PSD are valid for comparing with frequencies observed in the time history plots.

At FS 84.5 BL 14.0, the test and analysis responses are very definitive pulses in the lower frequency (< 100 Hz) regime as can be observed from the time histories in figure 4-15. The analysis peak amplitude is nearly twice as high as the test peak amplitudes from both sides, which are close in amplitude to each other. The unfiltered PSD analysis of this data is provided in figure 4-16. Unfiltered PSD data is used throughout this section of analysis because it does not alter any of the amplitudes and provides the full range of frequencies.

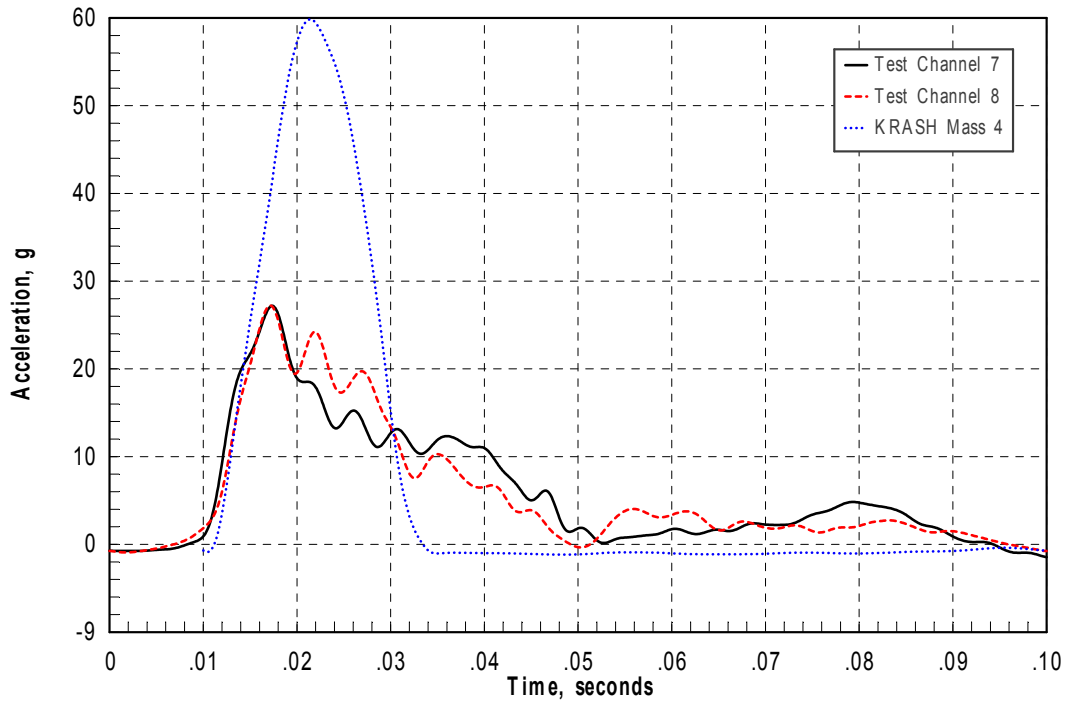


FIGURE 4-15. S1 SLAB AZ TIME HISTORY CORRELATION, FS 84.5 BL 14, SAE CLASS 180 FILTER

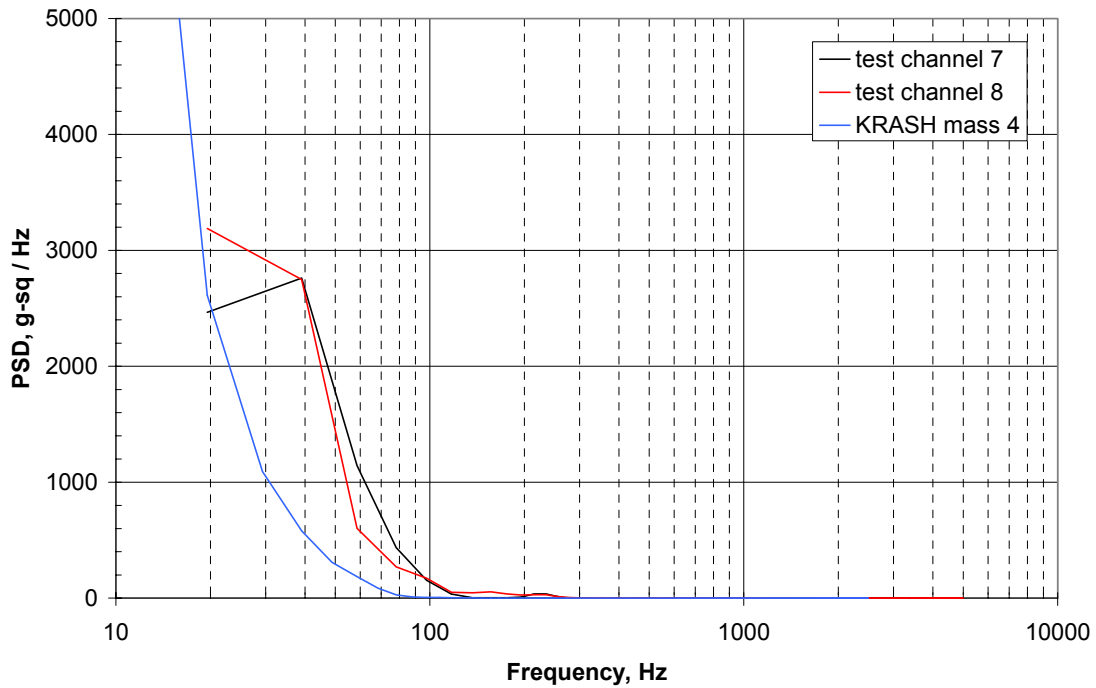


FIGURE 4-16. S1 SLAB AZ PSD CORRELATION, FS 84.5 BL 14, UNFILTERED LINEAR SCALE

Since a class 180 filter was used in the time histories, the PSD analysis confirms the time history results in that

- the test and analysis amplitudes are all relatively low frequency (< 50 Hz).
- the opposite side test responses contribute equally in amplitude and frequency.
- the analysis response amplitude is higher than the test response amplitude.

The difference between analysis and test results for this situation might in some way be altered. If this were a simple system, then increasing the KRASH model mass at this particular location might lower the amplitude and provide for a longer-duration response, both of which would improve correlation. Alternatively, changing the underside panel representation to reduce the water impact force might be appropriate.

Figures 4-17 through 4-19 present a comparison of acceleration data at FS 102 BL 37.3. The class 180- and class 60-filtered time history data are shown in figures 4-17 and 4-18, respectively. The latter is shown because it provides a clearer definition of a potential floor pulse. The opposite side test peaks differ by $\pm 22.7\%$ (class 180 filter) and 11.4% (class 60 filter) from an average of the two. The average of the test data differs by 28% (class 180 filter) and 5.8% (class 60 filter) from the KRASH analysis model for mass 62.

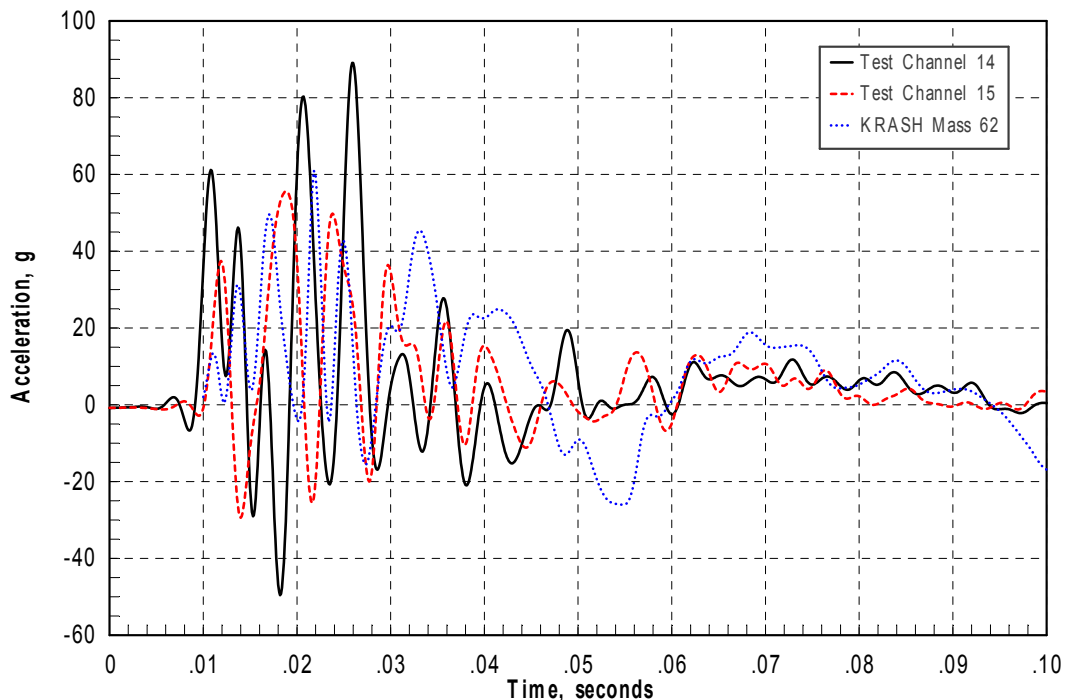


FIGURE 4-17. S1 FLOOR AZ TIME HISTORY CORRELATION, FS 102 BL 37.3, SAE CLASS 180 FILTER

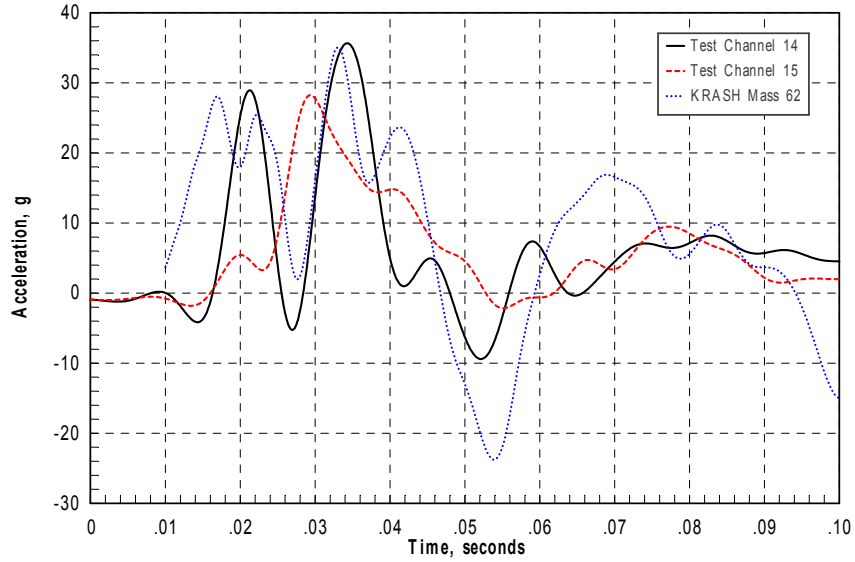


FIGURE 4-18. S1 FLOOR AZ TIME HISTORY CORRELATION, FS 102 BL 37.3, SAE CLASS 60 FILTER

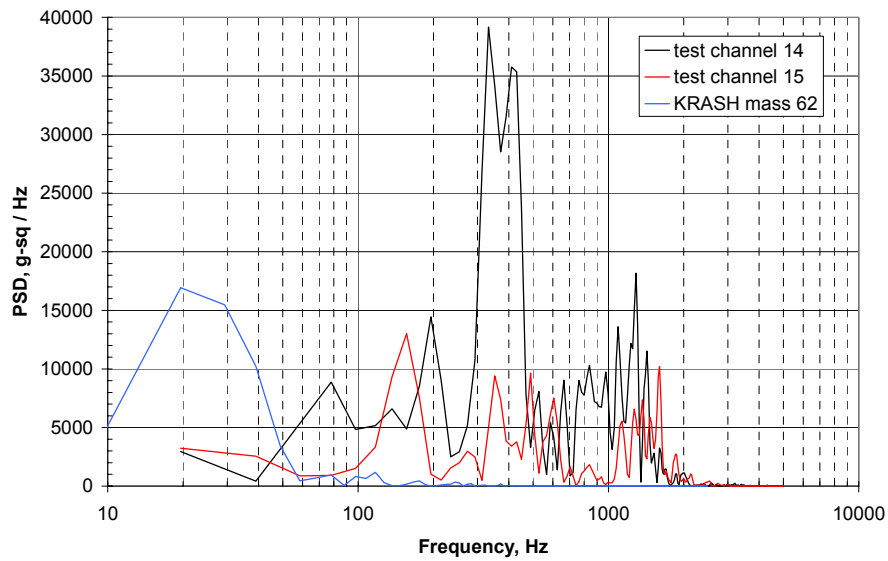


FIGURE 4-19. S1 FLOOR AZ PSD CORRELATION, FS 102 BL 37.3, UNFILTERED LINEAR SCALE

The PSD results for the responses shown in figure 4-19 indicate that the test amplitudes are associated with frequencies between 100 and 200 Hz. The peaks between 320 and 400 Hz for test channel 14 exist but cannot be compared to the time history frequencies because the latter used a class 180 filter with a 300 Hz cutoff frequency. For test channel 15, there are similar frequencies but at much lower amplitudes. The KRASH model mass 62 exhibits a primary response in the range of 20-30 Hz. What appears unusual about these plots is that the low-

frequency filtering clearly shows the two test channels and the KRASH mass as having relatively close peak acceleration amplitudes (figure 4-18) but different PSD frequency contributions below 100 Hz.

Figure 4-20 presents the floor az at FS 129 BL 36.3 using the class 180 filter. The corresponding unfiltered PSD is shown in figure 4-21. The left side (channel 11) and the right side (channel 13) test data clearly differ in amplitude in the time history plot, as they do in the PSD plot. They also exhibit different frequency contributions. The KRASH mass at 72 shows a peak response that is in between peaks of both test channels for both the time history and PSD plots. In the PSD plot, the analysis peak appears to occur at a lower frequency than the test peaks.

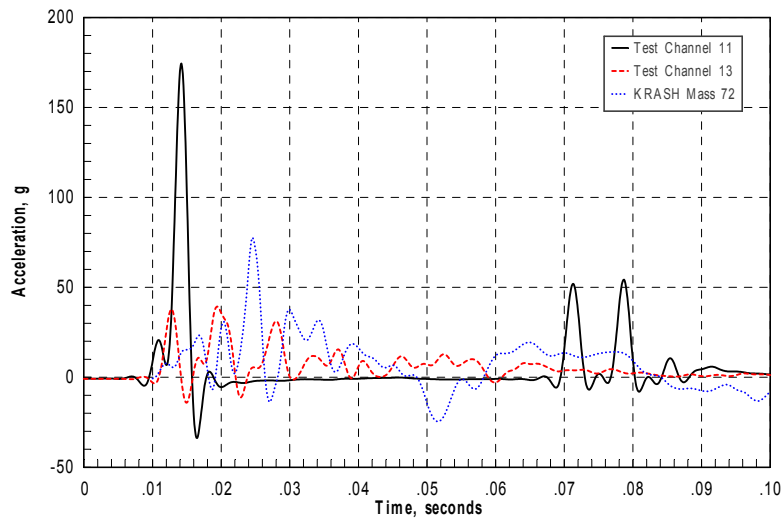


FIGURE 4-20. S1 FLOOR AZ TIME HISTORY CORRELATION, FS 129 BL 36.3, SAE CLASS 180 FILTER

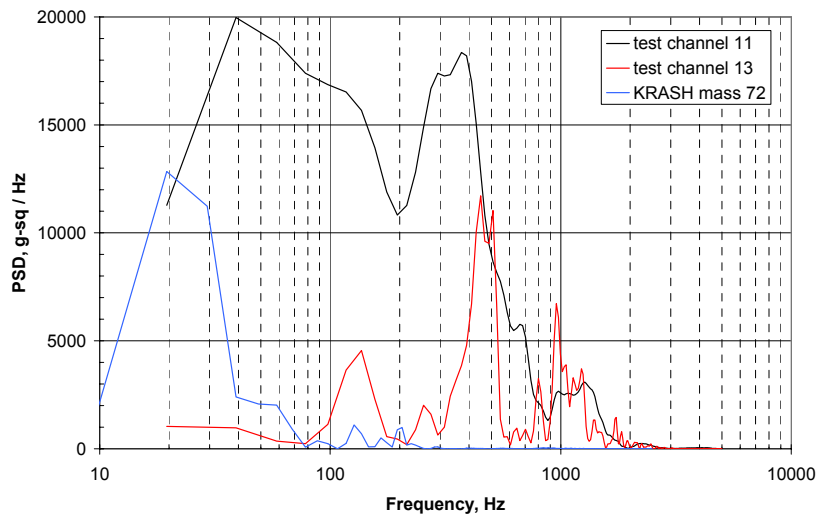


FIGURE 4-21. S1 FLOOR AZ PSD CORRELATION, FS 129 BL 36.3, UNFILTERED LINEAR SCALE

Figure 4-22 presents the floor az at FS 155 BL 14 and BL 20, using the class 180 filter. The corresponding unfiltered PSD is shown in figure 4-23. Typically, the analysis results at the two KRASH masses show the expected high short-duration peaks at mass 81 (6.3 lb.) and a lower longer-duration response at mass 6 (650 lb.). The peak accelerations associated with the two test measurements are fairly low. The PSD results do not correlate particularly well between test and analysis. However, the analysis results show that the higher slab mass has stronger low-frequency content relative to the lower floor mass. The test data PSD results show a strong 100 Hz component for the right channel, which is also very evident in the figure 4-22 time history.

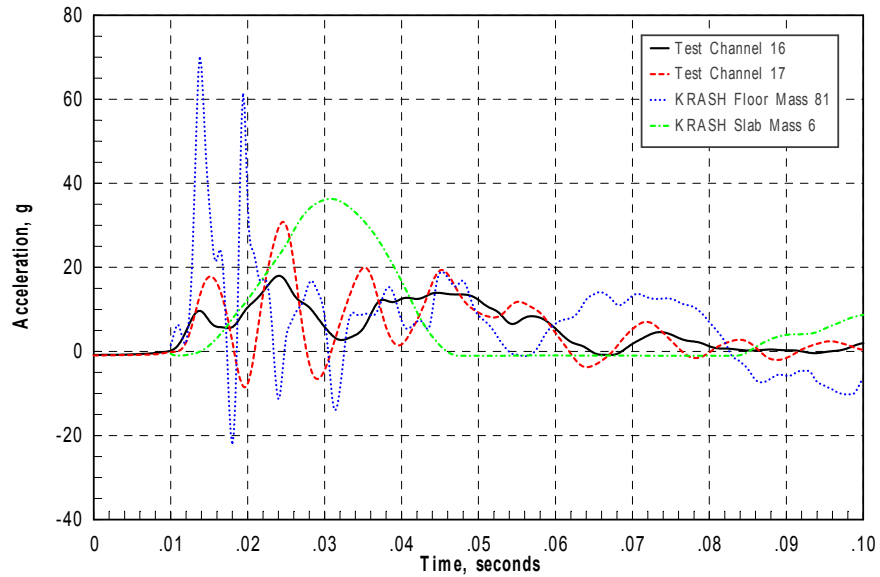


FIGURE 4-22. S1 FLOOR AZ TIME HISTORY CORRELATION, FS 155 BL 14 AND BL 20, SAE CLASS 180 FILTER

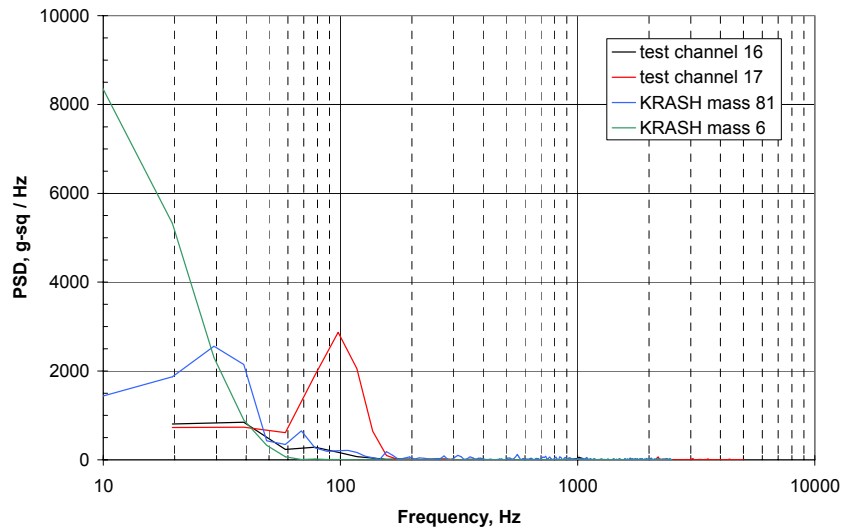


FIGURE 4-23. S1 FLOOR AZ PSD CORRELATION, FS 155 BL 14 AND BL 20, UNFILTERED LINEAR SCALE

Figure 4-24 presents the floor az at FS 155 BL 35 using the class 180 filter. The corresponding unfiltered PSD is shown in figure 4-25. Typically, the analysis results at a KRASH model lightweight mass show an expected high short-duration peak. The peak accelerations associated with the two test measurements are lower and consistent with each other. The PSD results indicate that all three responses have a frequency contribution at around 150 Hz. However, the test data shows additional higher-frequency modes, including a major input at around 700 Hz. Since the time history data is filtered at 300 Hz, it is not observed in the figure 4-24 plot.

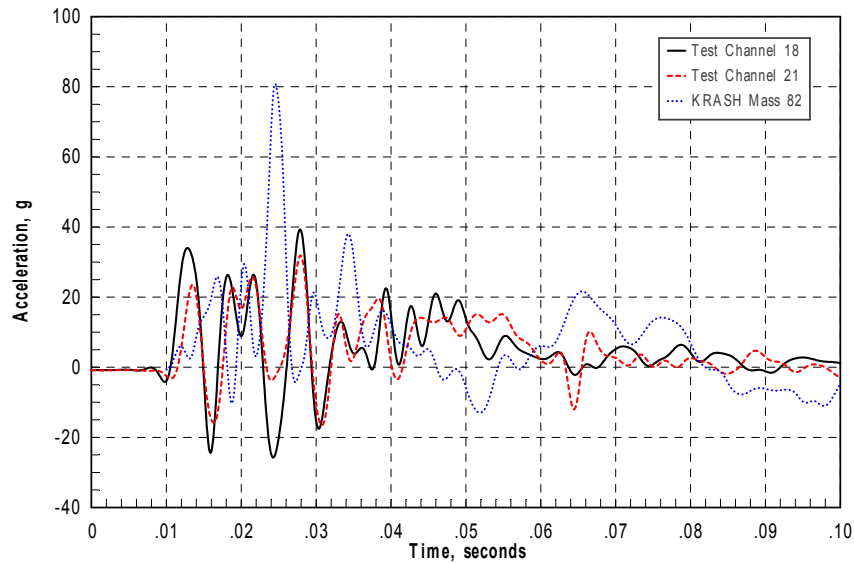


FIGURE 4-24. S1 FLOOR AZ TIME HISTORY CORRELATION, FS 155 BL 35.21, SAE CLASS 180 FILTER

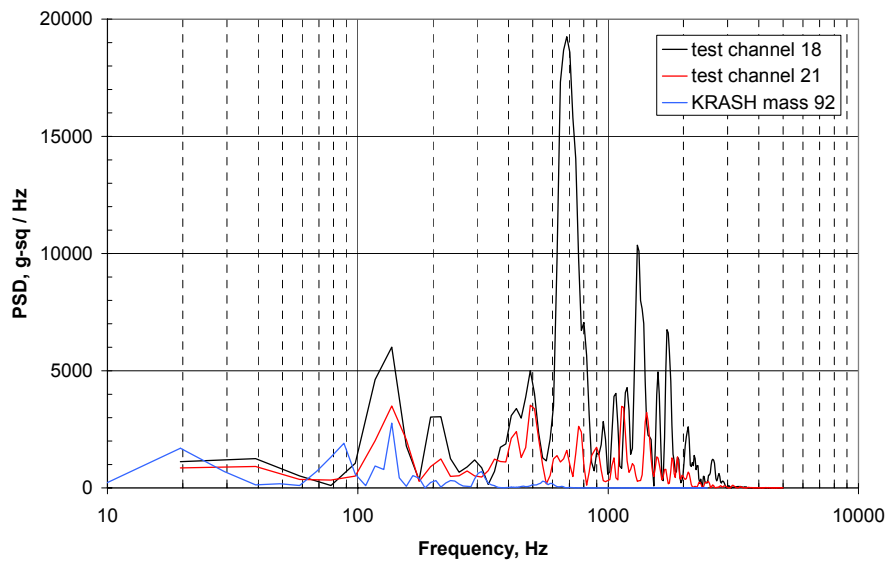


FIGURE 4-25. S1 FLOOR AZ PSD CORRELATION, FS 155 BL 35.21, UNFILTERED LINEAR SCALE

An attempt was made to compare time history amplitudes with PSD amplitudes. The difficulty encountered was in deciding what level of filtering to use, or if unfiltered data were appropriate. The problem with using unfiltered accelerations is, as was noted in the discussions about filtering effects, that some locations have such extremely high peaks that even normalization of data is misleading. Test pressures, as was also noted earlier, are also very sensitive to filter level, unlike the analysis results. Another problem in comparing PSD amplitudes with time history amplitudes is that the PSD amplitude is affected by sample size. The time history and PSD plots have different amplitude scales. The amplitude scale for a time plot is g. The amplitude scale for a PSD is g^2/Hz . The only possible attempt to compare amplitudes is by using normalized data.

Table 4-1 provides normalized time history and PSD data for class 60 and class 180 filters at several floor and slab locations. Normalized data does allow one to see that relative amplitude relationships in the time domain are also observed in the frequency domain. However, absolute amplitude matches are not possible.

TABLE 4-1. S1 NORMALIZED PEAK ACCELERATION AMPLITUDES

Location	SAE Class 180 Filter			SAE Class 60 Filter		
	Time	PSD	Frequency (Hz)	Time	PSD	Frequency (Hz)
FS 42 BL 14 (Slabs)						
Test channel 1	0.86	0.96	< 20	0.93	0.96	< 20
Test channel 4	1.00	0.90	< 20	0.82	0.90	< 20
KRASH mass 3	0.88	1.00	< 35	1.00	1.00	< 35
FS 84.5 BL 14 (Slabs)						
Test channel 7	0.50	0.50	40	0.42	0.50	40
Test channel 8	0.64	0.64	< 20	0.42	0.50	< 20
KRASH mass 4	1.00	1.00	< 15	1.00	1.00	< 15
FS 120 BL 37.3 (Floor)						
Test channel 14	1.00	0.62	300	1.00	0.50	
Test channel 15	0.62	0.33	150	0.80	0.17	
KRASH mass 62	0.68	0.43	20	0.93	1.00	20
FS 129 BL 14 (Floor)						
Test channel 10	1.00	1.00	200	0.30	0.50	
KRASH mass 71	0.87	0.47	30	1.00	1.00	30
FS 155 BL 14/20 (Slab)						
Test channel 16	0.50	0.08	20-40	0.45	0.13	20-40
Test channel 17	0.85	0.35	100	0.57	0.38	100
KRASH mass 6	1.00	1.00	< 20	1.00	1.00	< 20
FS 155 BL 35.2 (Floor)						
Test channel 18	0.50	1.00	125-150	0.38	0.90	30-40
Test channel 21	0.40	0.67	125-150	0.33	0.80	20-40
KRASH mass 82	1.00	0.50	125-150	1.00	1.00	20, 90

Comparisons of the frequency content in the time and frequency domains as well as the modal contributions are discussed in sections 4.3.3 and 4.3.4.

4.3.3 Analysis of UH-1H KRASH S1 and S2 Modal Contributions.

From the modal analysis of the KRASH UH-1H S1 and S2 models presented in section 3.3.3, it was shown that the first 40 to 50 flexible modes are less than 30 Hz. The modal analysis further indicated that the first 400 modes were below 180 Hz. With a multimass model, it would suggest that in addition to modes with simple characteristics, there are numerous modes with complex motions. The modal deflections of each mode were taken into consideration in determining potential contribution of modal frequencies to floor or floor slab vertical accelerations.

Animation of the mode shapes, along with vector analysis, indicates that for some modes there is an obvious dominant motion defining the mode, such as fuselage vertical bending, while for other modes there are several contributing motions.

The modal analysis showed that there are several important points to be considered:

1. The modal contributions are dependent on the loading of the structure. Thus, the contribution of modes during the S1 impact is different than for the S2 impact, beyond the differences due to structural configuration.
2. The modal analysis results are dependent on the location and type of structure, i.e., heavy- and lightweight masses will produce different frequency responses and modal contributions.
3. The final response is a summation of modal contributions and some modes can cancel out other modes.

The first 20 flexible modes for both the S1 and S2 KRASH models are provided in tables 3-13 and 3-14. The corresponding first 11 flexible modes from the FEM model of the S2 test configuration are shown in table 3-2. The latter is based on a weight of 8577 lb., while the S1 and S2 models are for weight configurations of 7571 and 7955 lb.

The KRASH hybrid and the FEM model configurations have differences. These differences include (1) the number of degrees of freedom, (2) the local mass-stiffness relationships, (3) the FEM data denotes only the first 11 primary modes, and (4) the FEM data show modal vectors.

Comparisons of the S1 and S2 KRASH model modes and FEM modes are provided in tables 4-2 and 4-3. The S2 model is a better representation to compare with the FEM flexible modes because the weight difference is less and the two configurations are closer (both have the tail section, landing skids, transmission, and engine included).

TABLE 4-2. RELATIONSHIP OF KRASH S1 FLEXIBLE MODES TO FEM MODES

KRASH S1 Modes			FEM Modes	
mode	freq - Hz	description	freq	description
1	6.05	fuselage 1st vertical bending	7.72	fuselage 1st vertical
2	8.49	fuselage torsion	6.45	fuselage 1st lateral
3	9.93	fuselage 1st lateral bending & torsion		
4	10.58	fuselage 2nd vertical bending - trans slab vertical	15.27	fuselage 2nd vertical
5	10.79	fuselage 3rd vertical bending - trans slab vertical		
6	11.39	fuselage 2nd lateral bending & torsion	16.55	fuselage 2nd lateral
7	11.91	forward fuselage vertical bending		
8	12.06	fuselage 3rd lateral bending - tail slab torsion		
9	12.58	fuselage vertical bending - floor slab vertical		
10	13.00	forward fuselage vertical bending - transmission slab		
11	13.03	forward fuselage vertical - aft fuselage torsion		
12	13.72	fuselage vertical & lateral bending - floor slab vertical		
13	13.90	roof vertical - floor slab & transmission slab vertical		
14	14.60	roof lateral		
15	14.70	roof vertical & lateral		
16	15.22	roof & forward fuselage torsion		
17	15.49	fuselage torsion, lateral & vertical bending	18.43	fuselage torsion
18	16.18	windshield lateral - floor slab vertical		
19	16.68	tail slab vertical bending - engine/trans slab vertical		
20	16.87	fuselage vertical bending - transmission slab vertical		

TABLE 4-3. RELATIONSHIP OF KRASH S2 FLEXIBLE MODES TO FEM MODES

KRASH S2 Modes			FEM Modes	
mode	freq - Hz	description	freq	description
1	3.01	fuselage vertical bending		
2	3.56	fuselage lateral bending	8.51	fuselage 1st lateral bending
3	3.92	fuselage vertical bending - rotor mast fore-aft	3.61	pylon pitch
4	5.39	fuselage torsion & lateral bending	3.37	pylon roll
5	7.45	fuselage torsion & tail rotor lateral		
6	7.79	fuselage vertical bending	6.71	fuselage 1st vertical bending
7	9.56	fuselage torsion & tail lateral bending	21.38	fuselage torsion
8	10.36	fuselage lateral bending & torsion	21.95	fuselage 2nd lateral bending
9	10.93	fuselage vertical bending - forward fuselage vertical		
10	11.53	fuselage vertical bending	17.4	fuselage 2nd vertical bending
11	14.06	fuselage vertical/lateral bending - engine, trans, skids	13.64	engine lateral
12	15.07	forward fuselage torsion - skids		
13	15.46	forward fuselage torsion - skids fore-aft & lateral		
14	15.60	engine/trans vertical - skids fore-aft & lateral	15.27	LG skid lateral
15	15.89	skids lateral & vertical	16.14	LG skid vertical
16	16.05	fuselage lateral bending - skids fore-aft		
17	16.20	fuselage lateral bending - skids fore-aft - trans vertical		
18	16.39	skids fore-aft		
19	16.53	fuselage vertical bending - skids & engine fore-aft		
20	17.00	fuselage lateral & vertical bending - skids & engine fore-aft		

The relationship between possible model changes and correlation results are:

- The KRASH model tail section appears to be too soft and contributes greatly to the two lowest frequency flexible modes (3.01 and 3.56 Hz). Stiffening these sections should alter these modes. However, the correlation results that have been presented earlier should not be materially affected by the modeling in this region since the primary accelerometer measurements are on the cabin floor.
- The KRASH fuselage model appears softer than the aircraft. There are several coupled bending and torsion modes from 3.92 to 7.79 Hz, which are lower than the FEM first vertical and lateral bending modes of 6.71 to 8.51 Hz. These coupled KRASH modes are much lower than the FEM first torsion and higher order bending modes (17.4 to 21.38 Hz). It appears that increasing fuselage stiffness would be worth investigating. However, since some of the modes, such as torsion and lateral bending, may not be significant in the test symmetrical impacts, the effect on the correlation results is uncertain.
- The KRASH model indicates appreciable transmission top mass motion in the 3.05 and 3.92 Hz modes as well as several higher modes. This seems reasonable based on the FEM model pylon modes at 3.37 and 3.61 Hz.
- The KRASH model indicates substantial movement of the skids at frequencies between 15 and 17 Hz. The FEM also shows landing gear skid modes in this range. However, since the skids are ineffective in water and ground impacts, this good correlation is not particularly relevant for crash conditions.
- The KRASH model contains a coupled mode with engine, fuselage bending, transmission, and landing gear motion. This mode is at 14.06 Hz. The lowest FEM engine mode shows lateral motion at 13.64 Hz.

Table 4-4 compares the frequency content observed in the frequency domain (PSD) with the frequency content from the time domain at two primary locations (FS 42 BL 14 and FS 129 BL 14). Also shown in table 4-4 are the frequencies predicted from modal analysis. The comparisons indicate agreement in the correlation between time and frequency domains with regard to common ranges of frequencies that exist, although it is hard to identify precise frequencies. However, relative contributions at each frequency cannot be related between the time and frequency domain. The slab analysis tends to lower frequency responses, as has been noted earlier.

Changes to the model to bring the modal frequencies and mode shapes in line with the actual configuration, as determined by FEM analysis, are warranted. That has to be done judiciously by establishing priorities with regard to which modes may be significant and examining each change independently of others.

How one interprets modal analysis results likewise has to be properly thought out. When looking at the response data, one has to bear in mind that the frequencies that are present are a

function of the modal contributions. One may not see all of the lowest frequencies, if in fact they are not major contributors, due to the manner in which the structure is excited.

It also has to be recognized that modal analysis is strictly a linear phenomenon and that crash impact accelerations usually are greatly influenced by nonlinear behavior.

TABLE 4-4. S1 ACCELERATION FREQUENCY CONTENT COMPARISON—TIME HISTORY VS PSD RESULTS VS MODAL CONTRIBUTION

Location	Time History* (Hz)	PSD (Hz)	Predicted Modal Frequency (Hz)
FS 42 BL 14			
Test channel 1	20, 166, > 200	< 20	NA
Test channel 4	20,	< 20	NA
KRASH mass 3	12	< 35	6, 15-28
KRASH mass 31	25, 200	30, 60, 90	6, 28, 54-88, 160-175
	200		
FS 129 BL 14			
Test channel 10	40, 140, 200	100, 200	NA
Test channel 12	40, 140, 200	100, 220	NA
KRASH mass 71	40, 100, 300	30, 70, 180	80-90, 135-177
KRASH mass 5	15	< 10, 40, 100	6, 12-17, 21-58

Note: Red= Indicates PSD peak amplitude occurrence

*Based on class 180 (300 Hz) cutoff frequency

4.3.4 Relationship Among Acceleration Time History, PSD Analysis, and Modal Analysis.

This section describes how the anticipated KRASH modes compare to the measured modes. For illustrative purposes, two floor locations (FS 129 BL 14.0 and FS 42 BL 14.0) are examined. These two stations represent occupant and seat locations.

Figures 3-11 and 3-16, provided in section 3.3.1 for the discussion on PSD analysis, are used in this section for FS 129 analysis. The analysis data are for both a lightweight floor mass and a substantially heavier slab mass. The following discussion relates S1 time history frequencies to PSD frequencies.

- From the acceleration time histories (figure 3-11) it may be possible to estimate a frequency for the test and analysis. Some frequencies that one might detect are approximately >100, 200-220 Hz for the test (channels 10 and 12), and lightweight analysis mass 71. The test channels and mass 71 also show a possible low frequency response component around 25-40 Hz. These results compare favorably with test PSD peak amplitudes (figure 3-16) that occur at a frequency around 200 Hz, with lesser peak responses at frequencies between 100-120 Hz. The PSD also shows that lightweight

KRASH mass 71 has a peak amplitude response at around 30 Hz with lesser responses at 70 and 180 Hz.

- The KRASH slab (mass 5) time history exhibits a primary response of about 15 Hz. The corresponding PSD for mass 5 shows a peak response at 10 Hz and other contributions at 40 and 100 Hz.

Similarly, the plots shown in figures 4-26 and 4-27 provide S1 time history versus PSD results at the other occupant and seat fuselage location (FS 42 BL ± 14).

- From the acceleration time histories (figure 4-26), frequencies that may be detected are similar to those for FS 129 accelerations. The test channels (1 and 4) and lightweight KRASH mass 31 responses exhibit high-frequency pulses (> 200 Hz), along with possible lower-frequency responses of around 25 Hz.
- The PSD results (figure 4-27) for both the test and lightweight KRASH mass 71 indicate a high response below 30 Hz. The mass 71 PSD also shows lesser contributions at 60, 90, and >110 Hz.

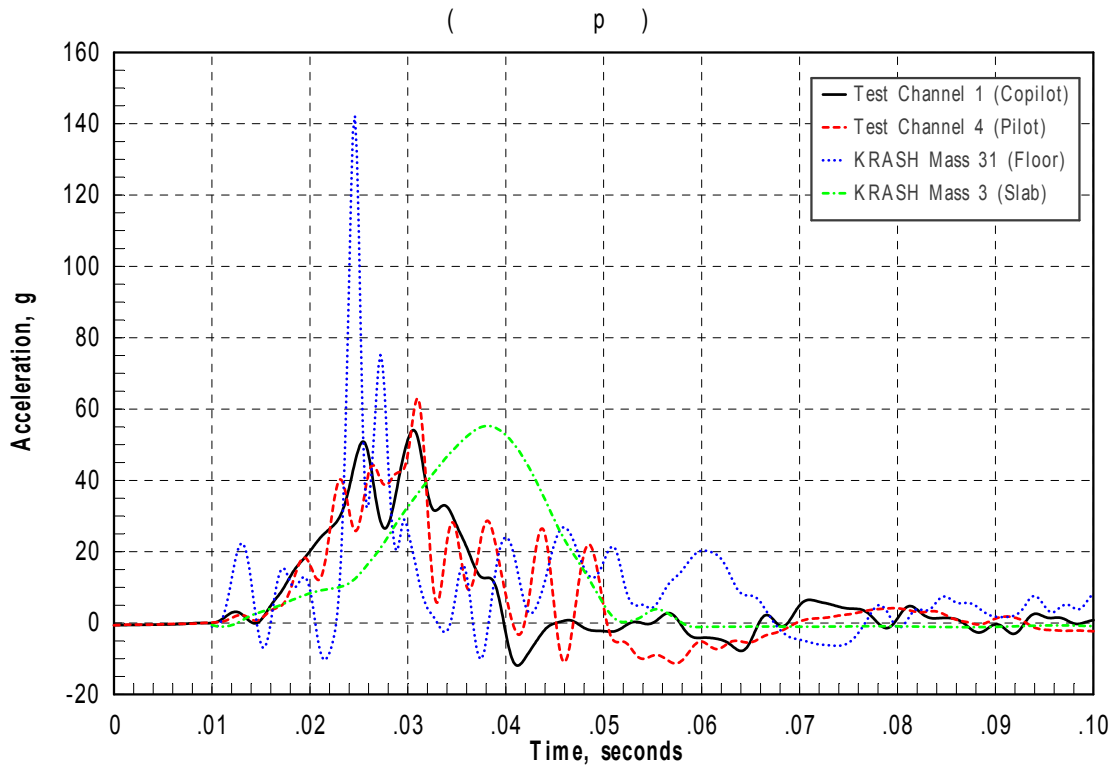


FIGURE 4-26. S1 FLOOR AND SLAB AZ TIME HISTORY CORRELATION, FS 42-47
BL 14-22, SAE CLASS 180 FILTER

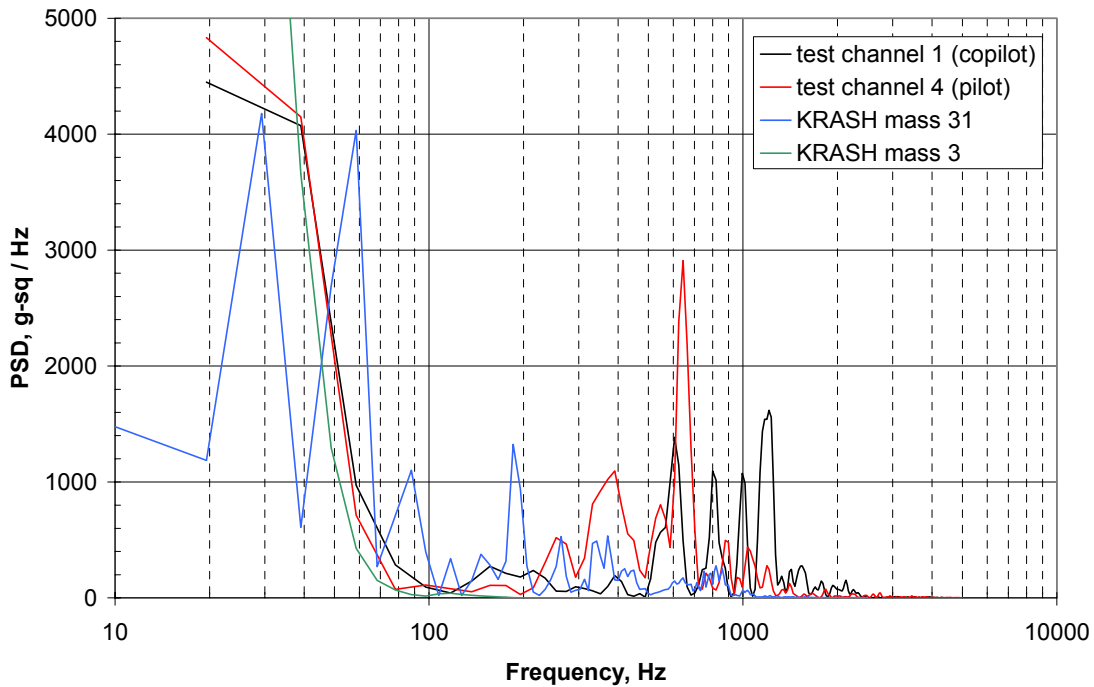


FIGURE 4-27. S1 FLOOR AND SLAB AZ PSD CORRELATION, FS 42-47 BL 14-22, UNFILTERED LINEAR SCALE

The modal analysis results presented in section 3.3 show that there are 90 modes below 40 Hz, with distinct bending, torsion, and lateral modes below 10 Hz. The available FEM modal analysis also indicates that the fuselage lower-order first lateral bending and vertical bending modes are in the range of 6.45-6.71 and 7.72-8.51 Hz, respectively. The KRASH modal analysis indicates these lower-order fuselage bending modes at 9.93 and 6.05 Hz, respectively. This appears consistent with (albeit softer than) the FEM modal data.

Of interest is whether the predicted KRASH model modal contributions show up in the test and analysis results. With this in mind, PSD frequencies of the KRASH model were compared to the predicted modes from the KRASH modal analysis. Modal contribution data from tables 3-16 and 3-17 for S1 and from tables 3-20 and 3-21 for S2 are used. These comparisons were performed at the same two locations previously discussed.

1. For the FS 129 BL 14 location

- The KRASH modal analysis suggests that the slab response (mass 5) could be greatly influenced by a 6.05 Hz fuselage first bending mode and several other frequencies up to and even above 60 Hz. This is consistent with time history and PSD results for this location, which both showed a significant response at < 25 Hz.

- The KRASH modal analysis shows the floor response (mass 71) to be sensitive to frequencies around 80-90 Hz and as high as 176 Hz. The PSD for the KRASH mass 71 shows a peak frequency around 30 Hz, which is not consistent with the potential lowest modal contribution. A 180 Hz response does show up in the PSD plot, which is consistent with the modal analysis range of 135-177 Hz. However, the acceleration time history shows a series of short-duration pulses, which indicate a frequency of 200 Hz.
- The test channel acceleration time histories and PSD results indicate a primary frequency contribution at or above 200 Hz. That frequency range represents a local mode that is difficult to visualize from the modal analysis, which shows the first 250 modes are below 200 Hz.

2. For the FS 42 BL 14 location

- The modal analysis indicates that the slab mass 3 response will be greatly influenced by the 6.05 Hz fuselage first bending mode, followed by several other contributing modes, ranging in frequency up to 30 Hz. The KRASH acceleration time history and associated PSD analyses show that the KRASH slab mass 3 response is indicative of a very low frequency (< 25 Hz). This is consistent with the modal analysis results.
- The modal analysis indicates that the floor mass 31 might be greatly influenced by the first mode (6.05 Hz), followed by several higher-frequency modes: 28.38 Hz, 50-80 Hz, and 160-175 Hz. The PSD for the lighter KRASH mass 31 shows a primary frequency contribution around 30 Hz and lesser contributions at various frequencies (60, 90, 110-300 Hz). The acceleration time history shows a series of short-duration pulses, indicating a frequency of 200 Hz or higher. This latter frequency does show up in the PSD analysis, but appears to be a lesser contributor.
- The test PSD results for this location suggest that the major frequency contributor is less than 40 Hz, with lesser contributions at various higher frequencies (400, 650, > 1000 Hz). This seems to be consistent with mass 31 results, where some higher-frequency responses are noted. The higher PSD frequencies are also noted in the mass 31 and test acceleration time histories. The shortness of the higher-frequency pulses (the same can be said for KRASH mass 31) may not produce substantial energy, which is symptomatic of lightweight structure responses.

The comparison of S1 time history, PSD, and predicted modal contribution frequency results is noted in table 4-4. The comparisons indicate agreement in the correlation between time and frequency domains and modal contribution results with regard to common ranges of frequencies that exist, although it is hard to identify precise frequencies.

The S2 results are shown to be similar to S1 results with regard to frequency content in the time domain, the frequency domain, and the predicted modal contributions. To illustrate this point,

the time and PSD results for a forward fuselage location are presented, and the PSD analysis frequency content versus the predicted modal contributions are compared for a forward and mid-fuselage location.

The acceleration time history and associated PSD analysis for the pilot/copilot location is shown in figures 4-28 and 4-29, respectively. The results are presented for the pilot/copilot test slab channels 1 and 4 (FS 55 BL ± 22) versus KRASH slab mass 3 (266 lb. at FS 60 BL 22) and floor lightweight mass 31 (12 lb. at FS 42 BL 14). The first three modal contributions for KRASH slab mass 3 are 24.4, 11.5, and 24 Hz (table 3-20). The first three modal contributors for KRASH floor mass 31 are 38.2, 46.6, and 59.1 Hz (table 3-21).

The PSD analysis shows a noticeable frequency contribution in the range of 22-28 Hz for mass 3 and a distinct 50 Hz frequency for mass 31. The test PSD results indicate very low (< 10 Hz) frequencies at both channels and some additional frequencies at 20-30 Hz. There is a modal frequency around 3 Hz, but it is not considered a top ten major contributor. The time history and PSD relative amplitudes both suggest mass 31 is much higher than the others. However, while the time history and tabulated data (table 3-7) suggest the mass 3 amplitude is higher than the two test channel amplitudes, the PSD indicates that substantial test amplitude exists at below 10 Hz for channel 1, far in excess of channel 4. This appears inconsistent with tabulated data, which shows test data fairly consistent at class 60 and class 180 filters.

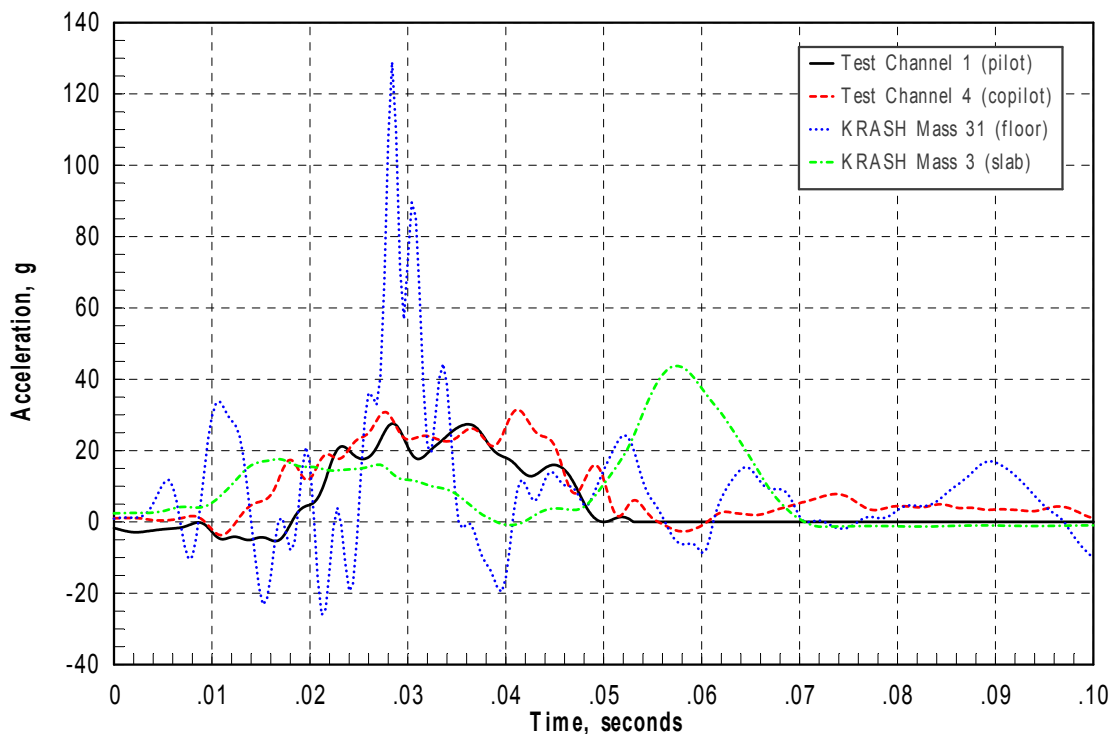


FIGURE 4-28. S2 FLOOR AND SLAB AZ TIME HISTORY CORRELATION, FS 42-60 BL 14-22, SAE CLASS 180 FILTER

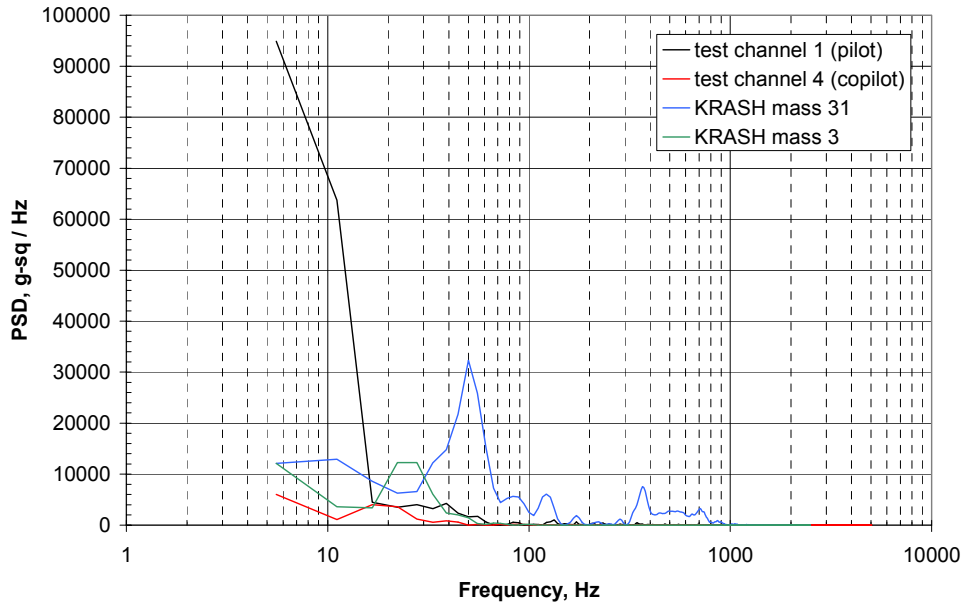


FIGURE 4-29. S2 FLOOR AND SLAB AZ PSD CORRELATION, FS 42-60 BL 14-22, UNFILTERED LINEAR SCALE

Table 4-5 presents the results for S2 PSD and the predicted modal frequency results. The comparisons indicate agreement in the correlation between frequency domain and modal contribution results with regard to common ranges of frequencies that exist, although it is hard to identify precise frequencies. The S2 results are also similar to the S1 results previously described, in that

- the frequency content of the time history and PSD results compares favorably.
- frequency content differences exist between slab or heavy floor masses and light floor weights.
- there is no clear indication that test PSD results are displaying distinct KRASH modes. The PSD results are displaying the S2 modal analysis potential contributing modes. However, since many of the KRASH modes exhibit coupled motions, it is difficult to say that any one mode predominates.

The fact that the KRASH model is softer than the FEM model suggests that future KRASH UH-1H models be improved in an effort to match some of the lower-frequency FEM modes better. Potential steps to alleviate these differences may be:

- Match analysis test weight representations
- Stiffen up local regions that show excessive motion
- Tune lower modal frequencies better before comparing with test data
- Refine how modal contribution factors are determined for different scenarios
- Obtain reliable PSD results at extreme low frequencies

TABLE 4-5. S2 ACCELERATION FREQUENCY CONTENT COMPARISON, PSD RESULTS VS MODAL CONTRIBUTION

Location	PSD ¹ (Hz)	Predicted Modal ² Frequency (Hz)
FS 42 BL 14		
Test channel 1	< 10, 20-30	NA
Test channel 4	22-28	NA
KRASH mass 3	50	24.4, 11.5, 24
KRASH mass 31	22-28	38.2, 46.6, 59.1
FS 129 BL 14		
Test channel 10	<10, 50-70	NA
Test channel 12	<10, 50-70	NA
KRASH mass 5	15-20	31.6, 16.2, 18.1
KRASH mass 71	70, 90	79, 46, 102

Note: Red= Indicates PSD peak amplitude occurrence

¹ Based on class 180 (300 Hz) cutoff frequency

² First three modal contribution frequencies

4.4 APPLICABILITY OF HILBERT SPECTRA AND HHT.

To help understand the potential application of the Hilbert Spectra to the crash impact scenarios, an evaluation of a sample channel of test data was performed by the NASA Goddard Space Flight Center. A 2.0-second trace of a test acceleration floor response (channel 1) at FS 42 BL 14 was used. The acceleration pulse was analyzed and the results of the HHT analysis are provided in figures 4-30 through 4-33.

The unfiltered acceleration versus time response from the test data at FS 42 BL 14 is shown in figure 4-30. The results in figure 4-30 indicate that the primary response occurs at less than 0.100 second after impact and is most prominent in the region of 0.030 to 0.040 second. Figures 4-31 through 4-33 provide Hilbert spectrum results. The plot in figure 4-33 shows that the more intense activity takes place in the 0.030- to 0.040-sec time frame, and there are several frequencies contributing with various intensities, as the intensity chart in figure 4-31 indicates.

Figure 4-32 is a three-dimensional (3D) plot (energy, frequency, and time) that shows the lowest frequencies provide the most energy throughout the 0.100-second postimpact interval shown. Figure 4-33 compares the marginal Hilbert and Fourier transform, the latter is used in the PSD process. The Hilbert transform represents a nonstationary and nonlinear process, whereas the Fourier transform represents a stationary and linear process.

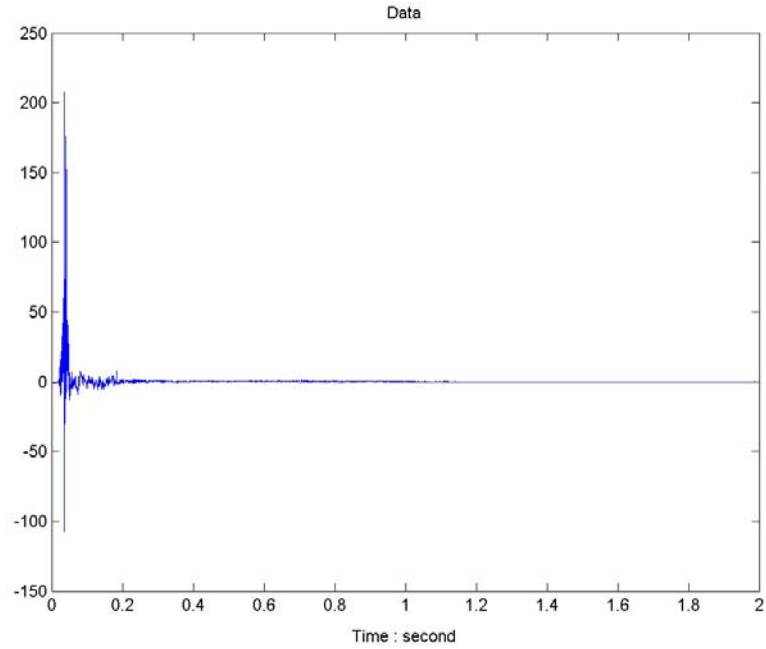


FIGURE 4-30. ACCELERATION 2.0-SECOND TIME HISTORY, FS 29 BL 22, TEST S1 CHANNEL 1

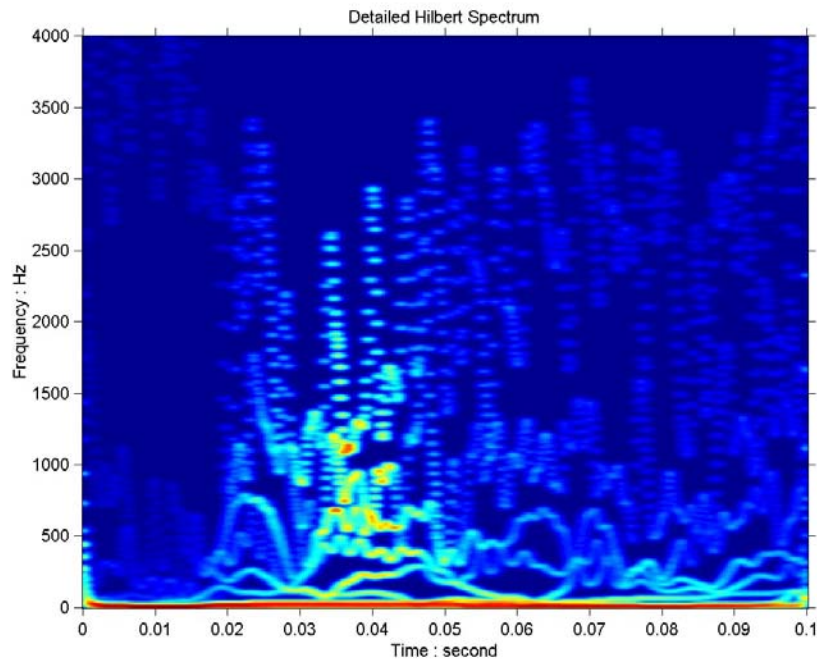


FIGURE 4-31. HILBERT SPECTRUM—FREQUENCY VS TIME—0.10 SECOND

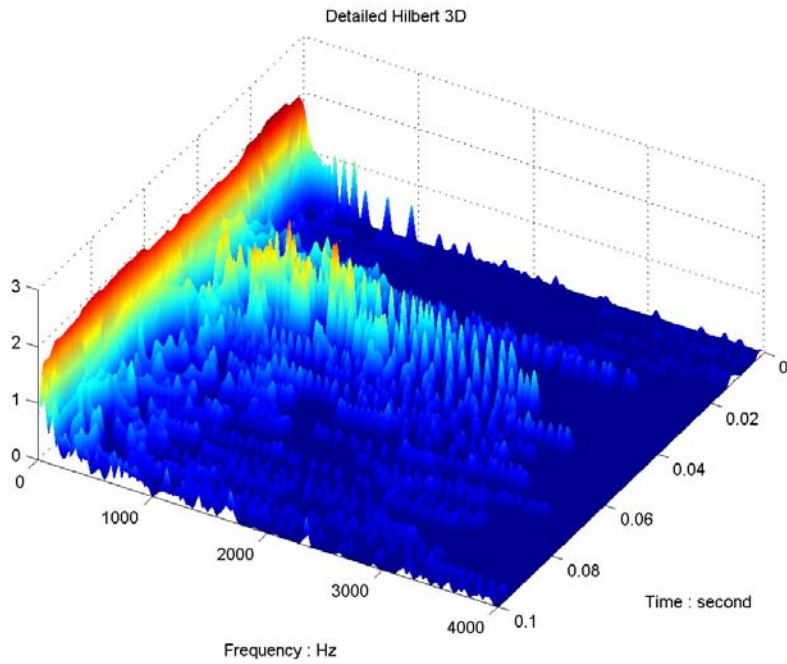


FIGURE 4-32. DETAILED HILBERT 3D SPECTRUM—AMPLITUDE-FREQUENCY-TIME—0.10 SECOND

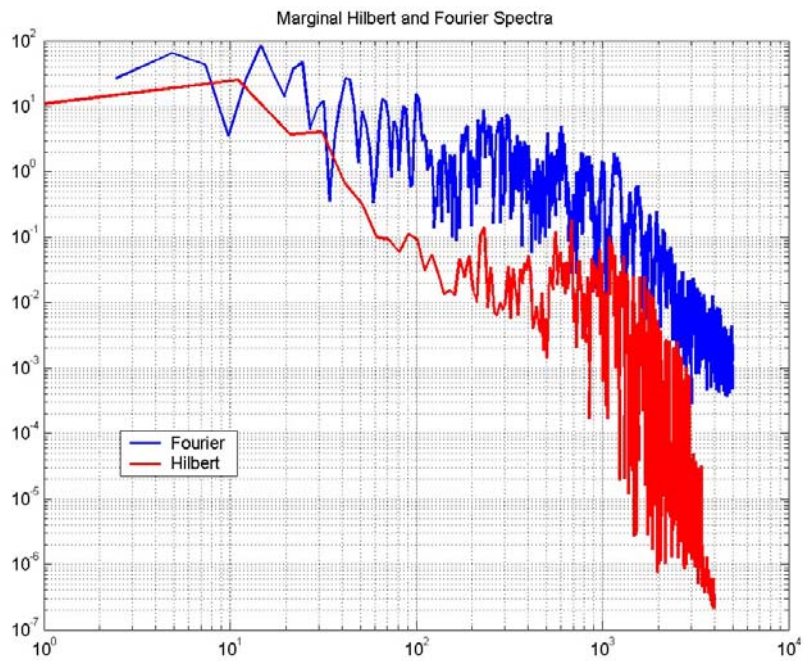


FIGURE 4-33. MARGINAL HILBERT AND FOURIER SPECTRA—AMPLITUDE VS FREQUENCY

The amplitude versus frequency content between the two spectra indicates that there may be higher-frequency contributions from the Fourier spectra than from the Hilbert spectra for this particular signal. However, in general, they both indicate higher amplitude in the lower-frequency regime (10-50 Hz). When one combines the results from figures 4-30 through 4-33, it can be observed that there are many frequencies throughout the response history, but that the most intense amplitude is at time < 0.100 second and closer to 0.040 second. The most intense energy levels are at the lowest frequency. From this set of results it is hard to pinpoint the frequency of most interest, but it appears to be the lower-frequency range.

When one reviews the sample HHT results and compares them to the evaluation of the PSD modal analysis results for this particular location, provided in section 4.3.4, it appears that they are consistent. The conclusions borne from the test data alone certainly indicate about the same interpretation and meaning. Since the KRASH analysis PSD and time histories at this location are in agreement with the test data, one would have to assume if the HHT were extended to the KRASH analysis data, it also would be consistent. However, as noted in section 4.3.4, at location FS 129 there can be differences between analysis and test results.

4.5 APPLICABILITY OF FORCE RECONSTRUCTION TECHNIQUE.

SNL considers the SWAT procedures more applicable than the DECON procedures for the water impact scenarios. This procedure uses the modal characteristics to calculate weighting functions, which allow summing acceleration measurements from different points on the specimen to reconstruct the force. The data requirements set forth by SNL include:

- A description (drawing) of the test article
- Description of the test
- List and description of test accelerometers (manufacturer, model, etc.)
- ASCII files of unfiltered test and analysis acceleration data and associated bandwidth
- Accelerometer test and analysis locations
- Description of the analytical model and analysis code
- Description of analysis input to the model for crash simulation
- Modal analysis results

All of the above data requirements are available. Unfortunately, a sample run of either a set of test or analysis data was not able to be obtained during this effort. Thus, an opportunity to examine the type of results that can be achieved from the Force Reconstruction procedure is not available.

Based on the example and the limitations described in section 3.5, it is difficult to fathom that this technique is applicable to crash testing. It appears that the technique is used to define the force that causes the responses measured. For the type of structure analyzed thus far, there is a limited and known force application location. In the S1 and S2 tests, there are multiple force inputs that occur randomly and over time. There are 30 panels at which impact forces enter. The influential airframe modes are closely coupled. Most of the measured responses are on the cabin floor and predominantly normal to the floor (vertical). For example, in the S1 test, there are 11 vertical-only accelerometer measurements and 4 triaxial measurements. Several fuselage

underside panels failed during the impact. Since the impact is primarily vertical and symmetrical and over a broad flatbottom fuselage, one might at best expect the Force Reconstruction technique to be able to determine a relatively uniform force over the bottom of the aircraft. From the analysis, these forces are provided. One might be able to compare these forces.

In the S2 test, there are five triaxial, three unidirectional (vertical) and three biaxial (vertical and longitudinal) cabin floor accelerometer locations. In addition, there are engine and transmission mass triaxial accelerometers. While the measurements are more conducive to obtaining an overall c.g. force or pulse, the impact condition is more complicated. The combined forward-vertical impact with a nose-up attitude means that the impact sequence is not flat and uniform. Several slab attachments also failed during this test. In water impact tests, there is no way to measure contact reaction forces. Thus, full-scale water impact testing may be a more difficult application for Force Reconstruction.

4.6 APPLICABILITY OF AUTOMOTIVE INDUSTRY REGULATIONS AND PRACTICES.

The automotive industry differs from the aircraft industry in several respects, including:

- The automotive industry has an extensive set of regulations that encompass specified impact conditions and injury criteria versus either a set of velocity envelopes or seat/occupant tests with limited injury criteria for the aircraft industry.
- Crash testing of complete automobiles is a routine event (some manufacturers do one test a day). The number of vehicles is many, the occupant dummy/seat/restraint systems are relatively few per vehicle and can be easily contained within the vehicle, and the cost per vehicle is relatively small when compared to civil or military aircraft. Testing of seat/occupant dummy/restraint systems subjected to a defined pulse is the closest the aircraft industry comes to a routine procedure.
- The automotive industry requires that compliance with the regulations come from testing and the analysis of the test data. This is not unlike the aircraft industry at this time, since civil CFR requirements emphasize seat dynamic testing and lumbar and head injury criteria. However, in the automotive industry, the manner in which injury is assessed is much more descriptive and detailed. Not only from full-scale crash test data, in which the occupant/restraint/protective system is included in the test vehicle, but also from component testing (i.e., FMVSS No. 201, as described in document NHTSA-96-1762 and the Federal Register). By contrast, in the aircraft industry, the occupant/restraint system is removed from the vehicle and tested to specified pulses intended to be representative of a survivable crash. While described in the respective CFR, the details are far less rigorous than that of the automotive counterparts.
- Car companies have large specialized departments devoted to crash modeling, in addition to separate crash test facilities. By way of contrast, aircraft manufacturers assign a crash specialist or two to model simulation.
- Crash safety is a major consideration in the car industry. Aircraft performance is the driving design consideration for the aircraft industry.

Crash design requirements are different for military and civil aircraft. The military is a customer that specifies the requirement for each new configuration or design. The design cycle, other than for derivatives, occurs every decade or two. The U.S. Army Crash Survival Design Guide provides a comprehensive set of crash design principles and guidelines, but is not a requirement by and of itself. The appropriate military service branch defines its own specifications. Performance, and not crashworthiness, is the major design and acceptance consideration.

Generally, the specifications define dynamic crash acceleration specifications such as those that relate to engine, transmission, and fuel tank, along with seat dynamic tests. The regulations for civil aircraft and the manner in which they are to be complied with are defined in the appropriate CFR. Seat dynamic testing and ditching scale model testing are specified, along with acceptable criteria for these respective tests. In some instances, derivatives of existing designs, i.e., ditching, are accepted by similarity.

In many respects, the state of the art in the use of analysis in the aircraft industry is on a par with the automotive industry. For example:

- There is no standard simulation code. Each company decides on their own simulation code. FEM codes such as MSC-DYTRAN are used in the U.S., and others such as PAM-CRASH or LSDYNA3D are used outside the U.S. for analysis of structure. A hybrid code such as KRASH is also used widely throughout the aircraft community. However, to date, the analysis of structures for compliance with the regulations is neither required nor has it been considered as an alternative approach to testing.
- There is no agreed definition of good correlation. The prevailing opinion seems to be that acceptable correlation is achieved when (1) peak values are within 20% agreement; (2) reasonable deformation and failure matches occur; (3) accountability for the kinematics of the impact simulation; i.e., velocity change is reasonable; (4) the sequence of events noted during the test are reproduced in the analysis; and (5) other parameters such as credible energy dissipation and distribution adds to the confidence level.
- Filtering of data, generally in accordance with SAE J211 standards, is used in both the aircraft and automotive industries.
- Injury assessment, while not always the same requirements or in the same detail between the two industries, is defined in the respective standards.

4.7 COMPARISON OF S1 AND S2 TEST AND ANALYSIS TRENDS.

Many relationships between the test-measured and analytically predicted quantitative results with regard to correlation criteria, filter level, modal analysis, PSD analysis, and other techniques has been discussed. Another significant relationship to help understand correlation results is the acceleration and pressure trends that exist between the S1 and S2 tests and analysis. These trends are noted in tables 4-6 and 4-7 and figure 4-34. Test S2 was much more severe than test S1, as measured by resultant velocities of 48 versus 26 fps and the posttest damage.

TABLE 4-6. S1 AND S2 FLOOR/SLAB ACCELERATIONS AND UNDERSIDE PANEL TRENDS—SAE CLASS 60 FILTER VS UNFILTERED

Impact Condition	S1	S2	S2/S1				
Vertical Vel - fps	26	28					
Longitudinal Vel - fps	0	39					
Resultant Vel - fps	26	48	85%				
Pitch attitude - deg.	0	4					
Average Acceleration (g)				Average Acceleration (g)			
	S1	S2	% diff. S2/S1		S1	S2	% diff. S2/S1
Analysis - SAE Class 60 Filter				Test - SAE Class 60 Filter			
Slabs only	4 pts	8 pts		Slabs only	6 pts	8 pts	
vertical	47.1	38.3		vertical	29	21.8	
longitudinal	0	11.8		longitudinal		8.6	
combined	47.1	40.1	-15%	combined	29	23.4	-19%
Floor only <100g	7 pts	2 pts		Floor only	8 pts	1 pt	
vertical	45.6	34.2		vertical	26.6	25	
longitudinal	0	14.5		longitudinal	0	5.9	
combined	45.6	37.1	-19%	combined	26.6	25.7	-3%
Slab and floor <100g	11 pts	10 pts		Slab and floor <100g	14 pts	9 pts	
vertical	46.2	37.5		vertical	27.6	22.1	
longitudinal	0	12.2		longitudinal	0	6.6	
combined	46.2	39.4	-15%	combined	27.6	23.1	-16%
No. total points	12	10		No. total points	14	10	
No. slabs	4	8		No. slabs	6	8	
Average Pressure (psi)				Average Pressure (psi)			
Analysis - Unfiltered				Test - Unfiltered			
all locations	27.4	39	42%	all locations	47	63	34%
Analysis - SAE Class 60 Filter				Test - SAE Class 60 Filter			
all locations	27.5	31.4	14%	all locations	21	22.2	6%
No. total points	21	20		No. total points	23	21	

TABLE 4-7. S1 AND S2 FLOOR/SLAB ACCELERATIONS AND UNDERSIDE PANEL TRENDS—SAE CLASS 180 FILTER VS UNFILTERED

Impact Condition	S1	S2	S2/S1				
Vertical Vel - fps	26	28					
Longitudinal Vel - fps	0	39					
Resultant Vel - fps	26	48	85%				
Pitch attitude - deg.	0	4					
Average Acceleration (g)				Average Acceleration (g)			
	S1	S2	% diff.		S1	S2	% diff
Analysis - SAE Class 180 Filter				Test - SAE Class 180 Filter			
Slabs-only	4 pts	8 pts		Slabs-only	6 pts	9 pts	
vertical	47.4	38.9		vertical	36.7	25.1	
longitudinal	0	13.7		longitudinal	0	10.5	
combined	47.4	41.2	-13%	combined	36.7	27.2	-26%
Floor only <100g	6 pts	0 pt		Floor only <100g	7 pts	1 pt	
vertical	68.8			vertical	52.5	71.6	
longitudinal	0			longitudinal	0	25.5	
combined	68.8			combined	52.5	76.0	
Floor and slab <100g	10 pts	8 pts		Floor and slabs	13 pts	10 pts	
vertical	60.2	38.9		vertical	45.5	29.7	
longitudinal	0	13.9		longitudinal	0	12.4	
combined	60.2	41.3	-31%	combined	45.5	32.2	-29%
No. total points	12	10		No. total points	14	10	
No. slabs	4	8		No. slabs	6	9	
Average Pressure (psi)				Average Pressure (psi)			
Analysis - Unfiltered				Test - Unfiltered			
all locations	27.4	39	42%	all locations	47	63	34%
Analysis - SAE Class 180 Filter				Test - SAE Class 180 Filter			
all locations	27.3	36.3	33%	all locations	29	38	31%
No. total points	21	20		No. total points	23	21	

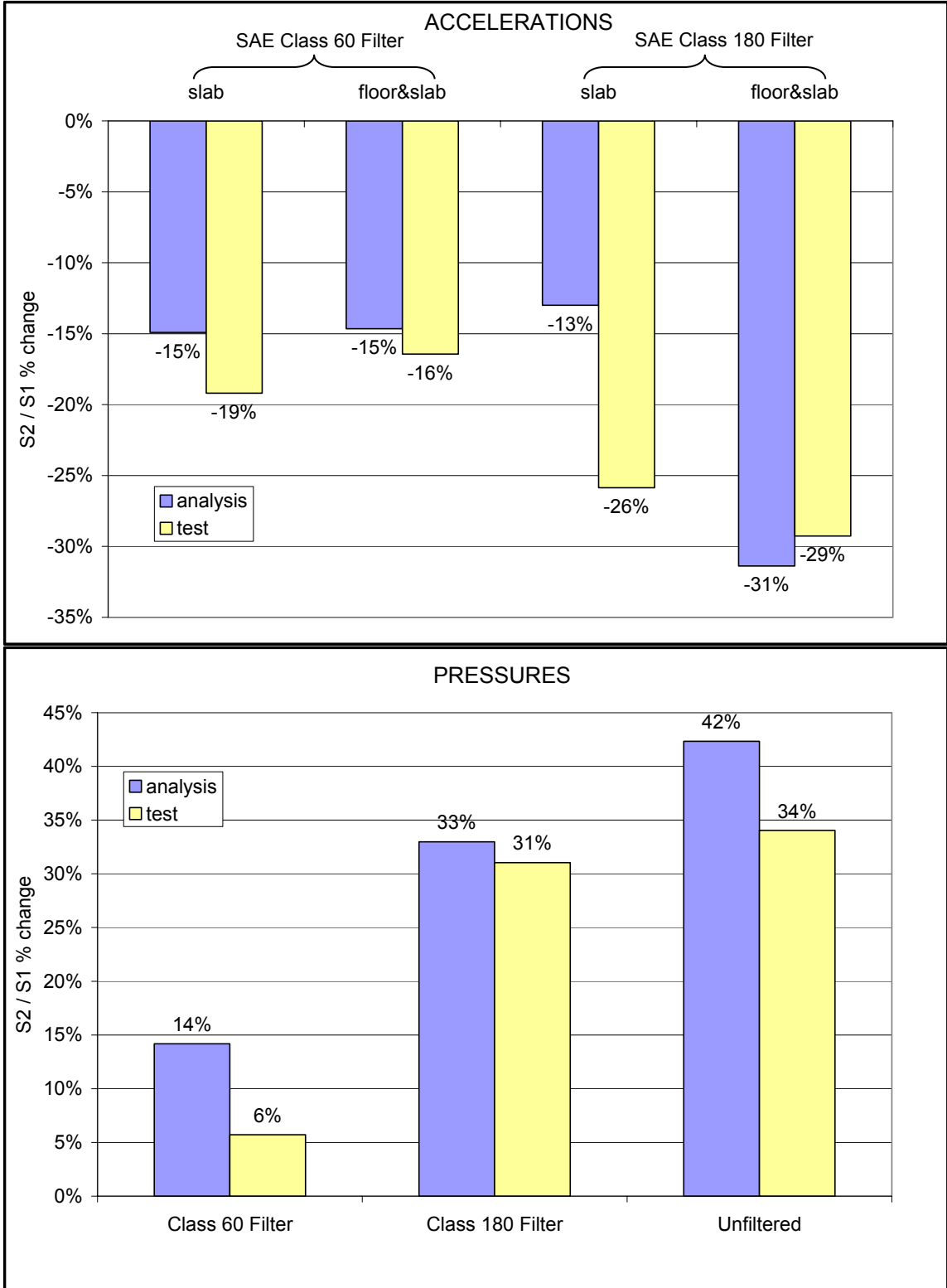


FIGURE 4-34. IMPACT SCENARIO TREND COMPARISON—ANALYSIS VS TEST—FLOOR AND SLAB—ACCELERATIONS AND UNDERSIDE PANEL PRESSURES

The acceleration trend from S1 to S2 for test and analysis are similar with regard to the acceleration for slabs and the acceleration for all responses, as are the test versus analysis pressure trends.

For the S2 test, all the filter comparisons for the underside panel pressures show increased pressures when compared to the S1 test results. The S2 to S1 test ratio results range from +6% for the class 60 filter to +34% for the unfiltered data. The S2 to S1 analysis ratio results range from +14% to +42%. Neither the analysis nor the test ratio increases are as large as one would expect from the magnitude of velocity increase from S1 to S2 (a factor of 1.85). The rationale for why the measured and predicted increases are not as large as anticipated, based on velocity increase, is as follows:

- The S1 test resulted in many panels experiencing pressure levels near to or at the failure design pressures. The S2 test, while much more severe than S1 resultant as noted by the additional panel failures, cannot produce higher underside panel pressures at the locations of the failed S1 panels. For panels that previously did not fail during the S1 test, the increase in pressure at best can produce only marginally higher underside panel pressures before failure will occur during the S2 test. Thus, the increase in pressure for S2 compared to S1 is inhibited by the limits of the panel design pressures. If one were to further increase the impact velocity, the likelihood would be that the measured underside panel pressures would not increase significantly. However, the increased forces from the higher velocities might have a greater affect on the interior structure, such as the passenger floor. To determine this affect, one would have to be able to measure passenger floor pressures or create a model to evaluate such behavior.

The class 60 and class 180 filter comparisons for the floor accelerations for slabs or for all floor responses (unfiltered not used) show negative or decreased acceleration levels for the more severe S2 test. For the class 60 filter, the test and analysis trends are almost identical, ranging from 15% to -19% regardless of location (slab and floor) or condition (test or analysis). For the class 180 data, the analysis slab responses show similar results to class 60 data (-13%), whereas the test results show a more substantial decrease (-26%). As noted in previous discussions, the analysis slab results are affected less than the test by filtering. The only other comparison for slab and floor locations show more substantial decreases (-29% to -31%) for test and analysis. However, tables 4-6 and 4-7, show that there is only one additional test point available, and that is in regard to S2 data. Thus, the comparison to include floor and slab accelerations is hindered by the limited data that is available. Since S2 is much more severe than S1, the initial expectation is that the S2 accelerations should be higher than S1 accelerations and substantially so. The possible contributing factors that may help explain the rationale for the test and the analysis results are:

- The vertical velocity component of S2 is 28 fps versus 26 fps for S1.
- The longitudinal forces may alleviate some of the vertical forces.
- The S2 test was conducted at a +4 degree nose-up pitch versus a flat S1 impact.

- The test pressures in some locations may not have increased from S1 to S2 due to design pressure limits as noted earlier.
- The number of slab points (which tend to give lower amplitudes) were much higher for both test and analysis for S2 versus S1 (6 to 9 versus 4 to 6).

4.8 ACCELERATION PRESSURE TRANSFER FUNCTION RELATIONSHIPS.

Previous discussions indicated that it is difficult to relate amplitudes between time and frequency domains. One very interesting aspect of the correlation between test and analysis, previously not addressed, is the relationship between the acceleration response and the pressure forces at various locations. In a ground impact, this relationship is the transfer of forces from the collapsible structure in contact with the ground and the floor acceleration response. Unfortunately, during most full-scale ground impact tests (particularly those that have combined vertical and longitudinal velocity), the ground reaction forces are not measured. During a water impact, panel underside force transducers provide pressure data, and analysis provides both underside panel hydrodynamic force and pressure data. Thus, for a water impact, it is potentially feasible to provide some relationship between floor acceleration response and underside panel pressure.

This is, in a sense, an acceleration to pressure (g/psi) transfer function. However, it is difficult to relate one particular acceleration point to one distinct pressure point because of the measurement locations versus analysis location and representation. Also, the choice of filtering and what class makes for difficult choices. Unfiltered acceleration data has been shown to be difficult to interpret and introduces some high peaks that can skew the data. Class 60 filters might provide unrealistic low test pressure data, as has been discussed. Thus, an attempt to develop a transfer function was performed for different regions and for class 180 filters.

Transfer functions are derived from the data in tables 3-4 through 3-9 and summarized with regard to several regions, averages, and using resultant S2 responses in table 4-8.

TABLE 4-8. S1 AND S2 ACCELERATION TO PRESSURE TRANSFER FUNCTIONS

S1	Test (g/psi)	Analysis (g/psi)	% Difference Analysis/Test
FS 42 BL 0-24	2.05	2.29	11.7
FS 85 BL 0-24	1.19	2.70	125.0
FS 105 BL 33-40	4.38	3.93	-10.3
FS 129 BL 14-22	2.59	2.91	12.3
FS 150 BL 14-22	0.29	0.40	37.9
S2			
FS 55 BL 22	0.53	1.81	241.5
FS 93 BL 14-22	1.24	1.43	15.3
FS 121 BL 0-22	1.01	0.55	-45.5
FS 150 BL 14-37	0.51	0.75	47.0

The data provided indicate that for the S1 impact condition, the test analysis transfer functions (TF) are consistent at several locations. At FS 85, the biggest disagreement exists. For the S2 impact, the TF at FS 55 is a major deviation. In general, the S1 test and analysis transfer functions are closer than the corresponding S2 transfer functions. Of interest is the S2 transfer functions are lower than the S1 transfer function. This might be related to the fact the S2 accelerations are lower than the S1 accelerations, while the pressure trends have increased, as noted in section 4.7.

Transfer functions have some viability in that there are two elements in play. The first is the amplitude of the hydrodynamic forces. The second is the ability of the model to transfer the hydrodynamic force through to the floor structure. If the analytically determined transfer function is in agreement with the corresponding test transfer function, then the model is doing something right, even if the hydrodynamic forces might be off. If the latter is the cause of disagreement between test and analysis, then the hydromodel might be altered, as has been previously discussed. If the transfer functions differ, then the potential model change might be associated with the structure representation, i.e., stiffness, frequency, and mode shape.

5. SUMMARY OF KEY POINTS.

This section summarizes some of the key findings of this effort. Included is a synopsis of some essential points related to the various aspects of correlation techniques that were investigated.

5.1 PREVIOUS S1 AND S2 CORRELATION RESULTS.

1. An SAE class 180 filter was used for the previous S1 and S2 test and analysis correlation. S1 and S2 comparisons between test and analysis showed
 - a. A difference of 6.9% to 22% for c.g. and average floor accelerations.
 - b. A difference of 4% to 8% for average fuselage underside panel pressures.
 - c. Underside panel failure rates of 80% to 90%.
 - d. Agreement between test and analysis for individual accelerometers (discrete locations) was between 25% and 33%.
 - e. Agreement between test and analysis for the corresponding individual underside panel pressures was between 18% and 25%.

5.2 CORRELATION CRITERIA.

1. Test S1 (symmetric impact, symmetric structure) shows opposite side variations on average between 20% and 23% and 0.002 to 0.007 second in time of occurrence of peak response.
2. Factors that contribute to test scatter include:
 - a. Location of instrumentation (desired versus actual)
 - b. Variation in effective weight where measurements are made on opposite side lightweight floor masses (< 10 lbs.)
 - c. Variation in placement of pressure transducers on opposite sides
 - d. Opposite side differences in design and layout of structure and panels
 - e. Inherent variation in test specimen manufacturing tolerances
3. Previous S1 and S2 test and analysis correlation was based on an acceptance criterion of 25% for peak amplitude and 10 msec. for time of peak occurrence.

5.3 FLOOR ACCELERATION SAE CLASS 60 FILTER VERSUS SAE CLASS 180 FILTER VERSUS UNFILTERED RESULTS.

1. Acceleration results at lightweight (< 10 lbs.) floor locations show high unfiltered floor responses (200-300 g) of short duration and cannot be used to characterize floor pulses.
2. Filtering results in a significant change in acceleration amplitude (50%-75%) from class 180 to class 60 for lightweight floor response results.
3. Filtering has little effect on heavy slab masses (250-650 lbs.), generally less than 10%.
4. Class 60 filtering improves correlation for lightweight floor accelerations but has no significant effect on heavier slab accelerations.
5. The use of class 60 filtering of floor accelerations is warranted in order to provide a floor pulse that can be characterized in a practical manner or can be compared to other pulses. Its use is better for purposes of seat dynamic testing, and it is also called for in the SAE guidelines.
6. Potential explanations for differences in accelerations obtained from the analysis versus test results are (1) the representative weight assigned to a particular location in the KRASH model versus the actual or effective weight at the corresponding test accelerometer location, (2) the model stiffness versus the actual aircraft stiffness either globally or at particular locations, and (3) hydrodynamic forces that are developed by analysis versus that produced during the tests.

5.4 PANEL PRESSURE SAE CLASS 60 FILTER VERSUS SAE CLASS 180 FILTER VERSUS UNFILTERED RESULTS.

1. The measured test pressures are sensitive to filter level. Class 60 filtering of test pressures reduced the average peak values to 21-22 psi, which is substantially below the estimated average design failure levels of around 39 psi.
2. The analysis pressures are unaffected by filter level for S1 (27.5 psi average). For S2 pressures, the corresponding range is from 39 to 38 to 31 psi for unfiltered, class 180 filter, and class 60 filter, respectively.
3. Class 60 filtering of test pressures reduces values to below estimated design failure levels.
4. The application of test-measured and analytically developed underside panel pressures to the water impact crash design process requires consideration as to what is appropriate filtering, or if filtering is even appropriate. Failure of the panels during both the S1 and S2 tests indicates that design pressures were reached at many panel locations. The use of unfiltered data or a class 180 filter provided test and analysis pressures, which are consistent with the observed damage. The test class 60 filter does not.

5. The interpretation of the meaning of test measurements obtained from a pressure transducer covering a small area versus a hybrid model, wherein the pressure represents an average panel response, is a matter of great concern. Add to this mix, the FEM pressures, being presented as contours, adds to the need to clarify how analysis and test pressure data are to be compared.
6. Potential explanations for differences in pressures obtained from the analysis versus test results are (1) the choice of representative area in KRASH that the calculated hydrodynamic force is divided by and (2) representative shape of a hydrodynamic surface that influences the calculated force.

5.5 POWER SPECTRAL DENSITY ANALYSIS OF TEST AND KRASH ANALYSIS DATA.

1. PSD analysis offers the opportunity to easily visualize the frequency content of the responses.
2. PSD analysis frequency range and amplitude results are dependent on the choice of parameter options: sample times, sampling rates (data interval), NPTS, and NFFT.
3. Linear amplitude scales more clearly define frequencies than do logarithmic amplitude scales.
4. It is difficult to relate to the meaning of the PSD amplitude contributions at the different frequencies in absolute terms.
5. PSD analysis adds another dimension to understanding test and analysis acceleration correlation results.

5.6 MODAL ANALYSIS OF THE KRASH MODEL.

1. A modal analysis of the analytical model is performed for the purpose of determining model mass and stiffness distribution as well as local and component mass/stiffness properties, as depicted by frequencies and mode shapes. Ideally, the analytical model is to have the same mass and stiffness properties as the test article. In reality, one cannot do a modal analysis of the test article but only of an analytical representation of the test article.
2. Not all modes in an aircraft are going to be excited. The modal analysis should be conducted to account for modal contributions at desired locations of interest. The modal contributions depend on the location where one is interested and the manner and location and sequence in which the structure is loaded. Thus, in some instances, higher-order modes could contribute more than some of the lower-order modes.
3. For the UH-1H S1 and S2 tests, the first-order vertical bending mode appears to be a major contributor at floor locations of interest. Higher-order modes also contribute.

4. The KRASH model of the S1 and S2 test articles appears to be softer in some areas compared to the FEM modal analysis results. It also has some modes that are not defined in the FEM model. Some changes to the model would be appropriate areas to investigate with regard to improving correlation. However, others that are not involved significantly in the floor response would not further the correlation effort.
5. Modal analysis offers the opportunity to improve analytical modeling and better understand test and analysis acceleration results.

5.7 RELATIONSHIP BETWEEN TIME HISTORY, PSD, AND MODAL ACCELERATION ANALYSIS RESULTS.

1. Acceleration frequencies estimated from time history plots can be confirmed with PSD plots.
2. It is difficult to compare absolute amplitudes, whether they be from test or analysis, between the time and the frequency domains. Thus, the use of normalized data between the two domains might be the best way to show relative contributions. Time histories (time domain) provide amplitudes that are based on all frequencies that contribute, while the PSD (frequency domain) is frequency-specific.
3. There are identifiable frequencies that are observed between time domain, frequency domain, and modal contribution analysis.
4. At some test locations, extremely high acceleration-related frequencies exist (> 300-700 Hz) that cannot be related to any meaningful mode. However, for class 60 and class 180 filter levels, these modes are irrelevant and will not show up.
5. PSD plots confirm that low frequencies (< 20 Hz) exhibit substantial and significant responses for both test and analysis in many instances, including those that appear to be higher frequencies in the time domain.

5.8 RELATIONSHIP OF FLOOR ACCELERATION AND PANEL PRESSURE TRENDS TO IMPACT SEVERITY.

1. The correlation results show that analysis and test both predict similar percentage increases in pressures for the more severe S2 impact condition versus the S1 impact condition but not as great as the velocity increase would suggest. This is related to the fact that design pressures at many panel locations are reached at the S1 impact level. Thus, at the more severe S2 impact level, there is a limited pressure increase available for the remaining panels.
2. The correlation results show that the analysis and test both predict similar percentage decreases in acceleration for the more severe S2 impact condition versus the S1 impact condition, contrary to an expected increase based on the velocity increase for S2 versus S1. Potential factors that influenced both test and analysis results are pitch attitude, vertical velocity component, more lower amplitude slabs modeled and measured during

S2, and limited pressure increases due to underside panel design pressures being exceeded.

3. The test and analysis acceleration and pressure trends as a function of impact severity are consistent and provide an increase in the confidence of the analytical model to simulate water impact scenarios.

5.9 RELATIONSHIP OF FLOOR ACCELERATION RESPONSE TO UNDERSIDE PANEL PRESSURE.

1. The correlation results showed agreement between the test and analysis floor acceleration response in relation to the panel underside pressure at several locations. This relationship can be defined as a transfer function with units of g/psi.
2. A g/psi transfer function provides insight into the ability of the analytical model to represent appropriate structural paths and, thus, is important to understanding test and analysis results and potential model changes.

5.10 OTHER TECHNIQUES.

1. The Hilbert Spectra/HHT analysis procedure is designed to analyze a nonstationary and nonlinear process, which the PSD and Fast Fourier Transform (FFT) are not. As such, it has the potential to determine frequency and energy both as a function of time. However, there are limitations associated with using this technique that marginalizes its benefits versus using the PSD and FFT.
2. The Force Reconstruction technique provides a method by which measured responses can be used to determine forces acting on the structure. However, there are several potential limitations to the use of this technique for full-aircraft water impact scenarios.

5.11 APPLICATION OF FEM PSD TAC TO HELICOPTER WATER IMPACT SCENARIOS.

1. The current application of PSD analysis to simple structures and correlation with FEM results has shown some promising results and concerns that require further investigation.
2. Correlation between test and analysis has shown strains are more easily reproduced than acceleration measurements, but neither with a high percentage of agreement.
3. It is difficult to relate the FEM PSD test-analysis correlation results of simple structures using strains to correlation for full-aircraft water impact test-analysis correlation using accelerations. There are many limitations on testing requirements and on the applicability of data from full-scale structure that are not present in simple structures.

5.12 AUTOMOTIVE INDUSTRY CORRELATION PROCEDURES.

1. The automotive industry has been extremely active in crash testing and modeling but offers no particular insight into improving an understanding of test and analysis results.

2. The automotive industry has far more comprehensive test requirements and defined procedures for analyzing test results than the aircraft industry.
3. There is no industry standard with regard to analysis programs, analytical modeling tolerances, and modeling techniques.

5.13 POTENTIAL KRASH IMPROVEMENTS.

1. Potential changes to the KRASH analytical model that can be identified and implemented to facilitate improved representation of test simulation are as follows.
 - In the KRASH model, hydrodynamic forces are influenced by the representation of the water impact surface contour or contact shapes. Changes to the representation of the hydrodynamic surface shape, shape parameters, and surface area will affect pressures.
 - The model weight distribution and stiffness can be altered to change some overall frequencies and local modes in an attempt to better match FEM-developed mode shapes and frequencies.
 - While changing weight and stiffness or underside panel, representations may alter results at one or more locations; there is no assurance that all the changes will result in positive improvements. The correlation results indicate that while the averages are within tolerance, the individual responses vary. This variation suggests that some analysis results are higher and some analysis results are lower than the corresponding test results. Thus, generic or overall changes affecting all responses up or down most likely result in both better and worse comparisons, while not necessarily affecting the averages. The results from selective changes in a multidegree of freedom system, unlike a single degree of freedom system, are very difficult to predict.
 - The performance of modal analysis prior to model applications to compare with available NASTRAN frequencies and mode shapes shows potential applicable mass and stiffness revisions.

5.14 TEST DATA GATHERING AND REDUCTION IMPROVEMENTS.

1. Recorded data should:
 - Attempt to record pressures at midpanel locations and with opposite side symmetry, where feasible.
 - Floor accelerations should be measured at major mass locations and, when appropriate, at locations in proximity to seat/occupant masses.

- As a minimum, the data should be recorded unfiltered or at a minimum of 1000 Hz filtered.
2. Data reduction should include SAE class 60 and 180 filtering of time history accelerations. The former to help define floor pulses for seat/occupant testing, and the latter to capture the effect of responses sensitive to frequencies up to 300 Hz. Unfiltered and filtered pressure data should be made available. All failures and damage should be recorded. In addition to determining impact attitude and velocity, the data reduction should provide computations of velocity change.
 3. Pretest analysis should be performed to help set impact conditions, anticipated response ranges, and level of impact severity to meet test objectives.
 4. Since a test is a one shot affair, the maximum set of data should be made available to compare with analysis results and assess the consequences of the impact.

6. CONCLUSIONS.

1. The use of power spectra density (PSD) analysis, modal analysis, and filtering has resulted in the following.
 - The S1 and S2 test and analysis correlation results are consistent with the characteristics of the aircraft configuration that was modeled and the structure that was tested. This provides confidence in the correlation results.
 - Some aspects of the analytical model can be altered so as to improve current and future hybrid models with regard to matching NASTRAN-provided data.
 - Not one of the techniques investigated is a stand-alone preferred correlation technique. However, the use of various techniques such as filtering, PSD analysis, and modal analysis each provide additional insight, which is useful in evaluating both test results and modeling representations.
2. Quantitative criteria used in correlating test and analysis results should be consistent with test data scatter or tolerances. Correlation criteria should include an assessment of whether key events noted in the test are satisfactorily matched by the analysis. This would include the kinematics, the response levels, time of occurrences, structural failures, as well as pressure and acceleration trends as a function of water impact severity.
3. Society of Automotive Engineers class 60 filtering is appropriate for correlating floor accelerations and defining floor pulses. While improving correlations at some locations, it does not improve correlation at all locations.
4. The relationship between underside panel force and floor acceleration response is important to understanding the test and analysis results as well as the correlation between them.
5. Frequency domain analysis does confirm time domain frequencies and is needed to determine relative frequency contributions. However, it is difficult to correlate time domain and frequency domain amplitudes, although some consistent trends can be shown with normalized data.
6. Force Reconstruction is not considered applicable to full-scale helicopter water impact scenarios. The Huang Hilbert Transform may be applicable but does not provide sufficient additional useful information compared to the Fast Fourier Transform, PSD, and time history procedures.
7. The automotive industry test requirements are different, but their correlation techniques are the same as current aircraft industry correlation techniques. The automotive industry has not developed any additional insight into test analysis correlation approaches.

7. REFERENCES.

1. Small Business Innovative Research (SBIR) Contract N698335-98-C-0035, March 1998.
2. Lindley Bark Report, Third International KRASH User's Seminar, ASU Phoenix, AZ, January 2001.
3. NASA Tech Briefs GSFC-13817- Technical Support Package, "Analyzing Time Series Using EMD and Hilbert Spectra."
4. Dr. Huang, et al., "The Empirical Mode Decomposition and the Hilbert Spectrum for Nonlinear and Non-stationary Time Series Analysis," *Proceedings Royal Society of London*, pgs 454, 903-995, 1998.
5. Dr. Bateman, et al., "Force Reconstruction for Impact Tests," *Journal of Vibration and Acoustics*, Vol. 113, April 1991.
6. Dr. Bateman, et al., "A Comparison of Force Reconstruction Methods for a Lumped Mass Beam," *Proceedings of the 63rd Shock and Vibration Symposium*, Vol. II, New Mexico, October 1992.